FUNCTIONAL CONTRIBUTIONS OF A SEX-SPECIFIC POPULATION OF MYELINATED AORTIC BARORECEPTORS IN RAT AND THEIR CHANGES FOLLOWING OVARIECTOMY

Grace C. Santa Cruz Chavez

Submitted to the faculty of the University Graduate School
in partial fulfillment of the requirements
for the degree
Doctor of Philosophy
in the Program of Medical Neuroscience,
Indiana University

May 2014

Accepted by the Graduate Faculty, Indiana University, in partial fulfillment of the requirements for the degree of Doctor of Philosophy.

_____
John H. Schild, Ph.D., Chair

_____
Grant D. Nicol, Ph. D.

Doctoral Committee

_____
Gerry S. Oxford, Ph.D.

April 28, 2014

_____
Daniel E. Rusyniak, M.D.

_____
Michael R. Vasko, Ph.D.

DEDICATION

I would like to dedicate this dissertation to my husband Andrew Whitaker, my children Carolina and Grace Whitaker, and my parents Lidia Chavez Garcia and Luis Santa Cruz Yabar.

ACKNOWLEDGEMENTS

The completion of my dissertation and Ph.D. could not have been possible without the invaluable support and professionalism of several people.

First, I would like to thank my research advisor, Dr. John H. Schild for being an exemplary mentor and colleague. His invaluable advice and encouragement have taught me about the process of conducting robust, evidence-based science and the importance of finding research focus and significance. Despite my many insecurities regarding my abilities as a scientist, he always encouraged me to find my own experimental recipe to conduct quality research. Next, I would like to thank my dissertation committee members Dr. Grant Nicol, Dr. Gerry Oxford, Dr. Daniel Rusyniak, and Dr. Michael Vasko for their advice, patience and guidance throughout my graduate work. This select group of outstanding scientists showed me genuine concern and faith in my work and thus motivated me to be the best that I could. I would also like to thank Dr. Bai-Yan Li, member of the Schild Lab, as he played an important role in training me as a scientist. I would like to thank my fellow doctoral students for their support, feedback, and friendship.

Finally, I would like to express my deepest gratitude and appreciation to my husband Andrew, my children Carolina and Grace, and my parents Luis and Lidia for their unconditional love, support, and encouragement.

Grace C. Santa Cruz Chavez

FUNCTIONAL CONTRIBUTIONS OF A SEX-SPECIFIC POPULATION OF MYELINATED AORTIC BARORECEPTORS IN RAT AND THEIR CHANGES FOLLOWING OVARIECTOMY

Gender differences in the basal function of autonomic cardiovascular control are well documented. Consistent baroreflex (BRx) studies suggest that women have higher tonic parasympathetic cardiac activation compared to men. Later in life and concomitant with menopause, a significant reduction in the capacity of the BRx in females increases their risk to develop hypertension, even exceeding that of age-matched males. Loss of sex hormones is but one factor.

In female rats, we previously identified a distinct myelinated baroreceptor (BR) neuronal phenotype termed Ah-type, which exhibits functional dynamics and ionic currents that are a mix of those observed in barosensory afferents functionally identified as myelinated A-type or unmyelinated C-type. Interestingly, Ah-type afferents constitute nearly 50% of the total population of myelinated aortic BR in female but less than 2% in male rat. We hypothesized that an afferent basis for sexual dimorphism in BRx function exists. Specifically, we investigated the potential functional impact Ah-type afferents have upon the aortic BRx and what changes, if any, loss of sex hormones through ovariectomy brings upon such functions.

We assessed electrophysiological and reflexogenic differences associated with the left aortic depressor nerve (ADN) from adult male, female, and ovariectomized female (OVX) Sprague-Dawley rats. Our results revealed sexually dimorphic conduction velocity (CV) profiles. A distinct, slower myelinated fiber volley was apparent in compound action potential (CAP) recordings from female aortic BR fibers, with an amplitude and CV not observed in males. Subsequent BRx studies demonstrated that females exhibited significantly greater BRx responses compared to males at myelinated-specific intensities. Ovariectomy induced an increased overall temporal dispersion in the CAP of OVX females that may have contributed to their attenuated BRx responses. Interestingly, the most significant changes in depressor dynamics occurred at electrical thresholds and frequencies most closely aligned with Ah-type BR fibers.

Collectively, we provide evidence that, in females, two anatomically distinct myelinated afferent pathways contribute to the integrated BRx function, whereas in males only one exists. These functional differences may partly account for the enhanced control of blood pressure in females. Furthermore, Ah-type afferents may provide a neuromodulatory pathway uniquely associated with the hormonal regulation of BRx function.

John H. Schild, Ph.D., Chair

TABLE OF CONTENTS

LIST OF TABLES

LIST OF FIGURES

LIST OF ABBREVIATIONS

ACh	Acetylcholine
ADN	Aortic depressor nerve
ANS	Autonomic nervous system
AV	Atrioventricular
BP	Blood pressure
BR	Baroreceptor
BRS	Baroreflex sensitivity
BRx	Baroreceptor reflex, baroreflex
CAP	Compound action potential
CNS	Central nervous system
CO	Cardiac output
CRWU	Case Western Reserve University
CV	Conduction velocity
CVD	Cardiovascular disease
CVLM	Caudal ventrolateral medulla
ENaC	Epithelial sodium channel
ER	Estrogen receptor
GABA	γ-aminobutyric acid
HF	High frequency
HR	Heart rate
HRV	Heart rate variability
IML	Intermediolateral
IX	Glossopharyngeal nerve
LCC	Left common carotid
LF	low frequency
LSA	Left subclavian artery
MAP	Mean arterial pressure
NE	Norepinephrine
NA	Nucleus ambiguous
NTS	Nucleus Tractus Solitarii
OH	Orthostatic hypotension
OVX	Ovariectomized
PNS	Parasympathetic nervous system
RMS	Root-mean-square
RVLM	Rostral ventrolateral medulla
SA	Sinoatrial
SD	Standard deviation
SLN	Superior laryngeal nerve
SNS	Sympathetic nervous system
SV	Stroke volume
TPR	Total peripheral resistance
TRPC	Canonical transient receptor potential
TTX	Tetradotoxin
VGC	Voltage gated channel

VLF	Very low frequency
X	Vagus nerve

CHAPTER 1: INTRODUCTION

The discovery of blood circulation was made nearly four centuries ago in 1615 by William Harvey (Ribatti, 2009). In his classic work, Harvey concluded that “the blood in the animal body moves around in a circle continuously and that the action or function of the heart is to accomplish this by pumping.” He also theorized that arteries and veins were connected to each other. With the discovery of capillary vessels by Marcello Malpighi in 1661 (Young, 1929), the cardiovascular circuit was completed.

The primary function of the cardiovascular system is to maintain adequate blood flow to all body tissues as the blood delivers nutrients and removes waste products (Kassab, 2006). To accomplish this, cardiovascular activity is regulated by homeostatic mechanisms of intrinsic or extrinsic nature (Table 1) (Bronzino, 2006). Intrinsic control is accomplished by the inherent physicochemical attributes of the cardiovascular tissues and organs themselves. In contrast, extrinsic control can be attributed to the effects other organ systems in the body have upon the cardiovascular tissue, most notably the autonomic nervous system (ANS) and the endocrine system. These regulatory mechanisms help maintain and adjust systemic hemodynamics.

Adequate performance of the cardiovascular system can be monitored by several hemodynamic measurements (Kuhn & Werdan, 2001). Most common of them all is the measurement of arterial blood pressure (BP). The relative stability of this hemodynamic parameter leads to the conclusion that it is a highly

Table 1: List of intrinsic and extrinsic factors regulating cardiovascular homeostasis

Intrinsic factors	Cardiac muscle Action potential of pacemaker cells Sequence of excitation of the cardiac conduction system Vasoconstrictor tone
Neural extrinsic factors	Neural control (parasympathetic and sympathetic) Baroreceptors Chemoreceptors Atrial receptor reflex
Humoral extrinsic factors	Renin-Angiotensin-Aldosterone system Vasopressin/antidiuretic hormone Atrial natriuretic peptide Epinephrine (released by adrenal gland) Thyroxin (released by thyroid gland) Glucagon (released by pancreatic α cells)
Renal extrinsic factors	Increased rate of kidney filtration Decrease amount of filtrate Increase reabsorption from filtrate to blood Renin-Angiotensin-Aldosterone system

controlled variable. Importantly, heart rate (HR) regulation plays a vital role in the maintenance of systemic arterial BP because BP is dependent on cardiac output (CO) and total peripheral resistance (TPR) (Hall *et al.*, 2012):

$$BP = CO \times TPR$$

CO, the volume of blood pumped by the heart, is determined by both stroke volume (SV) and HR:

$$CO = SV \times HR$$

Combining these two equations allow us to appreciate the major variables that directly influence arterial BP:

$$BP = (SV \times HR) \times TPR$$

Hence, any changes in BP must result from changes in one or more of these three variables.

The ANS plays a vital role in the control of HR, SV, and TPR through fast acting neural reflexes. These reflexes have high gain (i.e. performance, ratio of the reflex response and its error) and respond quickly compared to other extrinsic regulating factors (Guyton, 1980). For example, the baroreceptor reflex (baroreflex, BRx) initiated by baroreceptors (BR) responds to changes in BP within one heartbeat, while control of blood volume by the kidneys acts on a time scale of days. Therefore, short-term regulation of the cardiovascular system is predominantly under the control of the ANS through the synergistic actions of its sympathetic and parasympathetic arms. A long-term role for autonomic cardiovascular control has been proposed but remains controversial (Sleight, 2004; Thrasher, 2004).

In this dissertation, I focus on the BRx and how its response is modulated by the selective and graded activation of myelinated populations of aortic BR afferents. The BRx is a key regulatory mechanism of autonomic cardiovascular function. Activation of BR afferents innervating major blood vessels initiate the BRx resulting in the increase or decrease of sympathetic and parasympathetic nerves activity at effector organs and tissues. In addition to neural and humoral extrinsic factors that regulate cardiovascular function, gender and age have also been shown to influence cardiovascular performance and BRx function (Dart *et al.*, 2002; Huxley, 2007). A mechanism that could explain such observed effects other than sex hormones is not known and sex hormones have yet to be proven to be the sole contributors of the differences in BRx function between the sexes and in aging. In this dissertation, I propose a potential neural explanation to the sex differences observed in BRx function based on differential expression of functionally distinct subtypes of myelinated aortic barosensory afferent neuronal populations in male and female rats. To further examine this proposal I will determine whether the function of these myelinated afferents is affected by ovariectomy, a commonly used model of menopause and ovarian sex hormones deprivation (Diaz Brinton, 2012). The insights gained by the present work have the potential to not only advance our knowledge in the physiological mechanisms contributing to cardiovascular regulation in males and females, but also has the potential to provide with a novel venue for therapeutic interventions in cardiovascular care, especially in women.

I. Neural control of cardiovascular function

A. Role of the autonomic nervous system

The nervous system controls cardiovascular function almost entirely through the ANS (De Hert, 2012). Nervous control of BP is achieved by adjusting CO and peripheral resistance, thus providing adequate blood flow to vital tissues and organs. The ANS supplies sympathetic and parasympathetic innervation to cardiovascular tissues (except for capillaries, precapillary sphincters, and metarterioles), but their distributions are not equivalent (Robertson *et al.*, 2012). The sympathetic nervous system (SNS) is exclusively responsible for regulating circulation, whereas the Parasympathetic Nervous System (PNS) contributes specifically to regulation of heart function (Donald & Shepherd, 1980). Centers responsible for these regulatory activities include the cardiac and vasomotor centers of the medulla oblongata (Korner, 1971; Martini, 1998). Each cardiac center consists of a cardioacceleratory center, which increases CO through sympathetic innervation (Fukuda *et al.*, 1989), and a cardioinhibitory center, which reduces CO through parasympathetic innervation (Todo, 1977; Todo *et al.*, 1977). The vasomotor center contains two population of sympathetic vasomotor neurons, one responsible for widespread vasoconstriction, and the other responsible for vasodilation of arterioles in skeletal muscle and the brain (Martini, 1998). Furthermore, sympathetic nerves to the adrenal medulla causes these glands to secrete the catecholamines, norepinephrine (NE) and epinephrine, and neuropeptides into the blood (Robertson *et al.*, 2012). These hormones then circulate to all areas of the body and cause almost the same effect on the

circulation as direct sympathetic stimulation. The sympathetic vasomotor nerve fibers (from preganglionic cells) leave the spinal cord through all the thoracic spinal nerves and through the first one and two lumbar spinal nerves (Guyton, 2006). Then, they pass immediately into a sympathetic chain, one of which lies on each side of the vertebral column. Next, postganglionic nerve fibers pass to the circulation and innervate the vasculature of the internal viscera, heart, and peripheral areas. They also go directly to the heart and when stimulated, they markedly increase the activity of the heart increasing HR and SV (Randall & McNally, 1960). The PNS plays a supplementary role in regulation of the circulation. Its most important circulatory effect is to control HR via parasympathetic nerve fibers to the heart in the vagus nerve (cranial nerve X) (Higgins *et al.*, 1973). Parasympathetic stimulation causes a marked decrease in HR and a slight decrease in heart muscle contractility.

The ANS modulates the activity of target organs and tissues by the release of neurotransmitters at their junction with postganglionic autonomic neurons. The effects of autonomic ganglion cells on their smooth muscle, cardiac muscle, or glandular targets are mediated by two primary neurotransmitters: norepinephrine (NE) and acetylcholine (ACh) (Purves *et al.*, 2012).

Sympathetic adrenergic nerves innervate the sinoatrial (SA) and atrioventricular (AV) nodes, conduction pathways, and myocytes in the heart (Furukawa *et al.*, 1991). The release of NE from their postganglionic terminals binds to β_1 adrenoreceptors in the heart and increases the rate of cardiac pacemaker activity, enhances inotropy (i.e. contraction of myocardium) and

lusitropy (i.e myocyte relaxation). There are also β_2 adrenoreceptors in the heart and their stimulation by NE has similar cardiac effects as β_1 adrenoreceptor stimulation, but they constitute only 20% of the total cardiac β adrenoreceptor population (Bristow *et al.*, 1986; Wachter & Gilbert, 2012). α_1 adrenoreceptors in the human heart have been identified, however, their density is only 10 to 15% that of β adrenoreceptors (Brodde & Leineweber, 2004). Binding of NE to α_1 adrenoreceptors found on myocytes produce small increases in inotropy. NE released from the terminals of sympathetic postganglionic cells also acts on the smooth muscle of arterioles to increase the tone of peripheral vessels. Postsynaptic or postjunctional α adrenoreceptors in human blood vessels can be classified as α_1 and α_2, and both subtypes mediate vasoconstriction (van Brummelen *et al.*, 1986).

Parasympathetic control of the human heart is mediated by ACh receptors and the human heart possesses predominantly M_2 muscarinic cholinoceptors (Deighton *et al.*, 1990). ACh is released by parasympathetic cholinergic nerves derived from vagal nerves and binds to M_2 receptors in the cardiac muscle, especially at the SA and AV nodes where their density is greater. This gives rise to negative chronotropy (i.e. reduction in the firing of cardiac pacemaker cells and decreased HR) and negative dromotropy (i.e. decreased conduction velocity of AV node) in the heart (Brodde & Leineweber, 2004).

Notwithstanding the antagonistic actions of parasympathetic and sympathetic regulation of cardiovascular function, these neural systems work in tandem to provide very rapid control of systemic arterial pressure under a wide

range of circumstances (Glick & Braunwald, 1965; Olshansky *et al.*, 2008). This is achieved through precise arterial and non-arterial reflexes that detect and correct changes in BP (mediated by BRx), cardiac blood volume and chemical composition (cardiopulmonary reflex), and changes in blood carbon dioxide, oxygen, or pH levels (chemoreceptor reflex) (Vasquez *et al.*, 1997).

By far, the most studied and best known nervous mechanism that controls BP is the BRx since it is the fastest and impairment of the BRx brings about a variety of maladies ranging from increase in BP variability to aberrant pressure rises that augment the risk of fatal events such as myocardial infarction and stroke. Therefore, a properly functioning arterial BRx is necessary for appropriate cardiovascular performance.

As one of the purposes of this dissertation is to study the BRx function, the next sections will discuss the BRx circuitry with emphasis on its sensory components, the clinical measurements of BRx function, and the effects of gender and age on BRx function.

B. The autonomic components of the baroreflex

The ultimate goal of the BRx is to maintain BP homeostasis and this is achieved through a negative feedback loop that monitors mechanical or barosensory information of the arterial system. This information is provided by mechanoreceptors called baroreceptors (BR) that reside at major blood vessels and play a crucial role in determining the amount of parasympathetic or sympathetic activity supplied for cardiovascular control. The BRx buffers acute

BP fluctuations due to changes in posture, exercise, stress, drugs, and other stimuli. A sudden increase or reduction in BP results in corresponding increased or reduced firing of BR mechanosensitive terminals (Figure 1) primarily located in the adventitia of the carotid sinuses (innervated by the glossopharyngeal nerve, cranial nerve IX) and between the tunica media and tunica externa of the aortic arch (innervated by the vagus nerve) (Davos *et al.*, 2002). At these barosensory terminals, the mechanical deformation of the vessel wall is transduced into a train of frequency-modulated action potentials. This signal is relayed by sensory afferent fibers to the neurons located in the nucleus tractus solitarii (NTS) where it is processed and integrated with other neural information from the heart, circulation, lungs, etc (Miura & Reis, 1972; Andresen & Kunze, 1994; Hines *et al.*, 1994; Dean & Seagard, 1997; Chan *et al.*, 2000; Andresen *et al.*, 2004). From the NTS, the BRx bifurcates into two independently regulated pathways that differentiate in their functional effects: (1) a sympathetoinhibitory pathway that primarily controls TPR, and (2) a cardioinhibitory pathway that elicits rapid changes in HR (Benarroch, 2008).

The BRx sympathoinhibitory pathway involves a projection from the NTS to a group of γ-aminobutyric acid (GABA) releasing interneurons located in the caudal ventrolateral medulla (CVLM) that sends an inhibitory projection to sympathoexcitatory neurons residing in the rostral ventrolateral medulla (RVLM) (Pilowsky & Goodchild, 2002; Benarroch, 2008). The RVLM neurons send a direct excitatory glutamatergic projection to preganglionic neurons in the intermediolateral (IML) cell column and activate the sympathetic vasoconstrictor

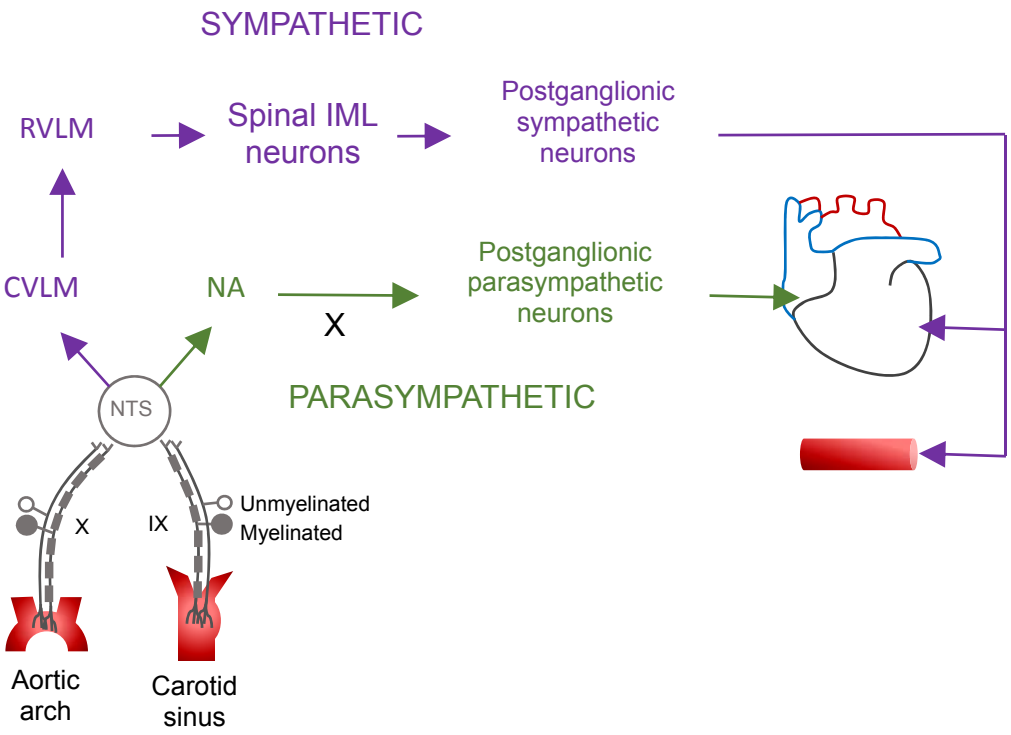

Figure 1: Simplified baroreflex circuit. The arterial baroreceptors located in the carotid sinuses and aortic arch respond to the mechanical deformation of the blood vessels elicited by rises and reductions in blood pressure. Baroreceptor afferent fibers provide monosynaptic excitatory input to the solitary tract where barosensory neurons initiate the sympathetic and parasympathetic pathways of the baroreflex. CVLM, caudal ventrolateral medulla; RVLM, rostral ventrolateral medulla; IML, intermediolateral; NA, nucleus ambiguus; IX, glossopharyngeal nerve; X, vagus nerve.

output to muscle, mesenteric, and renal blood vessels. The BRx cardioinhibitory pathway involves a direct input from the NTS to a group of preganglionic neurons residing in the ventrolateral portion of the nucleus ambiguus (NA) (Ciriello & Calaresu, 1979; McKitrick *et al.*, 1992; Benarroch, 2008). These cholinergic neurons project to the cardiac ganglion neurons that inhibit the pacemaker cells of the SA node and provide a beat-to-beat control of HR.

Collectively, the sympathetic and parasympathetic branches of the BRx function to regulate BP levels. If BP suddenly falls, decreased firing of the BR results in disinhibition of the sympathetic pathway (Pilowsky & Goodchild, 2002), increased firing of sympathetic nerves to the heart and vascular smooth muscle, and the augmentation of CO and peripheral resistance. Almost simultaneously, firing of parasympathetic nerves to the heart is decreased to assist in increasing CO. In the case of a sudden rise in BP, the barosensitive NTS neurons initiate the inhibition of vasoconstrictor and cardioaccelerator centers (Aviado & Guevara Aviado, 2001), resulting in the release of ACh into the SA node of the heart and a cardio-inhibitory effect. Consequently, the HR is lowered, CO diminishes and arterial BP decreases.

C. Role of arterial baroreceptors in baroreflex function

The idea that the arterial system contains pressure sensitive areas was introduced in 1902 by Koster and Tschermak (Koster & Tschermak, 1903). Later, in 1923, Hering showed that nerve fibers in the carotid sinus and in the common carotid artery bifurcation were responsible for the carotid sinus reflex (Hering,

1923). A noteworthy experimental contribution from Hering's work is that he introduced the use of electrical stimulation to activate the BR and elicit the reflex. Up until the 1920s, occlusion of the carotid arteries had been the preferred method to artificially evoke a rise in BP and HR (Janig, 2008). Soon after, BR function began to be described in terms of their discharge frequency (Adrian, 1926; Bronk & Stella, 1932; Ead *et al.*, 1952) proving useful in determining the dependency of BR activity not only on the mean level of BP, but also on the direction and rate of change of BP (Landgren, 1952a, b; Katona *et al.*, 1968; Arndt *et al.*, 1975). Therefore, BR activity will increase or decrease to a greater extent when the change in BP occurs more rapidly leading to a more effective reflex compensation (Robertson *et al.*, 2012). Similarly, these barosensory afferents demonstrate a phasic discharge with the arterial pulse, higher during the systolic phase and lower or absent during diastole, implying that threshold and range of operation contribute to the buffering capabilities of the BRx (Ead *et al.*, 1952). Interestingly, BR can adjust their range of operation in hypertension. Commonly referred to as resetting, this property includes an increase in threshold, a decrease in sensitivity, and usually a decrease in maximal impulse frequency (Coleridge & Coleridge, 1980). Resetting develops progressively with hypertension and when complete (i.e. the characteristic BR pressure-discharge curve has shifted to the left), the BR continue to function as if the BP had not been raised. Consequently, the general belief became that BR and the BRx are only effective to minimize acute fluctuations in arterial BP but not to regulate the level of BP, thus, they do not contribute to the long term control of mean arterial

pressure (MAP) (Cowley, 1992). In addition, several studies involving dogs had shown that chronic denervation of the BR (both at the aortic arch and the carotid sinus) did not affect the average level of BP (McCubbin *et al.*, 1956; Cowley *et al.*, 1973), although tremendous fluctuations of MAP were observed during their normal activities.

The dogma that arterial BR are not important for the regulation of long-term MAP has been refuted by Thrasher (2004) (Thrasher, 2004). He used dogs in which the aortic BR and the carotid BR on one side were chronically denervated while the left carotid sinus BR of the other side were left intact (Thrasher, 2002). The dogs exhibited normal levels of MAP. Next, he unloaded the remaining intact arterial BR by occlusion of the common carotid artery proximal to the innervated carotid sinus. Over 7 days, this procedure generated increases in arterial BP and HR, both returning to normal after removal of the occlusion. This experiment clearly shows that arterial BR are also important for the long term maintenance of arterial BP.

Considerable controversy still remains regarding the barosensory afferents and their association with long term control of MAP. Regardless, arterial BR are in the forefront of cardiovascular reflex control because they are the first stage in the neural feedback system that regulates BP and HR. Not surprisingly, BR dysfunction closely associates with a variety of cardiovascular pathologies such as unremitting hypertension and dysrhythmias (Ketch *et al.*, 2002). Importantly, clinical studies have demonstrated the prognostic value of quantitative measures of the BRx since changes in its function reflect alterations

in the autonomic control of the cardiovascular system. These measurements which include baroreflex sensitivity (BRS) and heart rate variability (HRV) have become robust and valuable tools that evaluate integrated ANS function.

D. Clinical quantification of baroreflex function

In baseline conditions, in young humans, there is an important amount of tonic vagal discharge and only a moderate amount of tonic sympathetic discharge (Jose & Collison, 1970; Opthof, 2000). The result of this interaction is that resting HR is about 30% lower than the intrinsic HR of 90 – 100 beats/min and a CO that is about 30% higher than in the absence of sympathetic discharge (De Hert, 2012). This ensures maintenance of the body's most basic function and that vital signs such as BP and HR remain within normal levels. The ANS plays an important role in the regulation of these indicators of cardiovascular health through variations in its sympathetic and parasympathetic activity. Even though the actions of these two neural systems are often, but not always, antagonistic, they work synergistically to maintain a balance (i.e. sympathovagal balance). Importantly, sympathetic and parasympathetic activities are regulated through BRx mechanisms that tightly control BP and HR. Changes in BRx function reflect alterations in the autonomic control of the cardiovascular system and impairment of BRx mechanisms is often exhibited in cardiovascular diseases. For example, reductions of inhibitory activity and imbalance in the physiological sympathovagal balance outflow to the heart result in chronic adrenergic activation or sympathoexcitation eliciting hypertension. Therefore, methods that quantify

autonomic function relative to sympathetic and parasympathetic activity such as BRS and HRV have become important prognosis indicators of cardiac health by clinical assessment (La Rovere *et al.*, 2008; Pagani *et al.*, 2012).

BRS is defined as alterations in the beat-to-beat interval (msec) per unit change in BP (mmHg). It can be determined pharmacologically (Oxford method) through injection of vasoactive substances, such as phenylephrine and sodium nitroprusside, and invasive determination of arterial pressure (Sleight, 1997). Non-invasive methods for BRS evaluation may be through measurements of HR *vs.* BP changes in response to deep breath, Vasalva maneuver (forced expiration against resistance), the neck chamber technique (which provides a selective manipulation of the carotid BR), or tilt testing (passive body movement from supine position to upright tilt) (La Rovere *et al.*, 2008; Campos *et al.*, 2013). These tests provide a synthetic index of BRx gain.

HRV is the variation of beat-to-beat intervals, also known as R-R intervals. HRV indexes are obtained by analyzing the interval between the R waves, which can be captured by non-invasive instruments such as an electrocardiograph (Campos *et al.*, 2013). Several methods of measuring HRV have been developed, each of which can fall under broader classifications of “time domain” and “frequency” analyses (Lahiri *et al.*, 2008). Time domain measures of HRV are assessed with calculations based on statistical operations of R-R intervals such as standard deviation (SD) of normal R-R interval, the root-mean-square (RMS) of successive R-R interval differences, and the percentage of normal R-R intervals that differ by more than 50 msec. Frequency domain measures use

spectral analysis of R-R intervals and provide information of how power is distributed (variance) as a function of frequency. Recordings yield up to 3 peaks in very low (0.003 to 0.04 Hz, VLF), low (0.04 to 0.15 Hz, LF), and high (0.15 to 0.4 Hz, HF) frequency ranges. The HF component is thought to reflect the modulation of vagus nerve discharge caused by respiration, whereas the LF and VLF components represent the variation in R-R interval caused by more gradual interplay between sympathetic and parasympathetic activities.

The prognostic value of BRS and HRV in cardiovascular disease is widely reported. Decreased HRV and BRS has been associated with increased mortality in patients after myocardial infarction and with heart failure and hypertension (Liao *et al.*, 1996; La Rovere *et al.*, 1998; La Rovere *et al.*, 2001; La Rovere *et al.*, 2002; Frenneaux, 2004). This inverse relationship between BRS/HRV and cardiovascular risks encourages targeting therapies that improve BRx function. For example, lowering the BP of hypertensive patients by pharmacological or dietary interventions shifts the BRx function curve to lower MAP (Patterson *et al.*, 2002; Straznicky *et al.*, 2005). A recent increased interest has been shown for chronic electrical stimulation of carotid sinus BR in dog models of hypertension and in patients with drug-resistant hypertension (Scheffers *et al.*, 2010; Jordan *et al.*, 2012). Favorable effects, such as lower BP and reduced end-organ damage, have been reported after increasing BR activity that extend far beyond short term control of MAP.

E. Effects of gender and age on baroreflex function

Cardiovascular disease (CVD) is caused by disorders of the heart and blood vessels and is the leading cause of death in women and men worldwide. In the United States, roughly 84 million American adults (>1 in 3) have 1 or more types of CVD (Go *et al.*, 2013). The estimated direct and indirect cost of CVD for 2008 was $297.7 billion. Between 2010 and 2030, the total direct medical costs of CVD are projected to triple (Heidenreich *et al.*, 2011) . Among the long-recognized risk factors of CVDs are age and sex (Coulter, 2011). For example, men are at higher risk of developing CVD than pre-menopausal women (Go *et al.*, 2013). Later in life and coincident with women's menopause, there is a sharp rise in CVD development in women compared to age-matched men (Hsia *et al.*, 2007). These disparities between men and women in CVD development and their outcome have been extensively documented, but no conclusive explanation(s) as to the underlying cause currently exists. Interestingly, there are notable examples of gender-related differences in the ANS control of the cardiovascular system (Curtis & O'Keefe, 2002; Conte, 2003). Compelling evidence exists in the clinical literature suggesting that the parasympathetic arm of the BRx (i.e. cardiovagal BRx) is markedly sexually dimorphic. Sex-related differences in cardiovagal BRS and the parasympathetic marker of HRV have been reported (Beske *et al.*, 2001; Sevre *et al.*, 2001; Christou *et al.*, 2005; Johnson *et al.*, 2011; Barnes *et al.*, 2012; Arai *et al.*, 2013). Collectively, these studies support the potential for sex differences in cardiovagal BRx-mediated control of baseline HR and mean arterial BP. Although sex hormones have been

shown to play a role in modulating autonomic function, they have not been proven to be the sole contributors. (Herrington, 1999; Grady *et al.*, 2002; Rossouw *et al.*, 2002; Manson *et al.*, 2003; Hendrix *et al.*, 2006). Furthermore, their effects on cardiovagal BRx function remain controversial (Tanaka *et al.*, 2003; Tank *et al.*, 2005; Kim *et al.*, 2012; Maranon & Reckelhoff, 2013). To the best of our knowledge, no other mechanism responsible for the sexual dimorphism observed in the cardiovagal BRx has been reported. Alternatively, we contend that these differences arise, at least in part, because of fundamental differences in afferent function. We base this hypothesis on our experimental findings that a greater numbers of myelinated aortic BR neurons in female rat exists due to the expression of a functionally distinct subtype of aortic myelinated barosensory neuron that is rarely found in male rats (Li *et al.*, 2008). These findings lead to questions regarding what the physiological significance of this sex-specific subpopulation of BR neurons is. Essentially, what is their role in cardiovascular regulation? Therefore, the central objective of this dissertation was to determine whether this additional subpopulation of BR afferents constitutes an additional myelinated pathway to the integrated BRx drive and what, if any, are its functional contributions to the BRx performance in females compared with that of males? Furthermore, because the loss of ovarian hormones in females is associated with a reduction in BRx performance, I studied the effects ovariectomy may have upon the function of this potential afferent neural pathway.

II. Arterial baroreceptors

Changes in blood pressure are “sensed” by the BR, the mechanosensitive nerve endings that activate by vascular distension during increases in intraluminal BP. The activity of carotid sinus and aortic BR increases when arterial BP rises and decreases when BP falls. These changes in BR activity are transmitted via afferent fibers to brainstem nuclei and evoke the BRx, a homeostatic negative feedback mechanism that buffers changes in arterial BP. Therefore, BR afferents are critically important for BRx function since the activation of these pressure sensors initiates the BRx.

A. Neuroanatomy and classifications

BR terminals are clustered at strategic compartments within the cardiovascular system such as the auricles of the heart, the venae cavae, carotid sinuses, and the aortic arch. Regardless of their location, BR function to provide the afferent signals that maintain MAP at normal levels.

The aortic BR sensory terminals present in the aortic arch (Koster & Tschermak, 1903) arise from the arterial surface and their axons form a common nerve bundle termed aortic depressor nerve (ADN), first described by Cyon and Ludwig in rabbits (Nonidez, 1935). The soma of aortic BR neurons are located in the nodose ganglion. These BR neurons are pseudo-unipolar neurons featuring one short process extending from the cell body that immediately divides into two very long processes: a peripheral axon in the ADN and a central axon that transmits information concerning BP to the NTS (Zhuo *et al.*, 1997). The aortic

BR terminals have been extensively studied using both light and electron microscopy (Abraham, 1969; Aumonier, 1972; Krauhs, 1979). Aumonier's optical studies identified BR terminals in the adventitia and the muscular layer of the aorta in rabbits, dogs, and cats (Aumonier, 1972), but the small dimensions of the receptor endings (10 to 100 μm) limited detailed analysis of the BR terminal ultrastructure. With the aid of an electron microscope, Krauhs carried out a detail analysis of the BR neural endings and showed that, in the rat, these "were observed only in the adventitia and in parts of the media layer into which the adventitia had apparently invaginated" (Krauhs, 1979). Furthermore, when entering the blood vessel wall, myelinated axons lose their myelin sheath. This distal nerve segment is termed the "premyelinated" axon and small unmyelinated nerves often wrap around "premyelinated" fibers to form a terminal complex that has long been considered to represent the neuroanatomical aspect of the pressure sensitive ending (Figure 2) (Krauhs, 1979; Taha *et al.*, 1983).

The location of sensory terminals in the carotid sinus is similar to that of the aortic BR, between two elastic laminae, the adventitia and media layer, and has been described by Bock and Gorgas (Bock & Gorgas, 1976). These investigators used light and electron microscopy to study BR axon terminals in the carotid sinus of guinea pigs and mice. Measured BR units 100 to 150 μm in diameter were arranged in a hexagonal pattern. Carotid BR do not seem to exhibit the large amount of coiling seen in the sensory terminals of aortic BR. Krauhs inferred that this may be due to the large amount of distension undergone by the aorta and the large amount of basal laminae around rat aortic BR may

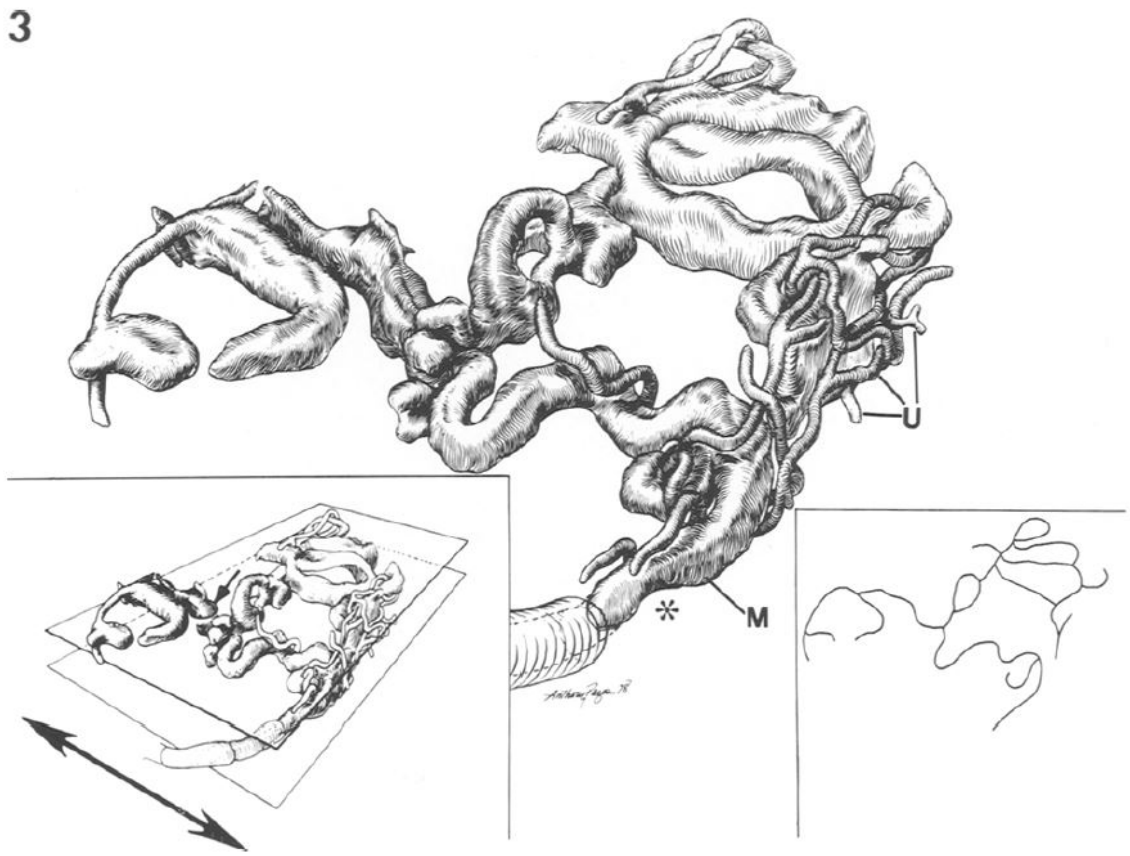

Figure 2: Aortic baroreceptor terminal endings. Three-dimensional reconstruction from electron micrographs of a rat aortic baroreceptor terminal complex consisting of a myelinated fiber (M) and intertwining unmyelinated receptors (U). The large myelinated axon (after the *) is much larger in length than what is depicted in Khraus' model. As shown in the right inset, the premyelinated axon had several branches and loops. Most of the terminal portions of the premyelinated axon are located between two sheets of elastic lamina, but one branch goes through a fenestration into another layer of adventitia (small arrow, left inset). Reprinted from (Krauhs, 1979), with kind permission from Springer.

help protect these sensory terminals (Krauhs, 1979). The small size of BR terminal endings and their extensive coupling with extracellular tissue makes them difficult to dissect. This renders it impossible to conduct direct receptor potential recordings that would provide essential knowledge regarding mechanotransduction following deformation of the blood vessel wall (Brown, 1980). However, electrophysiological studies of axonal discharge responding to BP pulse inputs in a variety of species (Katona *et al.*, 1968; Thoren & Jones, 1977; Coleridge *et al.*, 1987) have yielded details of the nerve endings strain-sensitive nature, and have led to widely utilized classifications of two functionally distinct BR afferents: those with myelinated axons or A-type, and those with unmyelinated axons or C-type.

A-type and C-type arterial BR afferents exhibit dissimilar patterns of discharge (Thoren & Jones, 1977; Coleridge & Coleridge, 1980; Schild & Kunze, 2012). Compared to their unmyelinated counterparts, myelinated afferents generally demonstrate lower thresholds for firing action potentials and higher discharge frequencies that are markedly less variable and faithfully encode the arterial pressure pulse. Conversely, unmyelinated afferents generally have discharge thresholds at pressures near or above normal MAP, have a narrower firing frequency range compared to the myelinated afferents, and typically exhibit irregular spike patterns per cardiac cycle.

Myelinated and unmyelinated BR afferent also present with contrasting neuroanatomical characteristics (Kirchheim, 1976). A-type BR afferent fibers are larger in diameter, ranging from less than 2 μm up to 10 μm, and are wrapped in

a sheath of fatty tissue called myelin manufactured by Schwann cells. The myelin layer and larger diameter of the myelinated axon help to support fast conduction speeds in A-type fibers, typically greater than 10 m/sec. On the other hand, C-type BR afferent fibers are smaller in diameter usually less than 2 μm, have no myelin sheath, and often conduct with speeds below 2 m/sec.

B. Ion channels at the terminal endings and soma

As the BP rises and the arterial diameter increases, BR terminals located within the arterial wall transduce wall deformation or strain into an electrochemical potential (i.e. generator potential) by the opening of mechanosensitive ion channels. If the resulting depolarization in the resting membrane voltage at the terminal ending is of sufficient magnitude, it will trigger a discharge of action potentials upon opening of voltage gated Na+ and K+ channels. The magnitude of the generator potential is encoded into the frequency of the action potentials propagated towards the central nervous system (CNS).

Understanding the basic mechanism(s) of mechanotransduction within the BR terminal endings begins with identifying the roles of the different ion channels that reside in the lipid membrane of BR terminals. Recent evidence implicates members of the epithelial sodium channel (ENaC) superfamily including acid-sensing ion channel (ASIC) 2 (Lu *et al.*, 2009). The γENaC subunit, perhaps in combination with other ENaC subunits, has been suggested as a component of a BR mechanosensitive channel complex (Figure 3) (Drummond *et al.*, 1998). Using immunocytochemical techniques, four canonical transient receptor

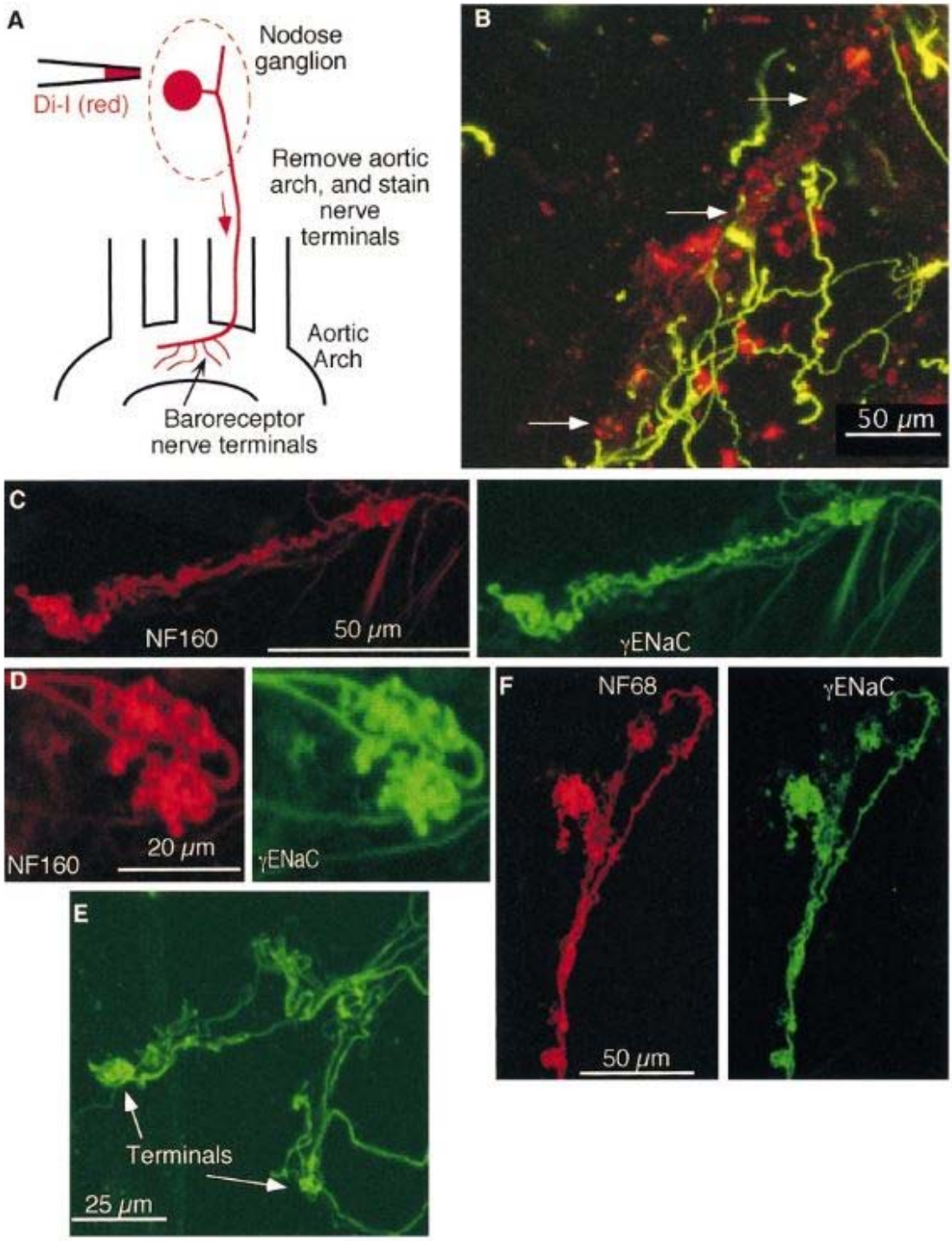
A
Nodose ganglion
Di-I (red)
Remove aortic arch, and stain nerve terminals
Aortic Arch
Baroreceptor nerve terminals
B
50 μm
C
NF160
50 μm
γENaC
D
NF160
20 μm
γENaC
E
Terminals
25 μm
F
NF68
50 μm
γENaC

Figure 3: Immunoflorescence localization of γ Epithelial sodium channels (ENac) in rat aortic arch and carotid sinus baroreceptor nerve terminals. (A) Diagram of fluorescent labelling of BR terminal in aortic arch with Di-l injection into the left nodose ganglion. Two weeks after the injection, the arch was removed and immunolabeled for γENac. (B) Colocalization (yellow) of Di-l (red) and γENaC (green) in a section of the aortic arch. (C and D) Rat aortic arch baroreceptor terminals immunolabeled with anti-NF-160, a neuronal marker, and anti-γENaC. (E) Aortic baroreceptor terminal expressing γENaC. Notice that many small fibers tend to associate with a slightly larger fiber. While the very small fibers appear to terminate as free endings, the slightly larger fibers appear to terminate in more complex structure. (F) Carotid sinus terminals expressing NF-68, aneuronal marker, and γENaC. Reprint from (Drummond *et al.*, 1998), Open Archive, Elsevier.

potential (TRPC) channels, TRPC1 and TRPC3-5, have also been identified to distribute at the peripheral axon and mechanosensory terminals, and may be involved in BR sensory transduction and/or signaling (Glazebrook *et al.*, 2005).

Importantly, a variety of voltage- and ligand-gated ion channels and membrane pumps modulate the membrane potential and excitability of BR endings and soma. The relative expression of each subtype has the potential to impact the total transmembrane current underlying the magnitude and time course of somal membrane voltage and integrated neural function (Schild & Kunze, 2012). Several specific types of voltage-gated channels (VGC) have been identified using pharmacological, electrophysiological, and immunohistochemical methodologies.

For example, critical in determining spike threshold and initiation, sodium channels such as $Na_v1.7$, which are blocked by tetrodotoxin (TTX), have been found in the soma of both A- and C-type BR neurons, whereas TTX-insensitive $Na_v1.8$ channels (along with $Na_v1.9$) are preferentially expressed in C-type BR (Schild & Kunze, 1997; Qiao *et al.*, 2009).

Potassium channels contribute to BR neuron discharge properties and have been suggested to participate in the function of BR sensory endings (Reynolds *et al.*, 1994). In the soma of aortic BR, four major K+ currents appear to be responsible for cell membrane repolarization : delayed rectifier (I_k), Ca^{2+}-activated K+ current ($I_{k,Ca}$), 4-aminopyridine-sensitive current with transient and slow decaying component ($I_{4\text{-}AP}$), and dendrotoxin-sensitive current (I_{DTX}) (Rudy, 1988; Hay & Kunze, 1994; Schild *et al.*, 2005; Li *et al.*, 2011). Interestingly,

Wladyka and Kunze showed that nodose neurons (Wladyka & Kunze, 2006), and a specific subset of these neurons innervating the aortic arch, express subunits of the KQT-like potassium channel subfamily (K_v7): KCNQ2, KCNQ3, and KCNQ5 (Wladyka *et al.*, 2008). Expression of these subunits in the BR endings was also confirmed.

Nodose afferents have been associated with a few isoforms of Ca^{2+} VGC: $Ca_v2.2$ (N-type); $Ca_v1.2$ (high threshold L-type), $Ca_v1.3$ (low-threshold L-type), $Ca_v2.1$ (P/Q-type), and $Ca_v3.2$ (T-type channel) (Schild & Kunze, 2012). However, a few studies suggest that mechano-transduction in aortic myelinated and unmyelinated baroreceptors does not require Ca^{2+} currents or that Ca^{2+} may only play a significant role in the generator potential (Kunze *et al.*, 1986; Andresen & Kunze, 1987).

C. Aortic baroreceptors and the aortic depressor nerve

In this study, I focus on the aortic BR as they are a group of the most sensitive BR and have the most robust and reliable response to changes in BP (Samodelov *et al.*, 1979; Sanders *et al.*, 1988; Kougias *et al.*, 2010). The aortic BR are pressure sensitive nerve endings that encode the magnitude and rate of change of arterial BP into a train of frequency-modulated action potential discharge initiated at the first node of Ranvier. This afferent information is continuously transmitted to the CNS through myelinated A-type and unmyelinated C-type BR axons or afferents, which have demonstrated distinct pressure encoding characteristics.

As Figure 4A shows, aortic BR terminals are located close to the apex of the aortic arch, between the left common carotid (LCC) and the left subclavian (LSC) arteries (Krauhs, 1979). The axons of the BR terminals form the ADN, a peripheral nerve bundle that in humans joins the vagus immediately after rising from the aortic arch. However, in rats, the ADN does not join the vagus until close to the nodose ganglion (Figure 4B) (Dworkin & Dworkin, 1995). Electrical stimulation of this readily identifiable, dissectible, and purely mechanosensory afferent fiber bundle initiates a rapid reduction in HR and BP solely via the aortic BRx (Sapru *et al.*, 1981; Kobayashi *et al.*, 1999).Therefore, rats are ideal animals for studying the pressure encoding properties of aortic BR.

Barosensory fibers of the ADN have long been classified as either myelinated A-type afferents with diameters in the range of 1 to 7 μm or unmyelinated C-type afferents with diameters in the range of 0.25 to 1.5 μm (Brown *et al.*, 1976; Fazan *et al.*, 1997; Fazan *et al.*, 1999). Due to widely known differences in fiber anatomy and ion channel distributions (Perge *et al.*, 2012; Schild & Kunze, 2012), myelinated A-type barosensory afferents have a threshold for electrical discharge well below that of unmyelinated C-type barosensory afferents. Low-threshold myelinated A-type fibers and neurons can sustain discharge rates well in excess of 50 Hz while higher threshold unmyelinated C-type fibers and neurons typically function at much lower rates and not often with steady nor sustained discharge beyond approximately 20 Hz (Li & Schild, 2002).

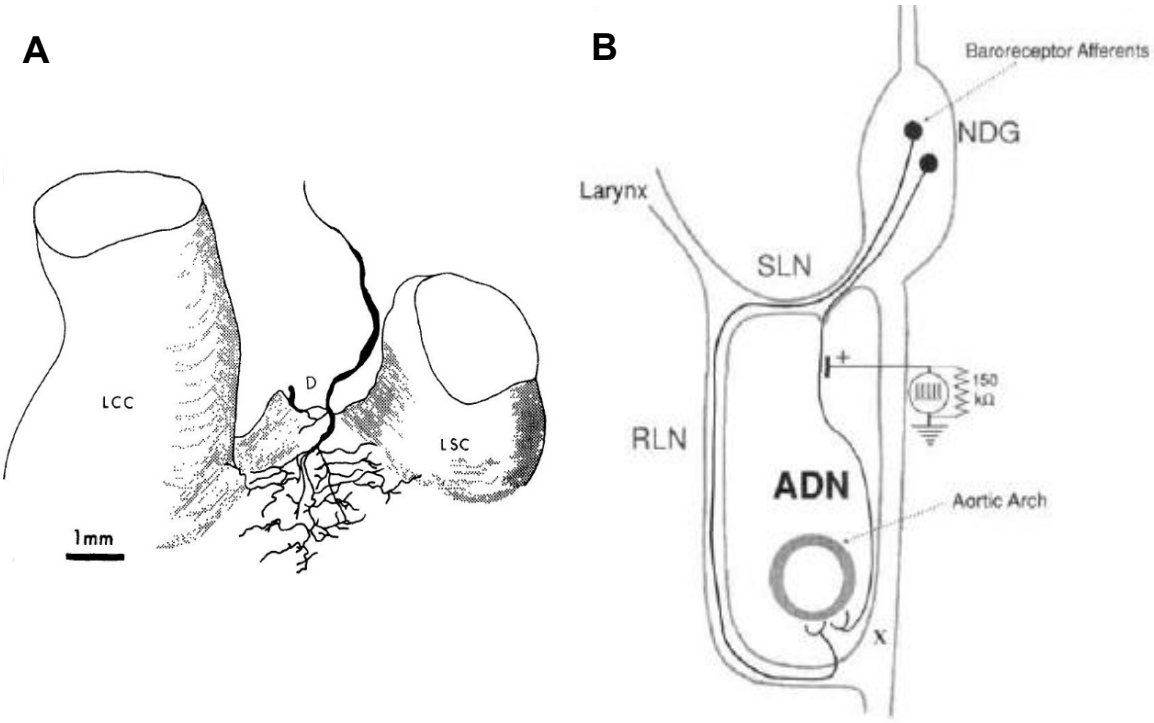

Figure 4: Aortic baroreceptor terminals and aortic depressor nerve.
(A) Drawing of aortic nerve as seen through the dissecting microscope. Part of the dorsal branch, D, is visible along with the ventral branch. LCC, left common carotid; LSC, left subclavian artery. Reprinted from (Krauhs, 1979), with kind permission from Springer. (B) The aortic depressor nerve, ADN, is most easily identifiable and located by reference to the superior laryngeal nerve, SLN. The ADN joins the SLN through a small “delta” of nerve and connective tissue. Reprint from (Dworkin & Dworkin, 1995), Copyright 1995, American Psychological Association, Inc.

III. The aortic baroreflex

A. Anatomy of the aortic baroreflex

Because the rat ADN remains as an isolated nerve until very close to the nodose ganglion and the AND nerve trunk contains mainly barosensory fibers, it serves as a biological model not only for understanding the pressure encoding functions of aortic BR, but importantly to investigate the impact of BR sensory information on reflex function. This line of BRx studies has usually been approached by quantification of BRx responses (i.e. changes in MAP) evoked by electrical activation of BR containing nerves such as rat ADN, and involves several interactions among groups of neurons both within and beyond the aortic BRx arch. Hence, it is essential that we understand the neuroanatomical basis of the aortic BRx as it will impact its function.

Briefly, the terminal endings of myelinated A-type and unmyelinated C-type aortic baroreceptors become depolarized upon the opening of stretch-activated channels. Both the arterial pressure and the rate of its change are reflected in the train of frequency-modulated action potentials generated at theses terminal and propagated by the BR fibers to the NTS region in the brain stem. In addition to innervation from the BR, the NTS receives projections from gastrointestinal, respiratory, and trigeminal sources as well as from other regions of the brain, such as the hypothalamus, parabrachialis and area postrema (Mraovitch *et al.*, 1982; Cai *et al.*, 1996; Duan *et al.*, 1999; Yu & Lindsey, 2003; Sabbatini *et al.*, 2004). All of these brain nuclei have demonstrated regulatory inputs to baroreflex activities.

From the NTS, the aortic BRx bifurcates into sympathetic and parasympathetic pathways that have opposite functional effects upon cardiovascular control. Up-regulation of sympathetic drive results in an increase in HR and vasoconstriction, eventually leading to an elevation in BP. Conversely, enhanced parasympathetic activation reduces the BP, mostly through decreases in heart rate.

Despite working together in regulating BP, there are significant differences in the time course of parasympathetic and sympathetic responses (La Rovere *et al.*, 2008). The parasympathetic or cardiovagal pathway of the aortic BRx evokes an immediate reaction, within 200 to 600 msec (Pickering & Davies, 1973). On the other hand, sympathetic activation occurs with a 2 to 3 second delay and reaches maximal effect even more slowly (Coleman, 1980). Therefore, the cardiovagal BRx pathway exerts a robust control over heart rate on a beat-to-beat basis and because it is the fastest, it is the least confounding to assess.

B. Frequency response characteristics of the aortic baroreflex

BRx control of cardiovagal activity is inextricably linked to the neural encoding properties of myelinated and unmyelinated barosensory afferents (Douglas *et al.*, 1956; Kardon *et al.*, 1975; Seagard *et al.*, 1993; Fan *et al.*, 1996). Classical bimodal classifications of the primary sensory neurons into myelinated A-type and unmyelinated C-type have been linked to differential expression of ion channels, receptors, and neurotransmitters (Jin *et al.*, 2004; Schild & Kunze, 2012). Similar bimodal presentations are evident in the frequency-dependent

reflex integration of barosensory fibers (Fan & Andresen, 1998; Fan *et al.*, 1999). For example, a significant depressor response consisting of bradycardia and hypotension can be elicited either through selective activation of low-threshold myelinated A-type BR fibers (with stimulus intensities up to 3 V) at rates in excess of 10 – 20 Hz or selective activation of high-threshold unmyelinated C-type afferents (with stimulus intensities greater than 15 V) at stimulation rates as low as 1 – 2 Hz (Figure 5) (Fan *et al.*, 1999). Furthermore, whole animal reflex studies suggest that myelinated BR are more sensitive than the myelinated ones and function more toward buffering acute changes in BP, whereas the less sensitive unmyelinated BR may function more to control MAP (Seagard *et al.*, 1993; Seagard *et al.*, 1995). Collectively, these studies suggests that the integration of A-type and C-type BR inputs is not equivalent and that processing of BR sensory input may differ in a pathway-specific manner. These disparities in sensory function are further complicated by recent cellular electrophysiological findings from our laboratory that in female rats an additional and distinctly functional population of myelinated aortic BR neurons exists, whereas in male rats they are rarely found (Li *et al.*, 2008). This raises questions regarding their functional contributions and whether the observed gender related differences in the cardiovagal BRx may have an afferent origin.

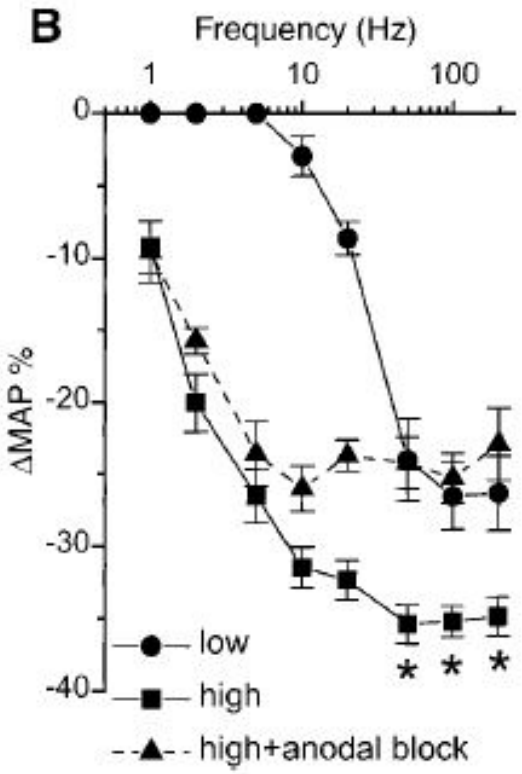

Figure 5: Reflex mean arterial pressure (MAP) responses to electrical activation of myelinated (A-type), unmyelinated (C-type), or both baroreceptors (BR) afferent fibers in aortic depressor nerve (ADN) of rat. Average % changes in MAP evoked by low (3 V, selective for myelinated BR activation) and high (18 V, activates both types of BR) stimulus intensities. High stimulus intensity plus anodal block activates mostly unmyelinated BR. A-type selective stimuli to the ADN evoked reflex responses when stimulus frequency exceeded 10 Hz. Frequencies as low as 1 Hz elicited substantial decreases in MAP when in combination with high stimulus intensities. C-type selective baroreflex responses demonstrates that unmyelinated BR input is necessary for low frequency (< 10 Hz) baroreflex responses. Reprint from (Fan *et al.*, 1999), Copyright 1999, The American Physiological Society.

IV. Sexual dimorphism in aortic baroreceptor afferents

Our lab has published cellular electrophysiological studies of BR afferent function in the rat that have led us to propose a novel alternative hypothesis concerning the origins of sexual dimorphism in the cardiovagal BRx (Li *et al.*, 2008). Namely, that in females there exists two functionally distinct and comparably sized populations (~50% each) of low-threshold myelinated BR afferents, whereas in males there exists a single homogeneous population (~98%) of low-threshold BR. This is significant because BRx control of cardiovagal activity is inextricably linked to the neural encoding properties of myelinated and unmyelinated barosensory afferents (Douglas *et al.*, 1956; Kardon *et al.*, 1975; Seagard *et al.*, 1993; Fan *et al.*, 1996). Differences in the distribution of low-threshold myelinated barosensory afferents between the sexes may account for, at least in part, the observed sex-related differences in cardiovagal reflex function (Dart *et al.*, 2002; Fisher *et al.*, 2012). This is because each population of barosensory neurons constitutes an afferent pathway that provides input to the CNS, where afferent summation (spatial and temporal) influences the magnitude of the effector response, in this case, a depressor response consisting of bradycardia and hypotension. However, definitive experimental evidence is lacking.

A. Cellular electrophysiological evidence for sexual dimorphism in the function of myelinated aortic barosensory neurons

To date, the most definite physiological explanation of afferent function related to the aortic BRx comes about through classifications of BR as having either

myelinated or unmyelinated axons. These two types of BR fibers have markedly dissimilar pressure-discharge characteristics and frequency-dependent reflex responses (Fan & Andresen, 1998; Fan *et al.*, 1999). A-type BR are often described as low-threshold pressoreceptors that are generally active at normal arterial pressures (Katona *et al.*, 1968), while unmyelinated BR are often described as high-threshold pressoreceptors that require more elevated arterial pressures for activation (Thoren & Jones, 1977). Interestingly, the threshold and repetitive discharge characteristics for a second population of myelinated vagal afferents with cell bodies in the nodose ganglion, herein referred to as Ah-type afferents, fall well within the range bounded by what are essentially two, non-overlapping distributions of electrophysiological properties associated with myelinated A-type and unmyelinated C-type afferents (Li & Schild, 2007; Li *et al.*, 2008; Qiao *et al.*, 2009). Somatic electrophysiological examination of fluorescently identified aortic BR neurons, a subpopulation of the vagal afferent neurons also with cell bodies in the nodose ganglion, from age-matched male and female Sprague-Dawley rats revealed that females exhibit two functionally distinct populations of A- and Ah-type barosensory neurons (Figure 6, left column) (Li *et al.*, 2008). Barosensory neurons classified as A-type exhibit low-threshold (~-44 mV), brief duration (< 1 msec) somatic action potentials. In contrast, myelinated Ah-type aortic afferent neurons exhibit somatic action potentials with significantly ($P < 0.01$) more depolarized thresholds (~-36 mV) and broader duration (~2 msec) than A-type neurons. All A-type barosensory neurons discharge repetitively at ~48 Hz in response to 300 pA depolarizing

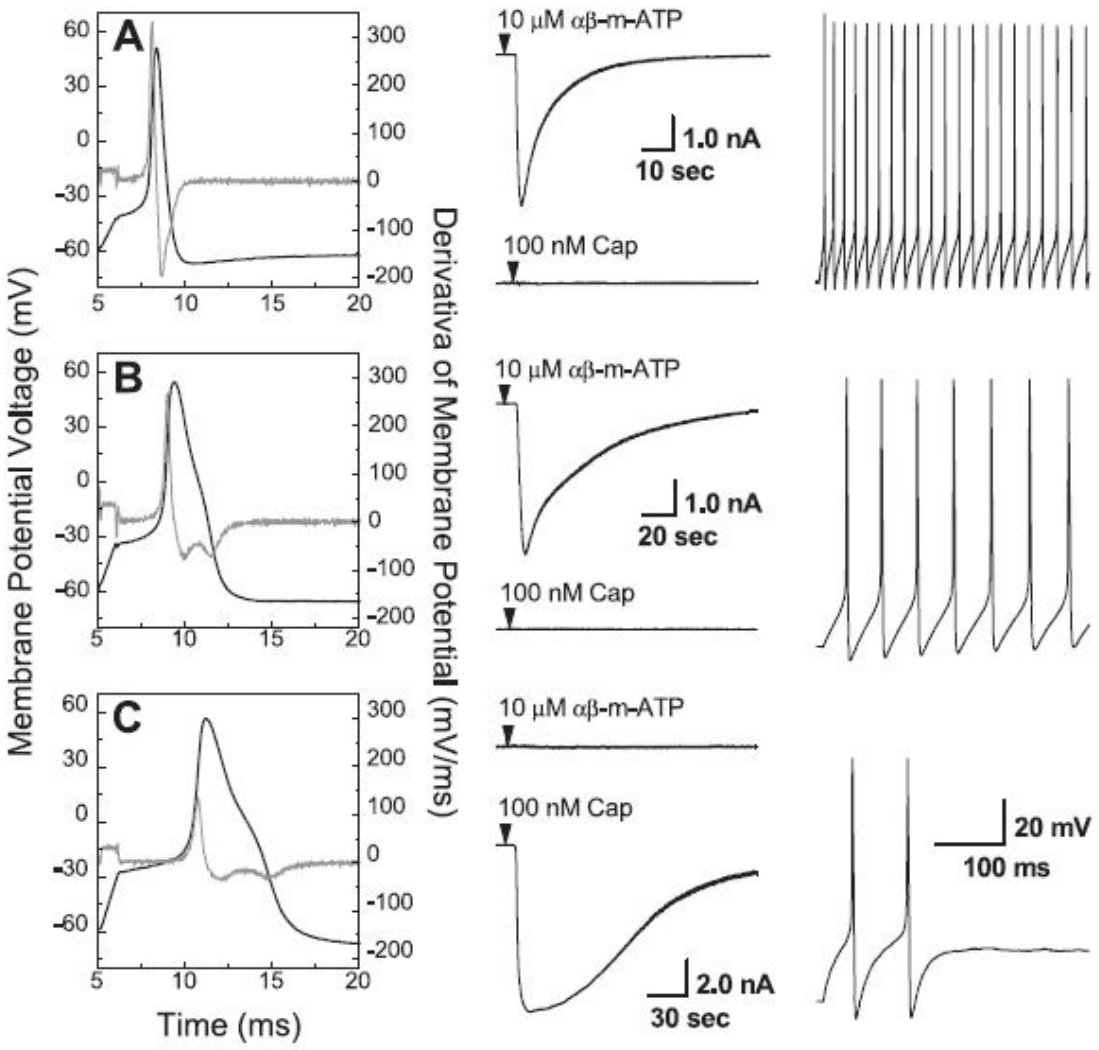

Figure 6: Electrophysiological and Pharmacological classification of aortic baroreceptor neurons as either myelinated A- and Ah-type, or unmyelinated C-type. Left column, representative somatic action potentials from fluorescently identified myelinated A-type (A), myelinated Ah-type (B), and unmyelinated C-type aortic barosensory neurons. Center column, pharmacological validation of afferent fiber type via chemosensitivity to P2X purinergic receptor agonist (αβ-mATP) and vanilloid receptor-1 agonist (capsaicin, Cap). Right column, Comparison of cell excitability in response to a constant step current input of 300 pA for myelinated A- and Ah-type neuron, and 600 pA for unmyelinated C-type neuron. Note the differences in action potential discharge frequency. Reprint from (Li *et al.*, 2008), Copyright 2008, The American Physiological Society.

currents whereas in Ah-type neurons, the same current input evoked one-third that repetitive discharge rate (Figure 6, right column). In addition, no differential sensitivity to pharmacological markers for myelinated neurons (i.e. αβ-mATP and Capsaicin) (Jin *et al.*, 2004) was found (Figure 6, center column).

B. Neuroanatomical evidence for sexual dimorphism in the population distribution of myelinated aortic barosensory neurons and afferents

Through functional classification of fluorescently identified aortic BR neurons, Li *et al.* (2008) demonstrated that myelinated Ah-type afferents are nearly five times more prevalent in females compared with male Sprague-Dawley rats (Figure 7) (Li *et al.*, 2008). Myelinated Ah-type afferents comprised 11% of the total population of aortic barosensory neurons from females but only 2.3% from males, whereas the percentages of myelinated A-type aortic barosensory neurons were comparable for male and female rats (15.9% *vs.* 15.6%, respectively). This means that there are nearly 1.5 times more myelinated afferents across the total population of aortic barosensory neurons from females compared with males (26.6% *vs.* 18.2%, respectively, $P < 0.01$). These results were consistent with correlative electron microscopic examinations of ADN cross sections that showed that across the total population of aortic BR afferents, female Sprague-Dawley rats exhibit a significantly greater percentage of myelinated BR fibers than age-matched males (24.8% *vs.* 18.7%, respectively, $P < 0.01$) (Table 2) (Li *et al.*, 2008).

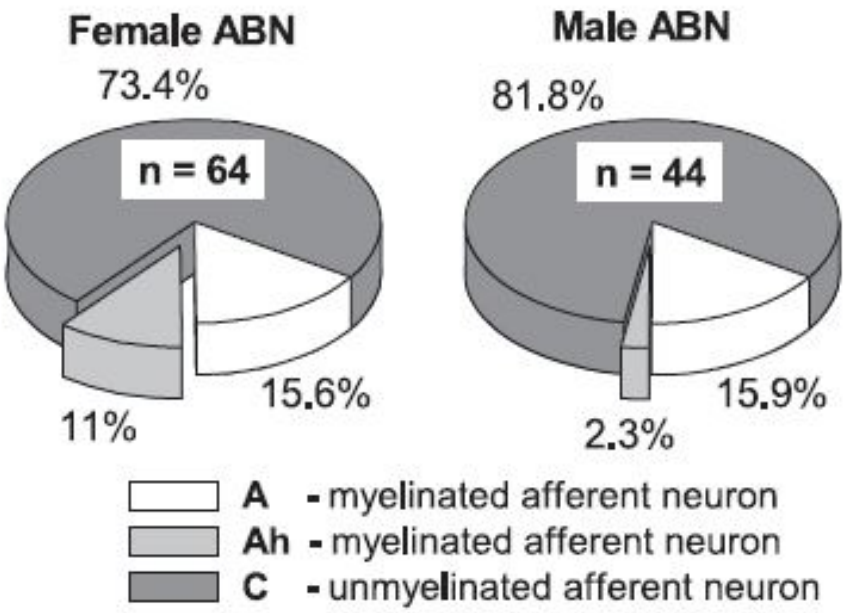

Figure 7: Distribution summary for aortic barosensory neurons functionally classified as either myelinated A- or Ah-type or unmyelinated C-type. Female Sprague-Dawley rats consistently showed a much greater propensity for myelinated Ah-type afferent neurons than males (Note light grey slices). Across the total population of aortic barosensory neurons, in females, roughly 27% were myelinated afferents, while in males these comprised about one-fifth of the total myelinated population. Reprint from (Li *et al.*, 2008), Copyright 2008, The American Physiological Society.

Table 2: Gender differences in morphology of aortic depressor nerve. Reprint from (Li *et al.*, 2008), Copyright 2008, The American Physiological Society.

	Female	Male
	Nerve Cross Section	
Area, μm^2	838±358*	1678±364
Diameter, μm	32.1±7*	46.0±5
	Myelinated Fibers	
Average	72.8±11*	103.5±20
Total	437	621
Myelin area, μm^2	2.76±0.3*	3.54±0.6
	Unmyelinated Fibers	
Average	221±36*	451±60
Total	1324	2703
	Relative distributions, %	
Myelinated fibers	24.8	18.7
Unmyelinated fibers	75.2	81.3

Data are presented as means ± SD of age-matched adult female (287 ± 11 g, $n = 6$) and male (330 ± 15 g, $n = 6$) Sprague-Dawley rats. *$P < 0.01$ vs. male.

C. Implications for aortic baroreflex function

Due to widely known differences in fiber anatomy and ion channel distributions (Perge *et al.*, 2012; Schild & Kunze, 2012), myelinated A-type barosensory afferents have a threshold for electrical discharge well below that of unmyelinated C-type barosensory afferents. Similar differences enable low-threshold myelinated A-type fibers and neurons to sustain discharge rates well in excess of 50 Hz while higher threshold unmyelinated C-type fibers and neurons typically function at much lower rates and not often with steady nor sustained discharge beyond approximately 20 Hz (Li & Schild, 2002). These bimodal presentations are also evident in the frequency-dependent reflex integration of these barosensory fibers (Fan & Andresen, 1998; Fan *et al.*, 1999). For example, a significant depressor response can be elicited either through selective activation of myelinated A-type BR fibers at rates in excess of 10 to 20 Hz or selective activation of unmyelinated C-type afferents at stimulation rates less than one-tenth that range. Interestingly, the threshold and repetitive discharge characteristics for Ah-type myelinated afferents span the previously described extremes associated with myelinated A-type and unmyelinated C-type afferents (Li and Schild, 2007; Li *et al.*, 2008; Qiao *et al.*, 2009). Therefore, a central objective of this study is to determine if the frequency-dependent reflex integration of low-threshold myelianted Ah-type afferents observed in female rat, differs from that of the A-type barosensory afferents.

D. Summary, hypothesis and specific aims

The arterial BRx is a key component of cardiovascular regulation. Changes in its function reflect alterations in the autonomic control of the cardiovascular system. The BRx is initiated by BR afferents residing in the aortic arch and carotid sinuses. Two major classes of BR exist: myelinated or A-type and unmyelinated or C-type. A-type BR are often described as low-threshold pressure receptors with higher mean discharge rates, whereas C-type BR typically demonstrate spontaneous subthreshold discharge. Based on their axonal conduction velocity (CV), myelinated A-type afferents propagate action potentials with higher speeds compared to unmyelinated C-type afferents. Similar bimodal classifications are evident in the frequency-dependent reflex integration of these barosensory fibers since significant depressor responses can be elicited either through selective activation of myelinated A-type BR fibers at stimulation rates greater than 10 Hz or by selective activation of unmyelinated C-type afferents at rates as low as 1 Hz. Due to these classifications, to date, the BRx has been thought to have a binary afferent input.

Regardless of type, BR function to provide feedback to the CNS about changes in systemic BP. For example, a rise in BP activates the BR and leads to the initiation of two pathways: sympathoinhibitory and cardioinhibitory. The cardioinhibitory pathway or cardiovagal BRx evokes an immediate reaction (between 200 and 600 msec) that is one of the most reliable and predictable effects of BR activation. Conversely, the sympathetic activation evokes a more sluggish response with a 2 to 3 second delay. Consequently, the cardiovagal

BRx pathway exerts a robust control over HR on a beat-to-beat basis and because it is the fastest, it is the least confounding to assess.

Interestingly, there are critically important gender differences in basal autonomic cardiovascular control that are inextricably linked to BRx function such as baseline MAP and HR. Consistent BRx studies suggest that women have higher tonic parasympathetic cardiac activation compared to men. Sex hormones may partly account for such sex bias, however, a comprehensive explanation remains elusive. Recently, our lab reported on an additional population of myelinated aortic BR afferents, termed Ah-type, that exhibits functional dynamics and ionic currents that are a mix of those observed in barosensory afferents functionally identified as myelinated A-type or unmyelinated C-type. Interestingly, Ah-type afferents constitute nearly 50% of the total population of myelinated aortic BR in female but less than 2% in male rat (Li *et al.*, 2008). Furthermore, ovariectomy, a commonly used model of ovarian sex hormone deprivation, greatly reduces the somatic *in vitro* excitability of the Ah-type vagal afferents, whereas A- and C-type vagal afferent excitability remains the same as in intact female rats (Qiao *et al.*, 2009).

These findings lead to questions concerning the physiological significance of the sex-specific myelinated Ah-type aortic BR afferent, its role in cardiac control, and whether their function may be affected by circulating sex-hormones. Therefore, the overarching hypothesis of the current work is that an afferent basis for sexual dimorphism in BRx function exist due to the functional contributions of Ah-type aortic BR afferents to the integrated afferent BRx drive in

females. Specifically, we propose to investigate the potential functional impact Ah-type afferents have upon the aortic BRx and whether their function is affected by the loss of ovarian sex hormones following ovariectomy. Our hypothesis was tested by means of the following specific aims:

Specific aim 1: To quantify differences in the parasympathetic mediated reduction of MAP (i.e. acute BRx depressor response) between adult male and female rats due to differential activation of myelinated aortic BR afferents

Specific aim 2: To determine differences in the parasympathetic mediated reduction of MAP between intact and ovariectomized female rats associated with the loss of sex hormones following ovariectomy.

This study will provide with neurophysiological explanation(s) for the differences in cardiac autonomic function between the sexes. Furthermore, this study has the potential to definitely clarify the role of the Ah-type barosensory neurons in the integrated afferent drive to the BRx in females and whether this sensory pathway may be affected by the loss of sex hormones, a common hallmark of aging. This study has the potential to lead to novel advances in the management of cardiovascular health and disease in the female population.

CHAPTER 2: MATERIALS AND METHODS

All animal use protocols were pre-approved by the Institutional Animal Care and Use Committee (IACUC) for the Purdue School of Science, Indiana University – Purdue University Indianapolis (IUPUI).

I. Introduction: morphometric analysis of myelinated aortic baroreceptor fibers

With the help from our collaborators in Case Western Reserve University (CWRU), Dr. Diana L. Kunze and Patricia A. Glazebrook, the Schild lab performed a morphological study of the myelinated fibers contained in the ADN of adult male (n = 7) and female Sprague-Dawley rats (n =7). The experimental protocols used for this study are described elsewhere (Santa Cruz Chavez *et al.*, 2014). Briefly, the left ADN of male and female rats were prepared for electron microscopic examination. Following microsurgical isolation, the ADN nerve tissue sample was fixated and embedded in epon-araldite. Next, the samples were sectioned to 90 nm, mounted, and imaged using a transmission electron microscope equipped with a digital camera. Digital images of each EM section of the ADN were then montaged for reconstruction of the whole nerve. These high resolution digital cross sections of the ADN were delimited to an eight-bit grayscale using ImageJ (Schneider *et al.*, 2012). The myelin area and the axon area for each myelinated nerve fiber within the ADN trunk was quantified using a pixel count (μm^2/pixel) from the original EM image. A common threshold adjustment was made to delineate the edges of the myelin sheath from the

surrounding tissues while also demarcating the circumference of the axon (Figure 8) (Santa Cruz Chavez *et al.*, 2012). A pixel count from each of the myelin and axon areas was then used to calculate an equivalent circular diameter for each myelinated fiber.

The purpose of this neuroanatomical study was two-fold. (1) To establish sex-related differences in the morphometry of the myelinated aortic BR fibers. It has long been established that factors such as fiber diameter and intermodal length affect action potential propagation in nerve (Waxman, 1995). Differences between the sexes in the speeds at which their aortic nerve fibers conduct may result in a sex bias towards afferent signal integration at the BRx brain processing centers, thus, promoting sexually dimorphic BRx responses. (2) To identify distinct myelinated population of A-type and Ah-type afferent fibers in male and female ADN nerve trunks. Previous work from the Schild Lab had shown in an *in vitro* rat nodose ganglion preparation that the presumably larger A-type vagal afferents conduct with faster speeds than the presumably lightly myelinated Ah-type vagal afferents (Li & Schild, 2007). Furthermore, the results of this study, which are described in the Results section of this dissertation, were used to calculate potential conduction velocity (CV) ranges of the aortic myelinated fibers based on long established linear and non-linear relationships between fiber diameter and CV (Coppin & Jack, 1972; Boyd & Kalu, 1979). These estimates of CV were correlated with our experimental estimates from ADN nerve conduction studies described below.

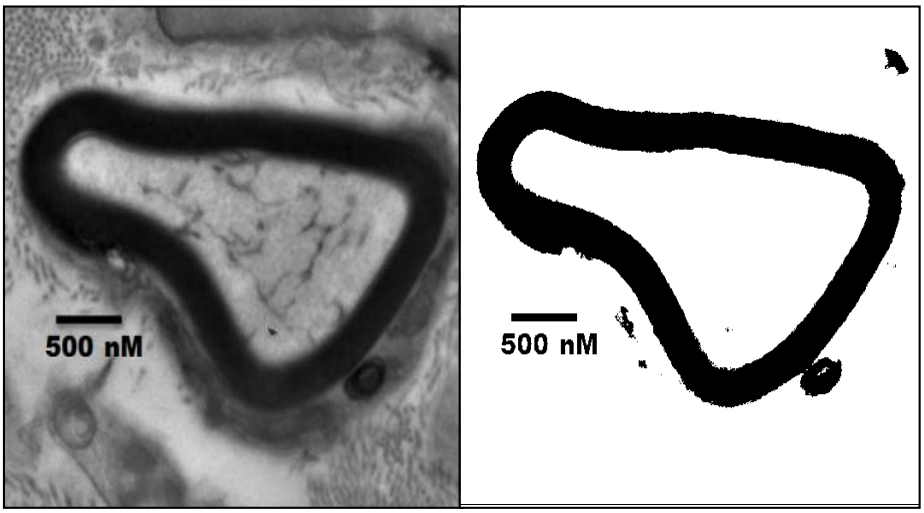

Figure 8: ADN myelinated fiber morphological analysis. Images of myelinated fiber (representative, left) were digitally processed (right) to contrast the myelin against the surrounding tissue. Black and white pixel counts were used to calculate the geometrical area of myelin and encapsulated axon. Reprinted from (Santa Cruz Chavez *et al.*, 2012).

The work from Dr. Schild's lab performed by the author consisted of two distinct experimental protocols that were designed to quantify the electrophysiological and reflexogenic differences associated with the left ADN from adult male (396 ± 45 g, n = 26), female (269 ± 27 g, n = 32), and ovariectomized (OVX, 307 ± 32 g, n = 25) Sprague-Dawley rats (Harlan, Indianapolis, IN), 12 to 20 weeks of age. Ovariectomy surgeries were performed at 9 weeks of age by the supplier. Rats were housed at Harlan for 7 days post OVX prior to shipment to IUPUI, where they were housed. Interventions started at day 28 (4 weeks) post OVX.

In addition, a separate cohort of OVX rats (225 ± 28 g, n = 20, 9 to 13 weeks) were utilized to investigate longitudinal changes in BRx response soon after ovariectomy, starting at day 4 up to week three after OVX. Ovariectomy surgeries were performed as described above, except here the rats were shipped to IUPUI 3 days post OVX and interventions started the day after.

For all intact female and OVX rats, no attempt was made to assess or control for the phase of estrous cycle.

II. Nerve conduction study of the aortic depressor nerve

A. <u>Animal preparation</u>

Nine male, fifteen female, and eight OVX unrestrained rats were placed in an airtight induction chamber for inhalation of the volatile anesthetic Isoflurane (Vedco Inc. St. Joseph, MO). Adequate depth of anesthesia was confirmed by lack of corneal reflex and lack of response to tail and paw pinch. Anesthesia was

maintained with 10 mL ketamine + 1.4 mL xylazine (0.1 ml/100 g, I.P. injection). The surgical area was shaved and an approximately 2 cm incision was made along the ventral side of the neck. Under stereo microscopy (×40 – Leica Microsystems Inc., Burr Ridge, IL), a blunt dissection of the superficial and underlying musculature exposed the left carotid artery and surrounding nerve trunks. The left ADN was identified.

B. Microsurgical isolation of rat aortic depressor nerve

The ADN was most easily identified rostrally as it joined the superior laryngeal nerve (SLN) through a small “delta” of nerve and connective tissue. This nerve junction was usually covered by a small pad of yellow fat, which was carefully removed. Distally, the ADN was also identified as it approached the wall of the aortic arch. We observed that the ADN would sometimes divide into two or more smaller nerves. The ADN usually included a small blood vessel, which lent some mechanical support and long-term viability, thus it was left intact whenever possible. The rostral and distal ends of the ADN were microsurgically separated from the vagus and sympathetic nerves. The rest of the ADN was left intact to prevent pressure or overstretching that could injure the delicate nerve fibers within the epineurium and affect action potential conduction.

C. Nerve stimulation and recording of compound action potentials

Simultaneous bipolar electrical stimulation and bipolar recording of compound action potentials (CAP) were utilized to construct ADN nerve conduction profiles

of adult male, female, and OVX rats. Microsurgical dissection of the ADN was performed as described above. In order to reliably discriminate the CAP from stimulus artifact, additional efforts were made to maximize the linear distance between the bipolar stimulating and recording electrodes which had a 1 mm hook diameter and an 800 μm spacing between the anode and cathode (FHC, Bowdoin, ME). The stimulating electrode was positioned close to the point of entry of the ADN into the chest cavity where it approached the wall of the aortic arch but well before any significant branching of the nerve trunk occurred. The recording electrode was rostral to the stimulating electrode, 5 to 8 mm from the vagal ganglion. The ADN was placed across both anode and cathode pairs and the separation distance, typically greater than 15 mm, was measured using a digital caliper (Marathon, Richmond Hill, Ontario, Canada). The nerve was then transected at both ends and covered with a mixture of petroleum jelly and mineral oil. The stimulus artifact was markedly reduced by an orthogonal arrangement of the anode and cathode pairs for each bipolar electrode. Electrical stimulation of the ADN was provided by a constant voltage stimulus isolation unit (Iso-flex, A.M.P.I., Jerusalem, Israel). Regulated monophasic voltage pulses, 200 μs in duration and ranging in magnitude from 0.1 to 20 V were delivered to the ADN at a rate of once per second (1 Hz). This event simultaneously triggered a digital data acquisition system (iWorx, Dover, NH) to record a 200 ms epoch of amplified (×50 to ×100k) and band passed filtered (1 to 5 kHz) nerve activity. A running average of 25 such recordings greatly improved the signal-to-noise ratio and formed a data set for each unique stimulus magnitude used in evoking a

graded CAP signal from the population of myelinated and unmyelinated aortic depressor nerve fibers.

D. Quantification of nerve conduction velocities and data analysis

The length of nerve separating the stimulation and recording electrodes divided by the time interval bounded by the stimulus artifact and a distinct CAP volley has long been used to reliably quantify nerve CV (m/sec) even in small diameter, Group III (< 5 μm) myelinated afferent fibers (Boyd & Kalu, 1979). Based on previous *in vitro* work (Li & Schild, 2007), CAP traveling at a rate in excess of 10 m/sec were presumed to arise from myelinated A-type afferents (Group III, Aαβ fibers) while those traveling at a rate less than 10 m/sec were presumed to arise from myelinated, Ah-type afferents (Group III, Aδ fibers). Axons with CV of less than 2 m/sec were functionally classified as unmyelinated afferents. In this manner, the average signal power arising from each distinct CAP (energy per unit time) can be quantified as a root-mean-square (RMS) value. Significant differences in the relative numbers of myelinated A- and Ah-type afferent fibers in the ADN of male and female rats can be expected to also present with significant differences in the RMS magnitude of the distinct CAP corresponding to each distinct fiber subtype. All measures are presented as mean ± SD. Statistical comparisons between groups was performed using a Student's t-test with differences noted as significant at $p < 0.05$.

III. Baroreflex protocols

A. Animal preparation

Cohorts of age-matched male (n = 17), female (n = 16), and OVX rats (n = 17), and an additional cohort of OVX rats (n = 20) were anesthetized through I.P. injection (0.8 ml/100 g) of urethane (800 mg/kg; Acros Organics, NJ) and α-chloralose (80 mg/kg; Fisher Scientific, Pittsburgh, PA). Adequate depth of anesthesia was confirmed by lack of corneal reflex and lack of response to tail and paw pinch. Anesthesia was maintained with supplemental I.P. injection of urethane and α-chloralose (10% of initial dosage). A heating pad was used to keep animals warm during the surgical procedure. The ventral neck area was shaved and an approximately 2 cm midline incision exposed the trachea for cannulation, which facilitated spontaneous respiration. Next, the femoral artery was exposed and catheterized using a short length (~10 mm) PE-10 tubing filled with heparinized saline (30 U/mL). The other end of the cannula was connected to a four-way stopcock with (1) a heparinized saline filled syringe used for flushing the cannula and (2) a pressure transducer. The physiological pressure transducer (Radnoti LLC, Monrovia, CA) provided linear transduction of BP (mmHg) into a voltage signal which was low pass filtered at 500 Hz and digitized at a rate of 1KHz using a Labview based data acquisition system (National Instruments, Austin, TX). Lastly, under stereo microscopy (×40 – Leica Microsystems Inc., Burr Ridge, IL), a blunt dissection of the superficial and underlying neck musculature exposed the left carotid artery and surrounding nerve trunks. The left ADN was identified.

B. Microsurgical isolation of rat aortic depressor nerve

The rat ADN was identified and isolated as previously described for the electrophysiological studies, except here only the distal end of the depressor nerve was microsurgically separated from the vagus and sympathetic nerves.

C. Baroreflex responses and data analysis

Electrical activation of aortic barosensory fibers contained in the ADN was carried out as previously described for the electrophysiological studies, but here without the rostral recording electrode. BRx protocols proceeded once the mean arterial pressure (MAP, mmHg) stabilized to within 10% of the target baseline of 100 mmHg, which was operationally defined as “resting” MAP. This was generally achieved within 15 to 30 min following final preparation of the left ADN. The depressor response was elicited using bipolar, constant voltage monophasic pulses from 1 to 5 V (0.5 V increments) and 6, 8, 10, 12, 15, 18, and 20 V at stimulation rates of 1, 2, 5, 10, 20, 30, 50, 75, and 100 Hz for each voltage magnitude. A single, unique pair of stimulus magnitude and rate was randomly selected without replacement from this combination set and applied for a duration of 30 sec (see example in Figure 9) (Santa Cruz Chavez *et al.*, 2012). Subsequent trials were not initiated until MAP recovered to resting values, typically within 1 to 2 min but never within less than 5 min. The numerical average of a 1 sec sample of the lowest arterial pressure associated with the depressor response was divided by the average of a 10 sec sample of arterial pressure measured just prior to nerve stimulation. This quotient was multiplied by

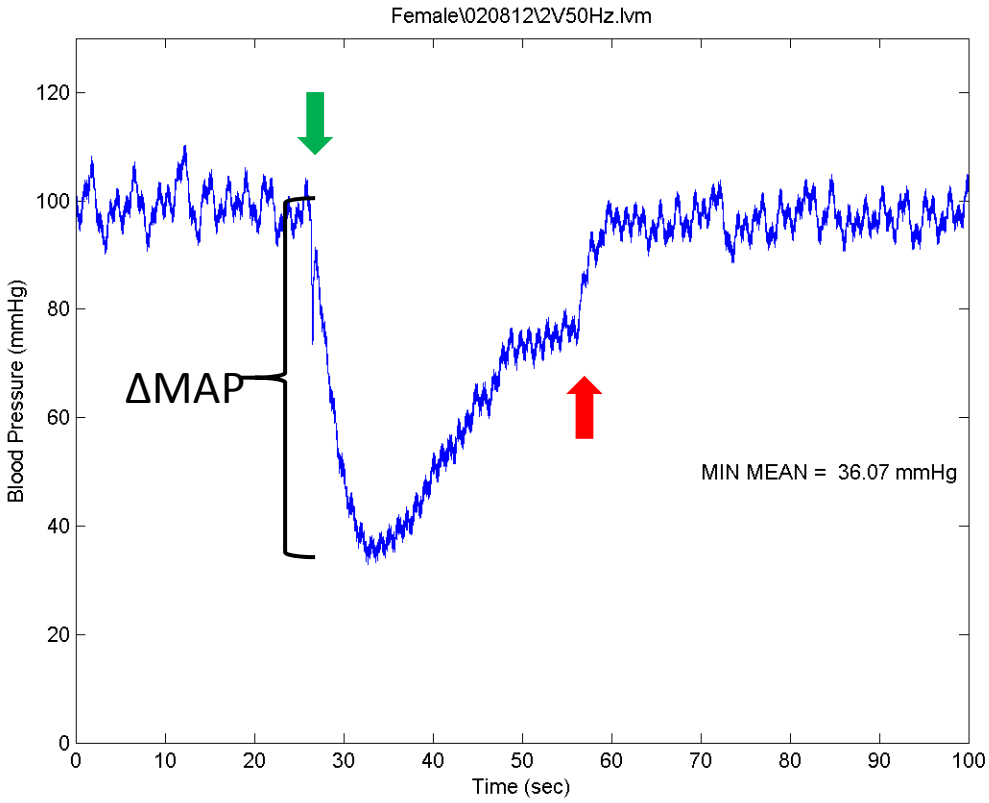

Figure 9: Changes in mean arterial pressure (MAP) in response to electrical activation of aortic barosensory fibers in rat aortic depressor nerve (ADN). A rapid reduction in MAP was observed upon electrical stimulation (green arrow) of the ADN. The stimulus was terminated (red arrow) after 30 sec and the maximum change in MAP (ΔMAP) was measured. This quantity was expressed as a percentage change with respect to baseline MAP (i.e. before stimulation). Reprinted from (Santa Cruz Chavez *et al.*, 2012).

100 to provide a peak change in MAP (ΔMAP, Figure 9) relative to the resting arterial pressure. Generally, only a subset of randomly selected intensity and frequency pairs could be completed within the 120 min the animal most reliably maintained a stable resting MAP. Rarely would an experimental protocol extend beyond 180 min and in such cases a supplemental I.P. injection of urethane and α-chloralose (10% of initial dosage) was often required to maintain anesthetization at resting MAP. All measures are presented as mean ± SD. Statistical comparisons between groups was performed using a Student's t-test with differences noted as significant at $p < 0.05$

CHAPTER 3: RESULTS

Distinct and complementary experimental protocols were used to quantify the electrophysiological and reflexogenic differences associated with the left ADN from male, female, and OVX rats. Concomitant with these experiments, a joint collaborative research study between scientists in CWRU and the Schild lab provided the morphometric data from ADN myelinated barosensory fibers in male and female rats.

A main objective of this dissertation was to investigate questions concerning the potential sexual dimorphism in the electrophysiological properties of myelinated aortic BR afferents. As the electrical threshold for neural discharge in myelinated axons is typically well below that for unmyelinated fibers, this population of larger diameter BR fibers of the ADN can be selectively recruited using incremental changes in the bipolar stimulus pulse magnitude (V) and the rate (Hz). These data were used, in turn, to establish nerve stimulation protocols to quantify the functional impact selective activation of low-threshold myelinated A- and Ah-type barosensory afferents may have upon the BRx.

Electrophysiological and reflexogenic studies performed by the author utilized male (n = 26), naive female (n = 32), and OVX (n = 45) Sprague-Dawley rats of approximately the same age, 15, 16 and 17 weeks, respectively. A longitudinal assessment of changes in BRx response post ovariectomy utilized OVX Sprague-Dawley rats of approximately 11 weeks of age.

I. Aim 1: To quantify differences in the parasympathetic mediated reductions of mean arterial pressure between male and female rats due to differential activation of myelinated aortic baroreceptor afferents

A. Introduction: Neuroanatomical evidence for sexual dimorphism in myelinated aortic baroreceptor fibers

Cross sections of the left ADN from a cohort of male (n = 7, 16 weeks) and female (n = 7, 16 weeks) rats revealed a significant trend toward a larger diameter nerve trunk ($P < 0.01$) in males as compared with females (42.4 ± 6 μm vs. 32.7 ± 5 μm). Female rats, however, had a greater number of myelinated fibers per nerve trunk on average as compared to male rats (61 ± 18 vs. 49 ± 25). From a large sample of male (n = 344) and female (n = 425) myelinated BR fibers, myelin and axon areas were measured and used to calculate equivalent estimates of fiber diameter and G-ratio (axon diameter/fiber diameter) as shown in Table 3. The calculated estimates of axon area, fiber diameter, and G-ratio were all suggestive of differences in fiber geometry between the sexes but only the measures of myelin area proved to be sexually dimorphic ($P < 0.03$). The average myelin area per fiber and the average fiber area (axon area + myelin area) in female rats were both significantly smaller ($P < 0.05$) than the same average measures from male rats. The frequency histograms for these two measures were mostly unimodal (Figure 10) with no compelling differences in the population profiles. One notable exception was the variance (σ^2) in the measures of myelin area, which was 8-fold broader in males as compared with females (note inset, myelin area distribution: $\sigma^2 = 33.63$ for males and $\sigma^2 = 4.41$ for

Table 3: Morphometric parameters of the myelinated fibers from aortic depressor nerve cross sections for male and female Sprague-Dawley rats.

	Male (n = 7)	Female (n = 7)	t-test (P-value)
Age (weeks)	16	16	-
Total fiber count	344	425	-
Ave. fiber per nerve trunk	69.71 ± 11.5	63.42 ± 7.5	-
Myelin area	3.68 ± 5.8	3.02 ± 2.1	0.029
Axon area	2.04 ± 3.5	1.73 ± 1.5	0.107
Fiber area	5.71 ± 9.25	4.75 ± 3.39	0.05
Equivalent diameter	2.45 ± 1.1	2.33 ±0.8	0.074
Myelin thickness	1.01 ± 0.5	0.94 ± 0.4	0.020
G-ratio	0.59 ± 0.1	0.60 ± 0.1	0.200

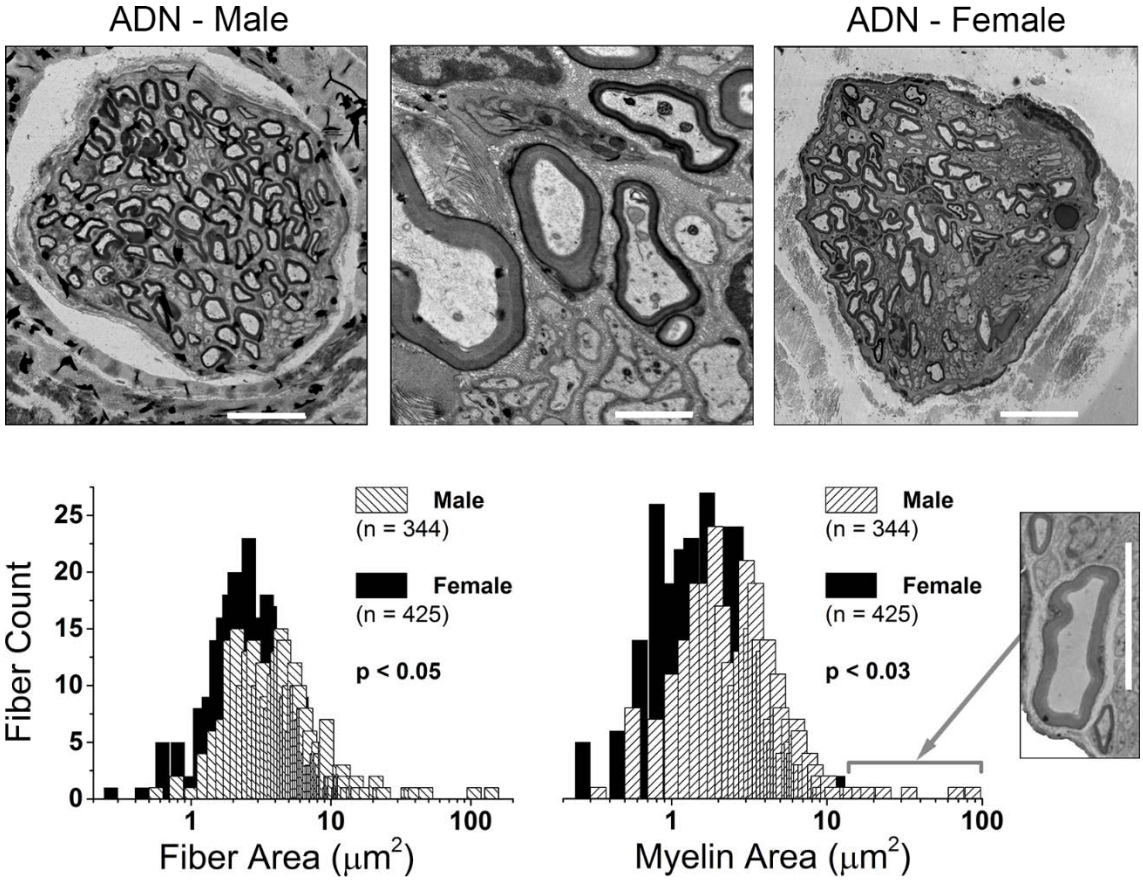

Figure 10: Sexual dimorphism in the myelination of rat aortic baroreceptor fibers. Upper panels: Electron microscopy images of the aortic depressor nerve (ADN) from an adult male and female rat. Scale bars represent 10 μm and 1.5 μm for low and high magnification, respectively. Lower panels: Frequency distribution of fiber (axon + myelin) and myelin cross sectional area (μm^2). From the sampled population of myelinated fibers in the ADN from male (n = 7) and female (n = 7) rats, only these two neuroanatomical measures were significantly different, with both trending toward smaller magnitudes in females. Bin centers increment in steps of 0.2 μm. INSET: Most male nerve trunks contained at least one large myelinated baroreceptor fiber with axon and myelin area that were 4 – 5 times greater than the population average. These large diameter fibers were not observed in the ADN of female rats. Scale bar for inset is 10 μm. Reprinted from (Santa Cruz Chavez *et al.*, 2014).

females). This may be the result of, at least in part, the regular occurrence of one or more, large diameter (> 10 μm) myelinated fiber in each of the left ADNs from male rats which skewed the male data distributions toward larger values of myelin and fiber area that were rarely observed in females (Figure 10, inset near myelin histogram).

B. Electrophysiological evidence for sexual dimorphism in myelinated aortic baroreceptor fibers

Fiber area and myelin thickness are well known to be reliably correlated with electrical threshold for fiber discharge and fiber conduction velocity (CV) (Waxman, 1980). *In situ* electrophysiological studies were carried out to determine if the observed differences in fiber and myelin area also present as quantitative differences in the electrically evoked compound action potential (CAP) from left ADN of male (n = 9, 16 weeks, 419 ± 41 g) and female (n = 7, 17 weeks, 279 ± 10 g) rats. Stable, low noise CAP with a modest stimulus artifact could be reliably recorded *in situ* from the left ADN at a minimum spacing between the stimulus and recording electrodes of 15 mm (Figure 11). At stimulus intensities as low as 0.1 – 0.3 V, recruitment of the lowest threshold and presumably largest A-type myelinated fibers presented as a distinct CAP volley, separate and delayed relative to the stimulus artifact. The CV of these fibers were estimated to be in the range of 60 m/sec for males and 50 m/sec for females but were not significantly different. Myelinated fibers with slightly higher electrical thresholds and presumably smaller diameters were recruited at 0.5 –

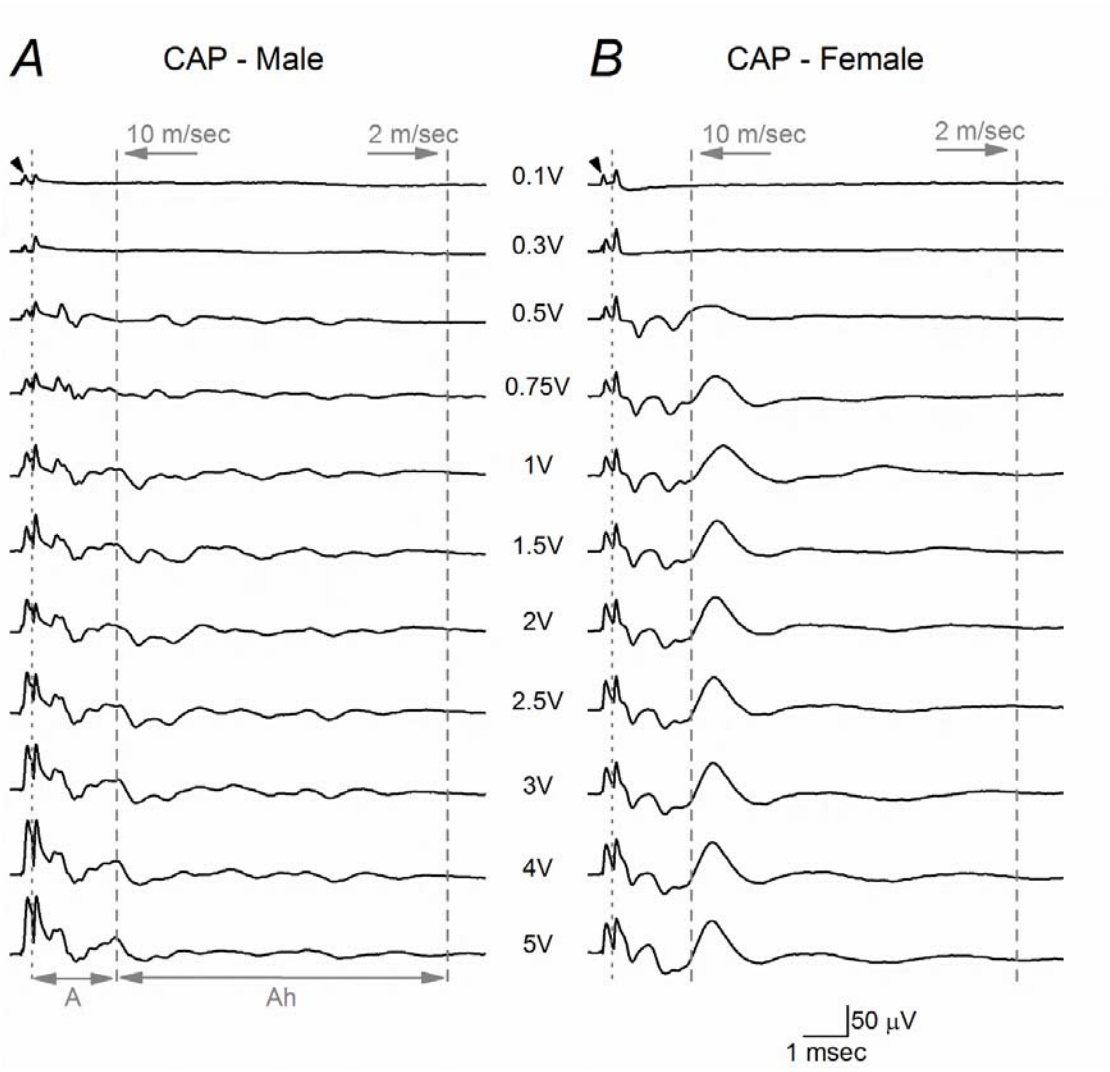

Figure 11: Compound action potentials (CAP) from the ADN of male and female rats. Bipolar, constant voltage stimulation (arrowhead) of the ADN in a male (A) and a female (B) rat showed clear differences in the magnitude and timing of the CAP evoked from low threshold myelinated baroreceptor afferent fibers. The CAP corresponding to the faster conducting A-type fibers was discernable at stimulation intensities as low as 0.1 V. The left most dotted line for each trace separates the stimulus artifact from the CAP for A-type fibers which extends through to the 10 m/sec demarcation (dashed line). The CAP corresponding to the slower conducting Ah-type fibers was bounded by the 10 m/sec and 2 m/sec demarcation lines. The CAP for the Ah-type baroreceptor fibers was apparent at low stimulus intensities (~ 0.5 V) in female rats but not in male rats. Each trace is an average of 25 recordings at a stimulus rate of 1 Hz. Reprinted from (Santa Cruz Chavez *et al.*, 2014).

1.0 V, which increased the complexity of the CAP within an epoch consistent with fiber CV in the range of 20 m/sec for males and 15 m/sec in females. Although not statistically different, this range of fiber CV is consistent with the continued recruitment of faster conducting and presumably larger diameter myelinated A-type fibers in both male and female rats. Use of a finer gradation in stimulation intensities provided an opportunity to quantify the root mean square (RMS) magnitude of the CAP signal energy as a function of stimulus intensity. The recruitment profiles for these lowest threshold and presumably largest diameter myelinated A-type fibers of the left ADN were remarkably similar between male and female rats. The A-volley CAP from both sexes exhibited an asymptotic increase in RMS magnitude with increasing stimulus intensity that plateaued around 1.25 – 1.75 V and remained within 14% of this stable magnitude through to 5 V of bipolar nerve stimulation (Figure 12A, gray arrow). Also starting at about 0.5 V of stimulation there was a distinct CAP volley in female rats that was quite delayed in time from the nerve stimulus and presumably related to the recruitment of the smaller diameter, myelinated Ah-type fibers with CV at or below 10 m/sec (Figure 11). This delayed CAP was not well represented in any of the nerve recordings from male rats. In female rats, starting at 0.4 V of stimulation the average RMS magnitude of this delayed CAP was significantly ($p < 0.05$) greater than the RMS of the corresponding epoch from male rats (Figure 12B) which failed to exhibit any obvious indication of a well defined, repeatable afferent volley (Figure 11). Further increases in stimulus intensity brought about a near linear increase in the RMS magnitude of the delayed CAP in female rats

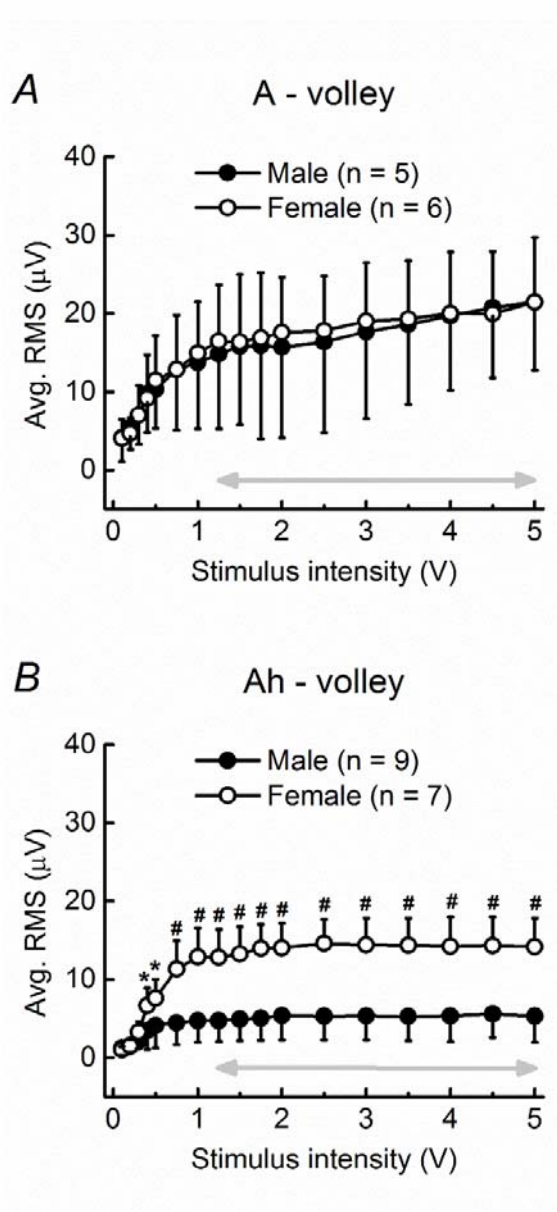

Figure 12: Low threshold myelinated Ah-type afferent CAP magnitude is larger in female rats. The average integrated magnitude (RMS) of the CAP from low threshold myelinated A- and Ah-type baroreceptor fibers are presented for each stimulus intensity. (A) The RMS of the CAP from A-type fibers in male and female rats were remarkably similar. (B) In stark contrast, the RMS of the CAP from Ah-type fibers in female rats were significantly greater than those from male rat over all but the lowest stimulation intensities (< 0.5 V). Double arrow highlights the range of suprathreshold activation, i.e. a CAP of constant magnitude and yet increasing stimulation intensity. Both populations of low threshold A- and Ah-type fibers exhibited graded recruitment at only the lowest stimulus intensities (< ~ 0.5V). * $p < 0.05$ and # $p < 0.01$. Reprinted from (Santa Cruz Chavez *et al.*, 2014).

that showed signs of saturation, starting just beyond 1.0 V of stimulation. Further increases in stimulation intensity through to 5 V brought about a remarkably stable plateau in the RMS magnitude of the CAP from Ah-type fibers (≤ 1% variation) that was significantly ($p < 0.01$) greater than the less synchronized, smaller magnitude response observed from male rat (Figures 11 and 12B). Such stability in the RMS magnitude of the CAP from Ah-type fibers is presumably a consequence of the complete electrical recruitment of all low threshold, myelinated baroreceptor fibers in the left ADN starting at about 1.25 V of bipolar stimulation (Figure 12, gray arrows).

At stimulus intensities beyond 5 V, a broad and less well defined CAP begins to appear in the left ADN from both sexes. These smaller magnitude and slower conducting CAP complexes presumably represent the recruitment of high threshold, unmyelinated C-type fibers of considerably smaller diameter than myelinated baroreceptor fibers and with CV of less than 2 m/sec (Figure 13A). At the maximum stimulation intensity tested the average magnitude of the CAP from these C-type fibers was never much greater than 5 μV RMS with remarkable similarity in the recruitment profiles from male and female rats (Figure 13B). Such low magnitude and desynchronized responses from these high threshold, slowest conducting unmyelinated fibers were in stark contrast to the more synchronized CAP arising from myelinated baroreceptor fibers. In female rat, the plateau exhibited in the RMS magnitude of the Ah-fiber CAP at low stimulation voltages was sustained through to 20 V of stimulation and remained significantly ($p < 0.01$) greater than the corresponding measure from male rats (Figure 13C,

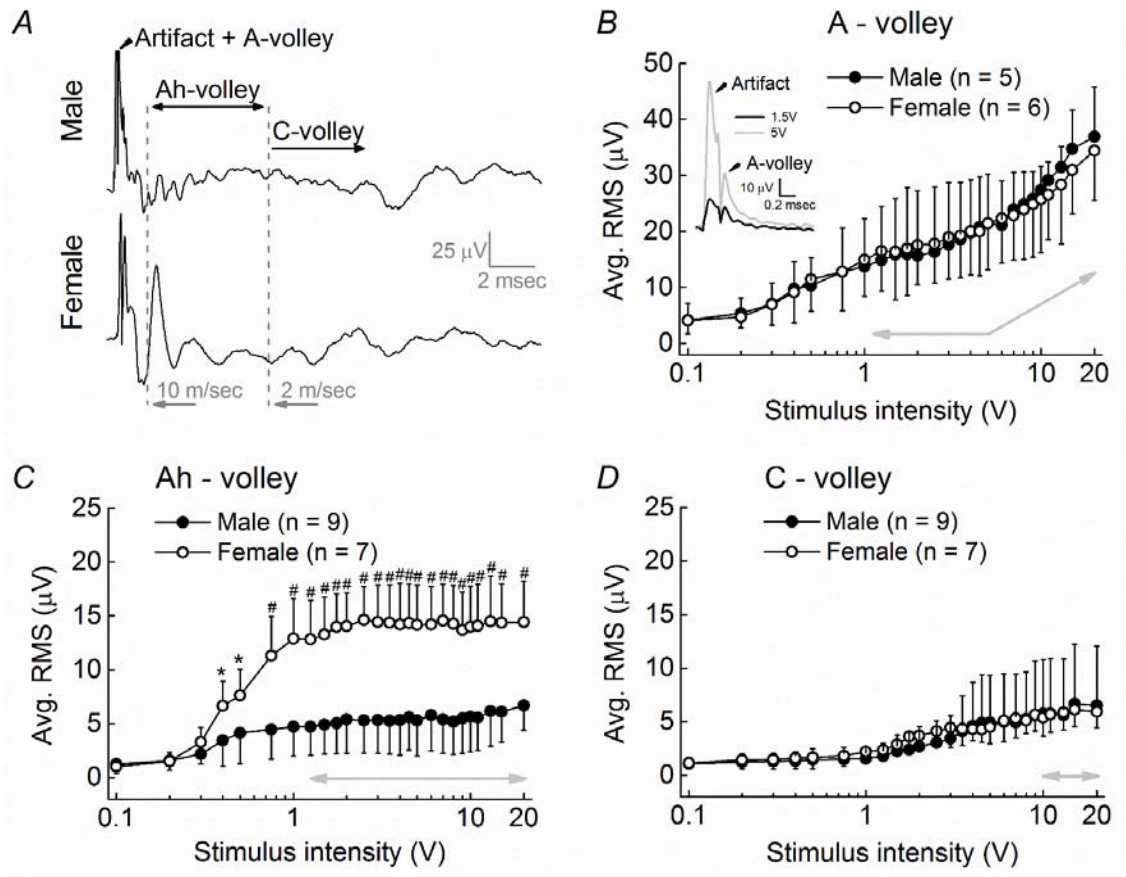

Figure 13: Ah-type afferent CAP is stable and persistent across suprathreshold stimulus intensities. (A) Representative CAP traces from the ADN of male and female rats at high intensity (20 V) stimulation. Starting at intensities greater than approximately 5 V the stimulus artifact extends into the recording epoch associated with A-type fibers (Artifact + A-volley). (B) As a result, beyond an initial saturation plateau the RMS magnitude of the CAP from the faster conducting (> 10 m/sec) A-type fibers increases proportionally with increasing stimulus intensity (note inset and gray arrows). The epochs associated with the CAP arising from the slower conducting (10 – 2 m/sec) myelinated Ah-type fibers (C) and the much slower (< 2 m/sec) unmyelinated C-type fibers (D) occur well beyond the duration stimulus artifact. As a result, the RMS magnitude of the Ah-volley from female rat is essentially the same magnitude across both low and high stimulation intensities and consistently greater than the Ah-volley from male rat (note horizontal gray line). Data are means ± SD, * $p < 0.05$ and # $p < 0.01$. Reprinted from (Santa Cruz Chavez *et al.*, 2014).

gray arrow). Interestingly, in male rats the average RMS magnitude of the Ah-fiber CAP never exceeded the average RMS for the CAP of unmyelinated fibers from either sex. The faster conducting myelinated A-type fibers exhibited a plateau in CAP magnitude from about 1.25 – 5 V of bipolar stimulation that was followed by a near linear increase in the average RMS magnitude as stimulus intensity approached 20 V. This was a consequence of the increasing stimulus artifact that was extending into the epoch for measuring the CAP arising from these faster conducting myelinated A-type fibers (Figure 13D, note inset and upward inflection of gray arrow).

C. Functional evidence for sexual dimorphism in the aortic baroreflex

In situ BRx studies were carried out to determine whether the electrical recruitment of low threshold, myelinated BR fibers in urethane and α-chloralose anesthetized male (n = 17, 14 weeks, 384 ± 43 g) and female (n = 16, 14 weeks, 254 ± 22 g) rats revealed evidence of sexual dimorphism in the reflex response, as might be inferred from the *in situ* nerve recordings (Figures 11 to 13). Femoral BP was monitored throughout each experiment. The average resting MAP in male rats was consistently higher than that in female rats, 100 ± 9.2 mmHg and 92.4 ± 7.9 mmHg, respectively. Once the nerve had been dissected away from the vagus and from the surrounding tissues, it was placed on a bipolar hook electrode and electrically activated using a 50 Hz burst of 3 V pulses. An abrupt and sustained depressor response that peaked within 2 – 4 seconds from the start of nerve stimulation confirmed that the hooked nerve was the left ADN,

which was then covered in a mixture of mineral oil and petroleum jelly. For this particular *in situ* BRx study (Figure 14) a bipolar stimulus of 1.5 V was utilized because this pulse magnitude had been shown to reliably recruit nearly all of the myelinated BR fibers in the left ADN of either sex as well as being far below what might be reasonably considered a minimum electrical threshold for unmyelinated C-type afferent fibers (Figure 13A and 13D). Increasing the rate of the 1.5 V stimulation clearly demonstrated a robust frequency dependent reduction in the MAP along a time course that was qualitatively similar between male and female rats. However, considerably higher rates of nerve stimulation were required in male rats in order to bring about a comparable peak reduction in the MAP evoked from female rats at much lower stimulation frequencies (Figure 14, inset). Indeed, in female rats a clear depressor response was reliably produced by 1.5 V pulses at stimulation rates as low as 5 Hz, whereas in male rats the first evidence of a reduction in MAP does not occur until 20 – 30 Hz of repetitive stimulation. The remaining studies were carried out to determine if such a functional bias was preserved across the 0.1 – 5.0 V stimulation magnitudes that are almost entirely associated with the selective recruitment of low-threshold, myelinated BR afferents (Figures 11 to 13). At a stimulation intensity of 1.0 V, the average normalized (with respect to baseline BP before stimulation) reduction in mean arterial pressure (ΔMAP) from female rats was considerably greater than that from male rats across all but the lowest stimulation frequencies (Figure 15A). As the stimulation intensity increased from 1.0 to 2.0 V the BRx in female rats brought about a significantly ($p < 0.01$) greater reduction in ΔMAP than was

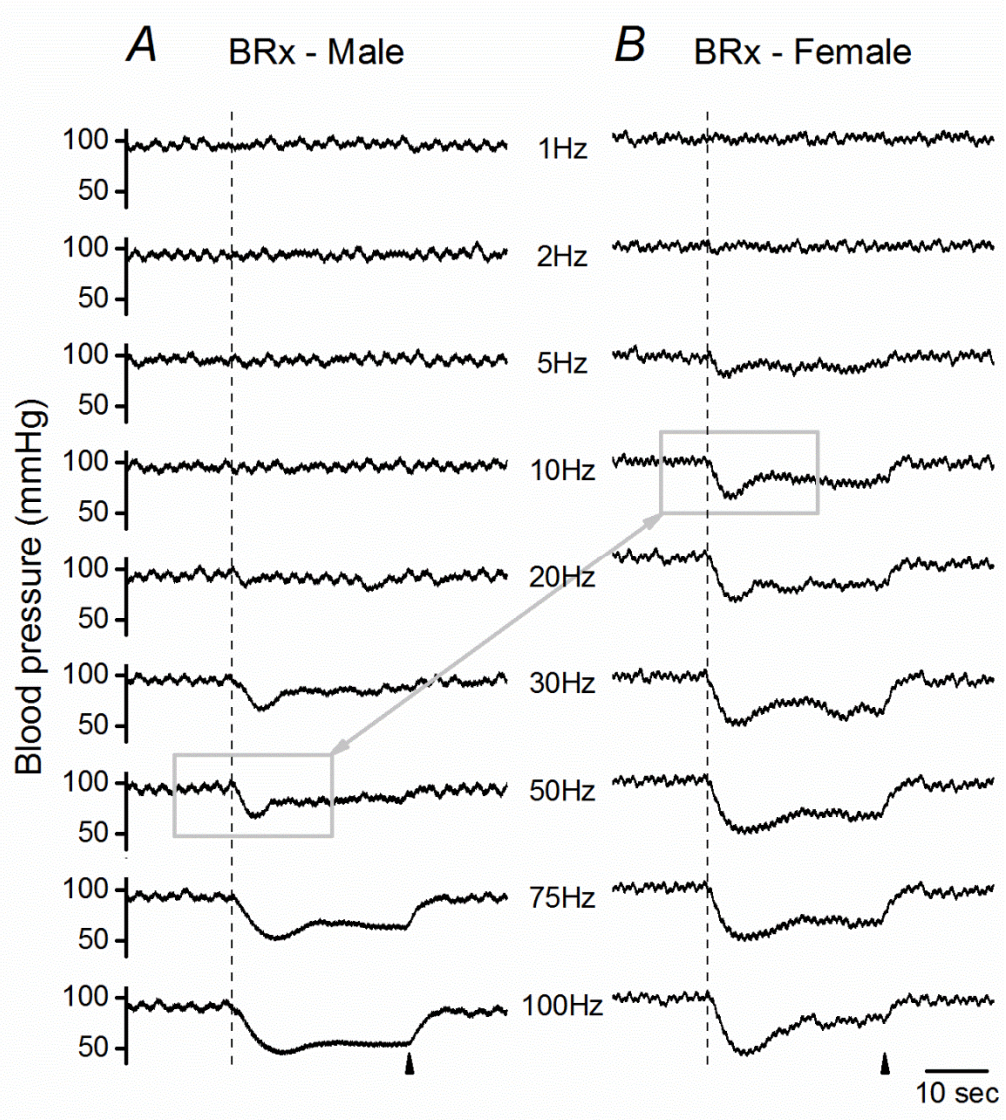

Figure 14: Low threshold myelinated afferents in female rats elicit the baroreflex at lower stimulation frequencies than in male rat. In situ, bipolar stimulation of the left ADN at 1.5 V. This elicited a rapid fall in femoral arterial pressure albeit with unique differences across the depressor responses from male (A) and female (B) rats. Each trial consisted of a 30 sec train of 200 μsec monophasic pulses at randomly selected frequencies, arranged here with an ascending order. Dashed line and arrowhead indicate the start and termination, respectively, of nerve stimulation. A depressor response was evident in female rats at stimulation rates as low as 10 Hz, well below the nearly 50 Hz stimulation rate required to elicit a comparable peak reduction in femoral MAP in male rats (n.b. gray boxes). Reprinted from (Santa Cruz Chavez *et al.*, 2014).

observed in male rats at nearly every frequency tested between 1 – 100 Hz (Figures 15B and 15C). Such a strong bias toward significantly greater reductions in the ΔMAP from female rats as compared to reductions in ΔMAP from male rats continued through to 3.0 V (data not shown). Beyond 3.0 V of nerve stimulation there continued to be a greater frequency-dependent reduction in ΔMAP in female rats as compared to that from male rats, although with an incremental loss in statistical significance as the stimulation intensities approached 5.0 V (Figure 15D).

D. Baroreflex response profile from selective activation of myelinated baroreceptor afferents

The normalized peak depressor responses (ΔMAP %) for a wide combination of stimulus intensities (1 to 5 V) and frequencies (1 to 100 Hz) from all male and female test animals were assembled into 3-dimensional profiles of the integrated BRx response. A linear interpolation was then calculated to join the data set into a single mesh surface for each sex (Figure 16A and 16B). Doing so revealed distinct regions within the recruitment profiles that differed considerably between male and female rats. Most apparent were differences at stimulation frequencies in the range of 1 – 2 Hz which resulted in a consistent peak reduction in the MAP of approximately 10% at all but the lowest stimulation intensities (< 1.5 V) in female but not in male rats. This trend toward greater evoked reductions in arterial pressures in female rats continued through to 20 Hz of nerve stimulation.

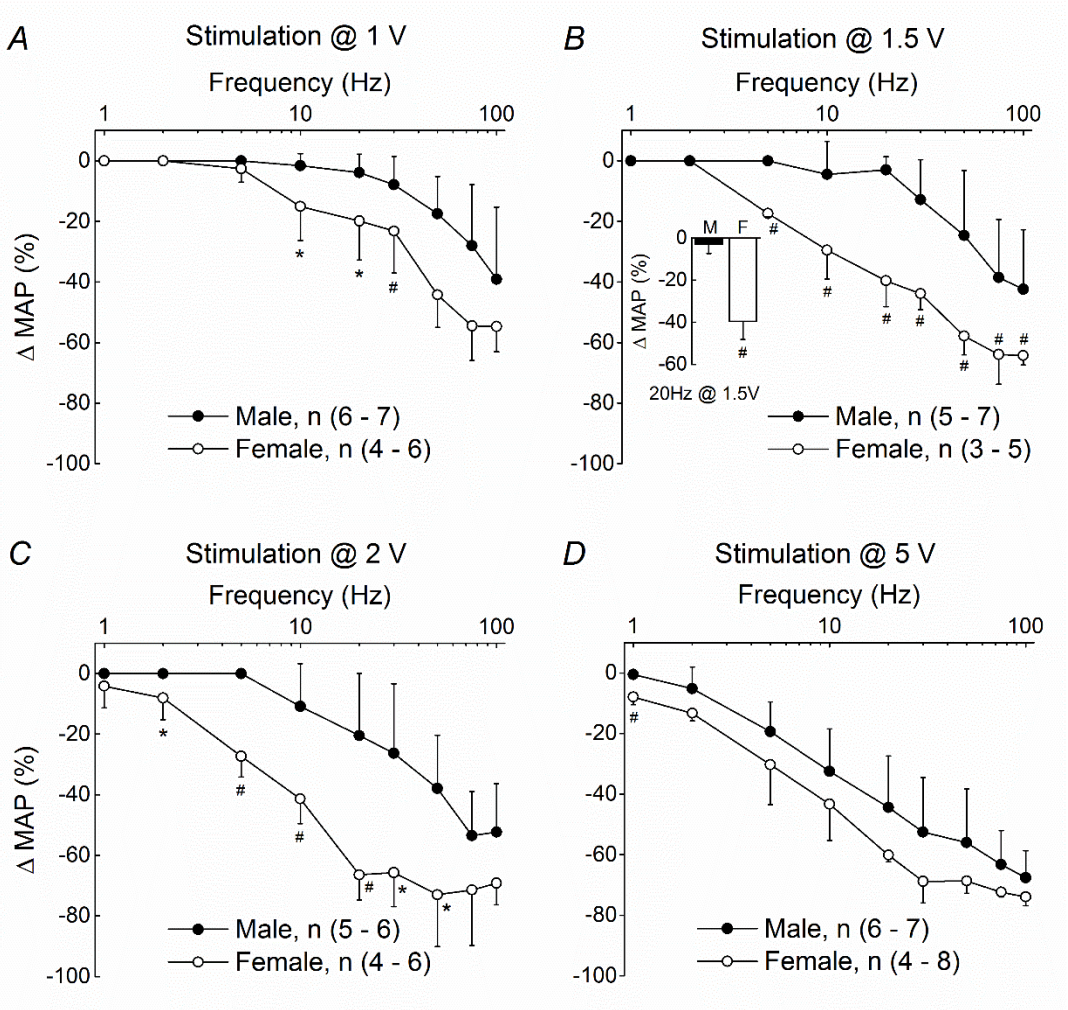

Figure 15: The baroreflex in female rats elicits a greater depressor response at low rates of bipolar stimulation of the left ADN than in male rats. Average % changes in left femoral MAP (Δ MAP) evoked through bipolar stimulation of the left ADN using randomly selected pairs of voltage (1 to 20 V) and frequency (1 to 100 Hz). (A - C) Low intensity (≤ 2 V), low frequency (≤ 20 Hz) stimulation of low threshold myelinated baroreceptor afferents evoked a substantial depressor reflex in female rats that was essentially lacking in male rats (see inset). Stimulation frequencies in excess of 30 Hz were necessary in order to elicit a comparable reflex response from male rats, although one that was significantly less than that from female rats. (D) Higher intensity (≥ 5 V) stimulation of the left ADN evoked a depressor reflex of comparable magnitude from male and female rats at all but the lowest rates (≤ 2 Hz). Results from the CAP studies suggest that beyond approximately 5 V of nerve stimulation there can be graded recruitment of the higher threshold, unmyelinated baroreceptor afferents which bring about a depressor response quite similar in male and female rats. Data are means ± SD, * $p < 0.05$ and # $p < 0.01$. Reprinted from (Santa Cruz Chavez *et al.*, 2014).

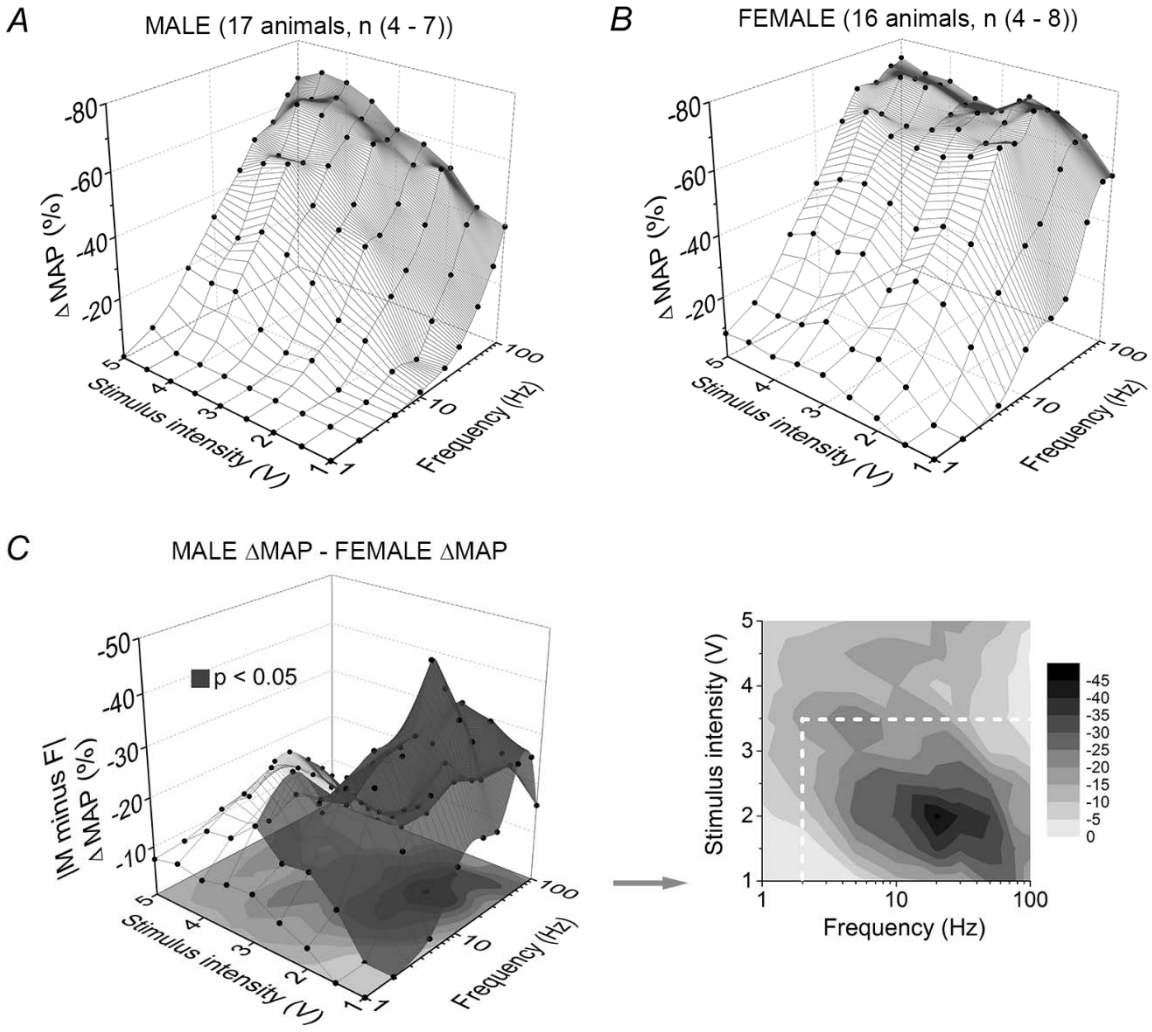

Figure 16: Peak depressor response resulting from the selective stimulation of low threshold, myelinated aortic baroreceptor fibers in male and female rats. Average change in left femoral MAP (Δ MAP) evoked through bipolar stimulation of the left ADN using randomly selected pairs of voltage (1 – 20 V) and frequency (1 – 100 Hz) stimuli applied to the left ADN of male (A, n = 17) and female (B, n = 16) rats, presented here as 3 dimensional plots. (C) Absolute difference in the average peak depressor response between male and female rats (male Δ MAP – female Δ MAP, i.e. Figure 16A minus Figure 16B). Shaded volume highlights the range of low intensity (1 to 3.5V) and low frequency (peak at 20 Hz) stimulation pairs that evoke a depressor response in female rats that is significantly greater than that from male rats. When presented as a 2-dimensional, gray scale contour plot the darker areas indicate those pairs of voltage and frequency stimuli that evoke a significantly greater depressor response in females as compared to male rats ($p < 0.05$, dashed enclosure). Reprinted from (Santa Cruz Chavez *et al.*, 2014)

As stimulation frequencies increased toward 100 Hz, the ΔMAP fromfemale rats remained 2 – 10 fold larger than that from male rats although the greatest differences were concentrated within a region of less than approximately 3.5 V. The numerical difference between these two data profiles revealed a range of stimulus pairs that consistently evoked a much larger reduction in the peak ΔMAP in female as compared to male rats (Figure 16C, shaded surface highlights differences greater than 10%). Presented as a 2-dimensional contour plot, the darker (i.e. greater reduction in MAP) regions outline an operational region in the electrical recruitment of myelinated BR fibers that consistently brought about a significantly greater BRx response from female as compared to male rats (Figure 16D, dashed box denotes $p < 0.05$). At stimulus intensities just beyond this boundary, the ΔMAP from females remained greater than that observed in males although not significantly so. Beyond approximately 5.0 V of nerve stimulation there was no apparent difference between the BRx reponse profiles of male and female rats which predominately involved the graded recruitment of the higher threshold, unmyelinated BR fibers (Figure 13).

II. Aim 2: To determine differences in the parasympathetic mediated reduction of mean arterial pressure between intact and ovariectomized female rats associated with the loss of sex hormones following ovariectomy

A. Electrophysiological evidence for changes in the myelinated compound action potential of myelinated aortic baroreceptor fibers after ovariectomy

The Schild lab had previously shown that ovariectomy lessens the excitability of myelinated Ah-type vagal neurons in the nodose ganglion but not their prevalence (Li *et al.*, 2008). This meant that we could reasonably expect the number of myelinated aortic BR fibers to remain unchanged after ovariectomy. However, progressive decline of peripheral nerve conductive functions due to aging that may be associated with the loss of sex hormones have been shown to be primarily related not only to a decrease in myelinated fibers numbers but also to changes in the structure of myelin sheaths (Sato *et al.*, 1985; Verdu *et al.*, 2000). Our *in situ* electrophysiological studies were carried out to observe quantitative differences in the electrically evoked CAP from left ADN of ovary intact (OVI, n = 9, 18 weeks, 288 ± 28 g) and ovariectomized (OVX, n = 8, 17 weeks, 307 ± 32 g) female rats.

As with the CAP recordings from male and female rats described above, we reliably recorded stable, low noise CAP with a modest stimulus artifact at a minimum spacing between the stimulus and recording electrodes of 15 mm (Figure 17). At stimulus intensities as low as 0.1 – 0.3 V, recruitment of the lowest threshold and presumably largest A-type myelinated fibers presented as a

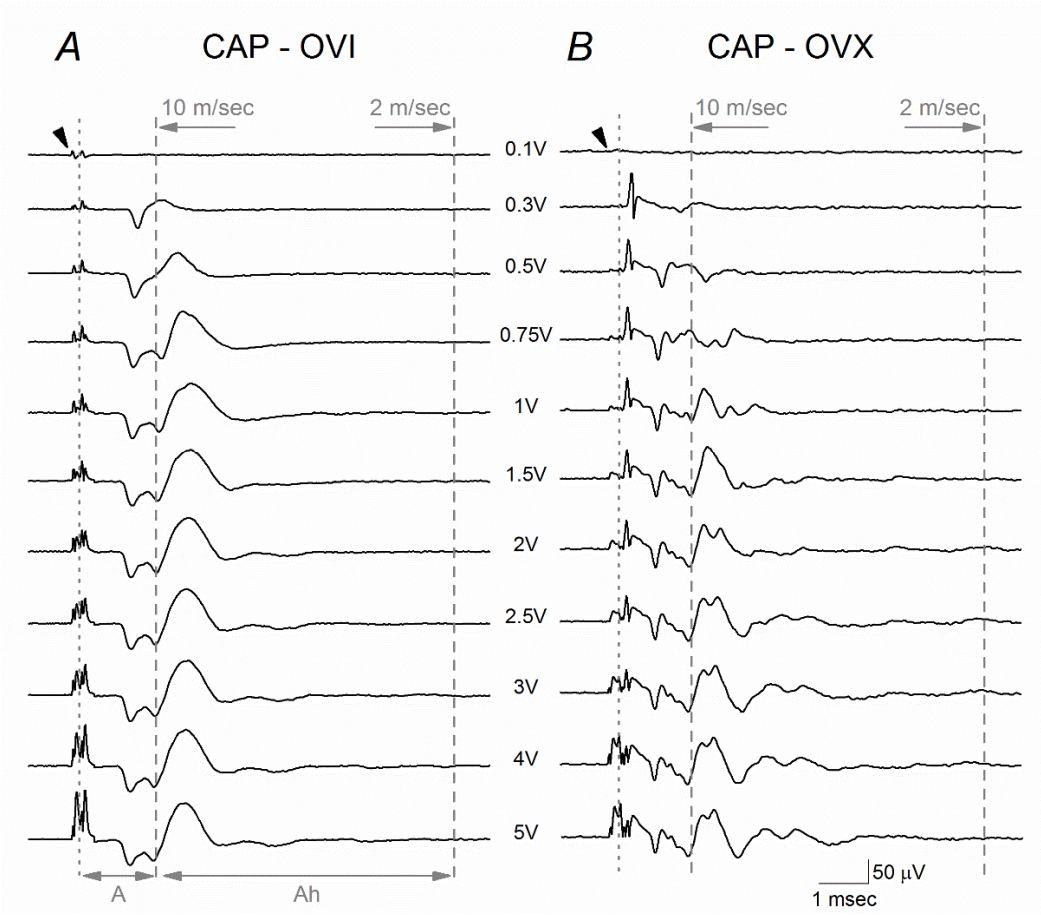

Figure 17: Compound action potentials (CAP) from the ADN of intact and ovariectomized female rats. Bipolar, constant voltage stimulation (arrowhead) of the ADN in an ovary intact (OVI, A) and an ovariectomized (OVX) female rat (B) showed differences in the synchronization of the CAP evoked from low-threshold myelinated baroreceptor afferents. The CAP corresponding to the faster conducting A-type fibers was discernable at stimulation intensities as low as 0.1 V. The left most dotted line for each trace separates the stimulus artifact from the CAP for A-type fibers which extends through to the 10 m/sec demarcation (dashed line). The CAP corresponding to the slower conducting Ah-type fibers was bounded by the 10 m/sec and 2 m/sec demarcation lines. The CAP for the Ah-type baroreceptor fibers was apparent at low stimulus intensities (~0.5 V) in both OVI and OVX rats. Each trace is an average of 25 recordings at a stimulus rate of 1 Hz. Reprinted from (Santa Cruz Chavez & Schild, 2014).

distinct CAP volley, separate and delayed relative to the stimulus artifact. The CV of these fibers (measured at the 1st positive peak in the A-type fiber volley) were estimated to average 35 ± 14 m/sec for OVI rats and 45 ± 13 m/sec for OVX rats but were not significantly different ($p = 0.25$). Myelinated fibers with slightly higher electrical thresholds and presumably smaller diameters were recruited at 0.5 – 1.0 V, which increased the complexity of the CAP within an epoch consistent with fiber CV in the range of 14 m/sec for OVI rats and 13 m/sec for OVX rats (measured at 2nd positive peak of A-type fiber volley). Although not statistically different ($p = 0.45$), the variance (σ^2) in the measures of these CV for OVX rats was almost 6-fold broader as compared with OVI rats ($\sigma^2 = 7.92$ for OVX and $\sigma^2 = 1.93$ for OVI). This increased spread of CV in the myelinated A-type CAP of OVX rats observed across all stimulus intensities tested may be the result of changes in the geometry of individual axons or structure of the myelin sheaths which brings about conduction delays and desynchronization in the summation of myelinated fiber responses (Kimura, 1984; Debanne *et al.*, 2011). Use of a finer gradation in stimulation intensities provided an opportunity to quantify the root mean square (RMS) magnitude of the CAP signal energy as a function of stimulus intensity. The recruitment profiles for the lowest threshold and presumably largest diameter myelinated A-type fibers of the left ADN were remarkably similar between OVI and OVX rats (Figure 18A). The A-volley CAP from both OVI and OVX rats exhibited an asymptotic increase in RMS magnitude with increasing stimulus intensity that plateaued around 1.25 – 1.75 V and remained within 14% for OVI rats and 23% for OVX rats of this stable magnitude

through to 5 V of bipolar nerve stimulation (Figure 18A, gray arrow). Starting at about 0.5 V of stimulation, a distinct CAP volley quite delayed in time from the nerve stimulus and presumably related to the recruitment of the smaller diameter, myelinated Ah-type fibers with CV at or below 10 m/sec presented in the left ADN nerve recordings for both OVI and OVX rats (Figure 17). This delayed CAP appeared smaller in peak magnitude and desynchronized over its time course in OVX rats as compared to OVI rats. Despite these evident differences in the Ah-fiber volley shape between OVI and OVX rats, no significant differences in average RMS magnitude were found between them across all stimulus intensities tested (Figure 18B) which demonstrated that the Ah-type afferent fiber volley in OVX rats was repeatable.

Further increases in stimulus intensity brought about a near linear increase in the RMS magnitude of the Ah-type afferent CAP in both OVI and OVX rats that showed signs of saturation, starting just beyond 1.0 V of stimulation. Further increases in stimulation intensity through to 5 V brought about a remarkably stable plateau in the RMS magnitude of the CAP from Ah-type fibers (≤ 7% variation for both OVI and OVX rats) that was not significantly different between OVI and OVX rats (Figures 18B), despite the slightly smaller OVI RMS magnitude. Such stability in the RMS magnitude of the CAP from Ah-type fibers is presumably a consequence of the complete electrical recruitment of all low threshold, myelinated BR fibers in the left ADN starting at about 1.25 V of bipolar stimulation (Figure 18B, gray arrows).

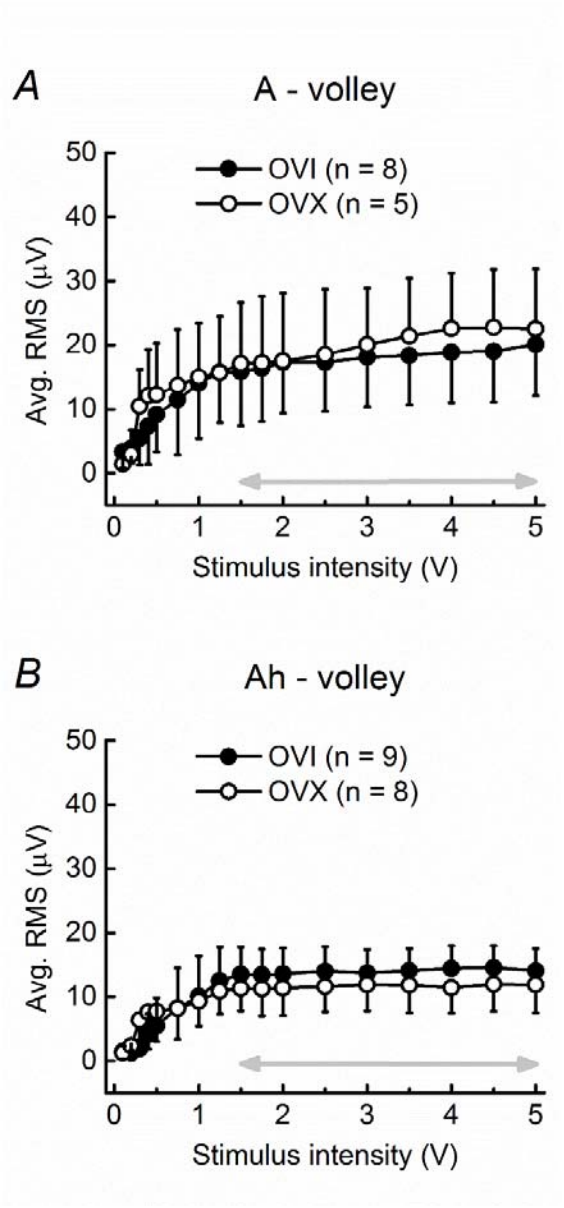

Figure 18: Myelinated Ah-type afferent CAP magnitude are similar in ovary intact (OVI) and ovariectomized (OVX) female rats. The average integrated magnitude (RMS) of the CAP from low threshold myelinated A- and Ah-type baroreceptor fibers are presented for each stimulus intensity up to 5V. The RMS of the CAP from A-type fibers (A) and Ah-type fibers (B) in OVI and OVX rats were remarkably similar over all stimulation intensities with no significant differences between their average RMS magnitudes. Double arrow highlights the range of suprathreshold activation, i.e. a CAP of constant magnitude and yet increasing stimulation intensity. Both populations of low threshold A- and Ah-type fibers exhibited graded recruitment at only the lowest stimulus intensities (< ~ 0.5V). Data are means ± SD. Reprinted from (Santa Cruz Chavez & Schild, 2014).

At stimulus intensities beyond 5 V, a broad and less well defined CAP begins to appear in the left ADN from both OVI and OVX rats. These smaller magnitude and slower conducting CAP complexes presumably represent the recruitment of high threshold, unmyelinated C-type fibers of considerably smaller diameter than myelinated BR fibers and with CV of less than 2 m/sec (Figure 19A). At the maximum stimulation intensity tested the average magnitude of the CAP from these C-type fibers was slightly greater than 5 μV RMS with remarkable similarity in the recruitment profiles from OVX and OVI rats (Figure 19D). In female OVX and OVI rats, the plateau exhibited in the RMS magnitude of the Ah-fiber CAP at low stimulation voltages was sustained through to 20 V of stimulation and no significant differences were found compared to the corresponding measures from OVX rats (Figure 19C, gray arrow). Noteworthy is the observation that using a semilog plot to display the superimposed RMS magnitudes of OVI and OVX rats revealed that the OVI RMS magnitude at stimulus voltages below ~ 0.75 V was greater than the corresponding measures of OVX rats, albeit not significantly different. This was also observed in the RMS magnitude semilog plot for the faster conducting A-type afferent volley at similar nerve stimulations (Figure 19B). Furthermore, the A-type fibers exhibited a plateau in CAP magnitude from about 1.25 – 5 V of bipolar stimulation that was followed by a near linear increase in the average RMS magnitude as stimulus intensity approached 20 V. This was a consequence of the increasing stimulus artifact that was extending into the epoch for measuring the CAP arising from these faster conducting myelinated A-type fibers (Figure 19B, gray arrow).

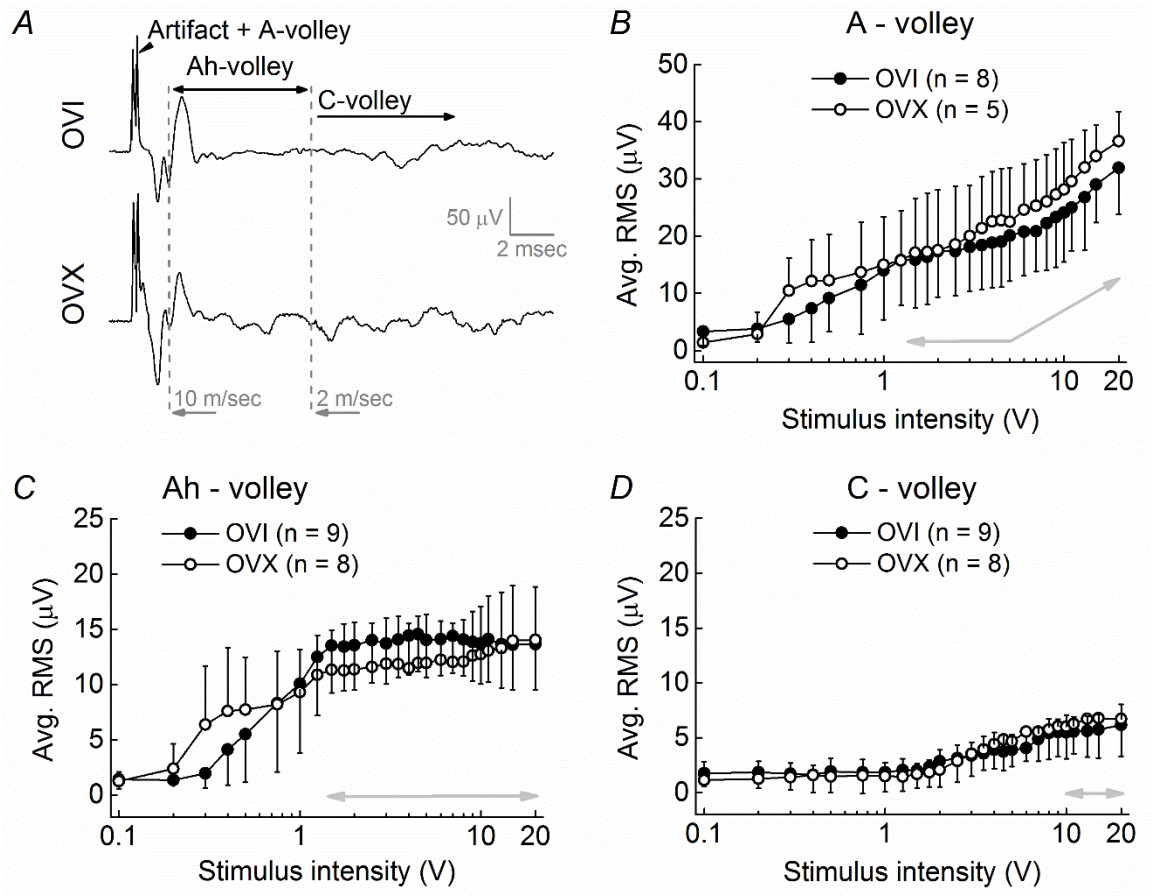

Figure 19: Ah-type afferent compound action potential (CAP) is stable and persistent across suprathreshold stimulus intensities in ovary intact (OVI) and ovariectomized (OVX) female rats. (A) Representative CAP traces from the ADN of OVI and OVX rats at high intensity (15 V) stimulation. Starting at intensities greater than approximately 5 V the stimulus artifact extends into the recording epoch associated with A-type fibers (Artifact + A-volley). (B) As a result, beyond an initial saturation plateau the RMS magnitude of the CAP from the faster conducting (> 10 m/sec) A-type fibers increases proportionally with increasing stimulus intensity (note gray arrows). The epochs associated with the CAP arising from the slower conducting (10 – 2 m/sec) myelinated Ah-type fibers (C) and the much slower (< 2 m/sec) unmyelinated C-type fibers (D) occur well beyond the duration of stimulus artifact. As a result, the RMS magnitude of the Ah-volley from OVI and OVX rats is essentially the same magnitude across both low and high stimulation intensities (note horizontal gray arrow). No significant differences were found between OVI and OVX RMS magnitudes of A-, Ah-, and C-type afferent CAP. Data are means ± SD. Reprinted from (Santa Cruz Chavez & Schild, 2014).

B. Functional evidence for changes in the aortic baroreflex response after ovariectomy

In situ BRx studies were carried out to determine whether the electrical recruitment of low threshold, myelinated BR fibers in urethane and α-chloralose anesthetized OVI (n = 16, 16 weeks, 269 ± 27 g) and OVX (n = 17, 17 weeks, 307 ± 32 g) rats revealed evidence of differences in the reflex response, despitesimilar *in situ* nerve recordings (Figures 17 to 19). Femoral BP was monitored throughout each experiment. The average resting MAP in OVI and OVX rats was 92.7 ± 7.7 mmHg and 97.8 ± 8.5 mmHg, respectively (p = 0.07). Identity of the ADN was confirmed as described in the Results for male vs. female BRx studies. Briefly, ADN myelinated nerve fibers were electrically activated using a 50 Hz burst of 3 V pulses. An abrupt and sustained depressor response that peaked within 2 – 4 seconds from the start of nerve stimulation confirmed that the hooked nerve was the left ADN, which was then covered in a mixture of mineral oil and petroleum jelly. For this particular *in situ* BRx study (Figure 20), a bipolar stimulus of 2 V was utilized because this pulse magnitude had been shown to reliably recruit nearly all of the myelinated BR fibers in the left ADN of either OVI or OVX rats as well as being far below what might be reasonably considered a minimum electrical threshold for unmyelinated C-type afferent fibers (Figures 18B and 19D). Increasing the rate of the 2 V stimulation clearly demonstrated a robust frequency dependent reduction in the MAP along a time course that was qualitatively similar between OVI and OVX rats. However, considerable higher rates of nerve stimulation were required in OVX rats in order

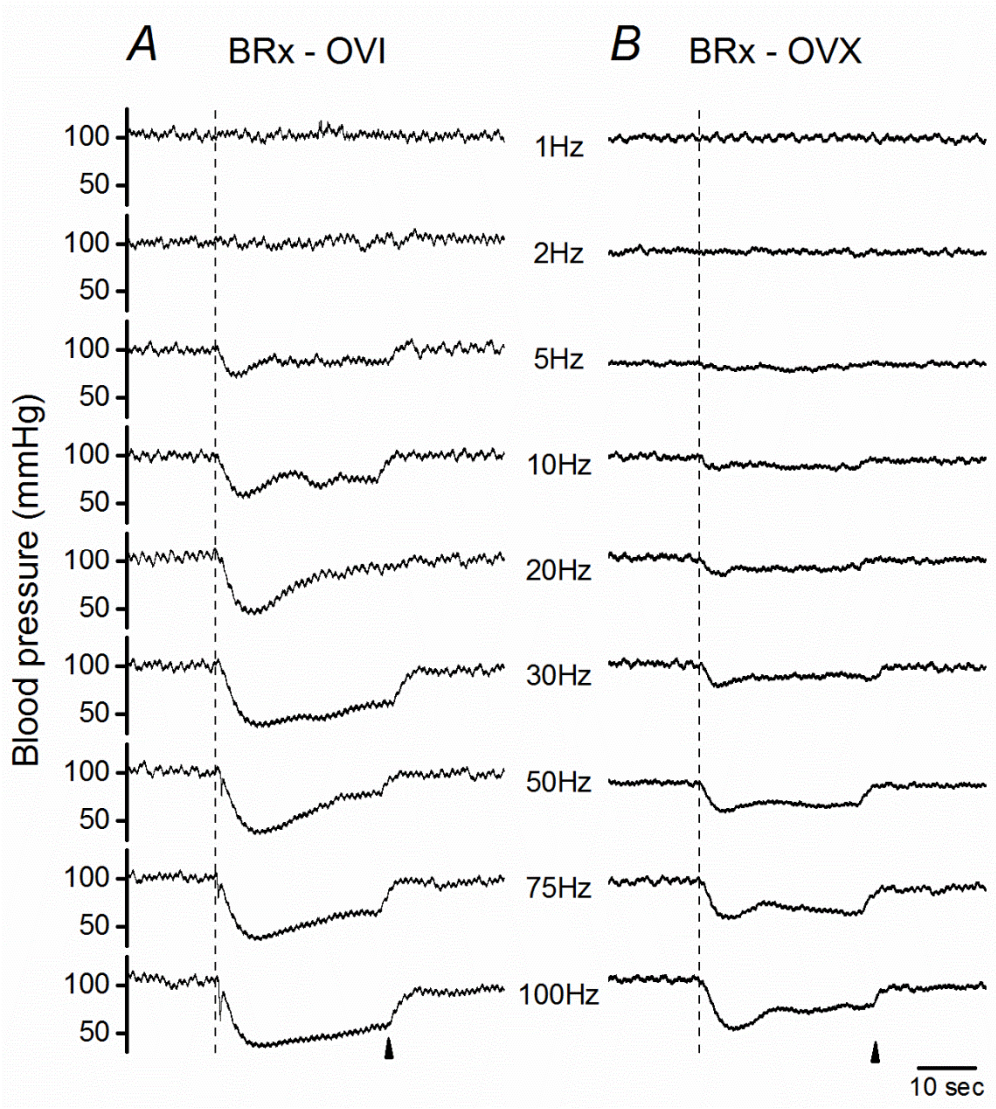

Figure 20: Low-threshold myelinated afferents in ovary intact (OVI) female rats elicit the baroreflex at lower stimulation frequencies than ovariectomized (OVX) female rats. In situ, bipolar stimulation of the left ADN at 2 V provided selective, suprathreshold activation of all A- and Ah-type myelinated fibers (see Figure 17). This elicited a rapid fall in femoral arterial pressure albeit with unique differences across the depressor responses from OVI (A) and OVX (B) rats. Each trial consisted of a 30 sec train of 200 μsec monophasic pulses at randomly selected frequencies, arranged here with an ascending order. Dashed line and arrowhead indicate the start and termination, respectively, of nerve stimulation. A depressor response was evident in OVI rats at stimulation rates as low as 5 Hz, well below the nearly 50 Hz stimulation rate required to elicit a comparable peak reduction in femoral MAP from OVX rats. Reprinted from (Santa Cruz Chavez & Schild, 2014).

to bring about a comparable peak reduction in the MAP evoked from OVI rats at much lower stimulation frequencies (Figure 20, compare 5 Hz in OVI rat to 50 Hz in OVX rat). In general, in OVI rats a clear depressor response was reliably produced by 2 V pulses at stimulation rates as low as 5 Hz, whereas in OVX rats the first evidence of a reduction in MAP does not occur until 20 to 30 Hz of repetitive stimulation. The remaining studies were carried out to determine if such a functional difference was preserved across the 0.1 – 5.0 V stimulation magnitudes that are almost entirely associated with the selective recruitment of low threshold, myelinated BR afferents (Figures 17 to 19). At a stimulation intensity of 1.0 V, the average normalized reduction in mean arterial pressure (ΔMAP) from OVI rats was considerably greater than that from OVX rats across all but the lowest stimulation frequencies (Figure 21). As the stimulation intensity increased from 1 to 2 V, the BRx in OVI rats brought about a significantly ($p < 0.01$) greater reduction in ΔMAP than was observed in OVX rats at nearly every frequency tested between 1 – 100 Hz (Figures 21A and B). Significantly greater reductions in the ΔMAP from OVI rats as compared to reductions in ΔMAP from OVX rats continued through to 5 V (Figure 21 C). Beyond 5 V of nerve stimulation there continued to be a greater frequency-dependent reduction in ΔMAP in OVI rats as compared to that from OVX rats, although with an incremental loss in statistical significance except at the lowest stimulus rates (Figure 21D). For example, at stimulus intensities equal to 10V, significant differences between the ΔMAP in OVI and OVX rats were only found at stimulus rates below 10 Hz (data not shown). Increasing the stimulus intensity to 18V

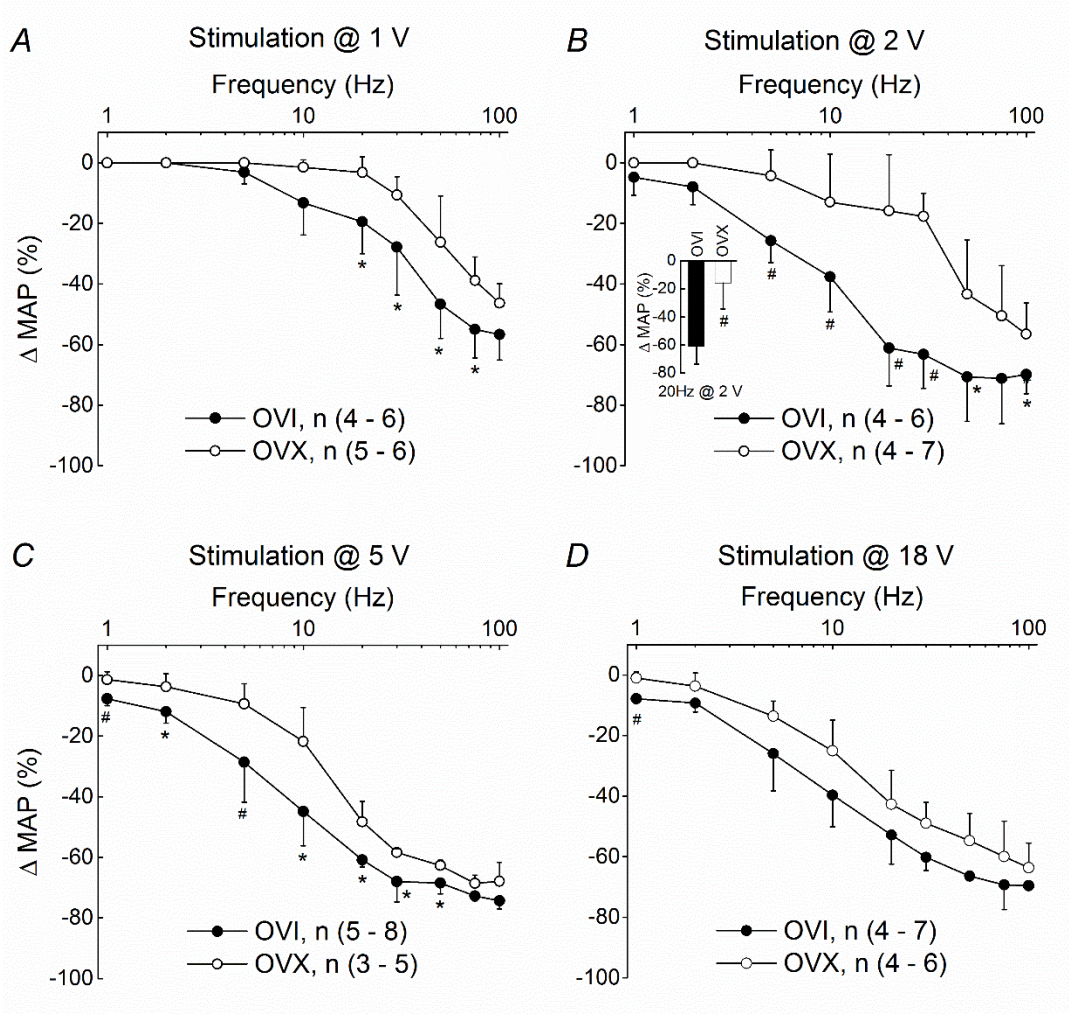

Figure 21: The baroreflex in ovariectomized (OVX) female rats elicits a significantly attenuated depressor response as compared to ovary intact (OVI) female rats at low intensities of bipolar stimulation of the left ADN. Average changes in left femoral MAP (Δ MAP) evoked through bipolar stimulation of the left ADN using randomly selected pairs of voltage (1 to 18 V) and frequency (1 to 100 Hz). (A - C) Low intensity (≤ 5 V) stimulation of low-threshold myelinated baroreceptor afferents evoked a substantial depressor reflex in OVI rats that was significantly attenuated in OVX rats (see inset). At 2 V, stimulation frequencies in excess of 50 Hz were necessary in order to elicit a comparable reflex response from OVX rats. (D) Higher intensity (≥ 5 V) stimulation of the left ADN resulted in graded recruitment of the higher threshold, unmyelinated baroreceptor afferents (see Figure 19) and incremental loss in statistical significance except at the lowest stimulus rates. Data are means ± SD, * $p < 0.05$ and # $p < 0.01$. Reprinted from (Santa Cruz Chavez & Schild, 2014).

resulted in significant differences in ΔMAP between OVI and OVX rats at 1Hz only (Figure 21D).

C. Longitudinal baroreflex study

The ovariectomized rat is a commonly used animal model of human menopause. Experimental intervention occurs either at the time of ovariectomy or commences once 17β-estradiol has reached a low to non-detectable level in plasma (Diaz Brinton, 2012). This typically occurs within 1 to 2 weeks post ovariectomy. As a discovery strategy, we wished to investigate whether progressive changes in BRx response could be identified within the first three weeks after ovariectomy. Reproductively mature female rats were ovariectomized (OVX, n = 20, 11 weeks, 224 ± 11 g) and interventions started at day 4 until day 22 post ovariectomy. *In situ* BRx studies were carried out as previously described only here we focused on a bipolar stimulus of 2 V since our electrophysiological studies (Figures 17 to 19) had shown that this pulse magnitude reliably recruits nearly all of the myelinated BR fibers in the left ADN of either ovary intact (OVI) or OVX rats (at least 24 days post ovariectomy) without activating unmyelinated C-type afferent fibers (Figures 18B and 19D). Femoral BP was monitored throughout each experiment. The average resting MAP in this group of OVX rats was slightly higher than in OVI rats, 94.8 ± 9.6 mmHg and 92.7 ± 7.7 mmHg, respectively. However, this difference was not statistically significant ($p = 0.15$). OVX rats were initially divided in 3 groups according to weeks post ovariectomy: week 1 or day 4 to 7 post ovariectomy, week 2 or day 8 to 14 post ovariectomy, week 3 or day 15

to 22 post ovariectomy. All OVX animals demonstrated a robust frequency dependent reduction in the MAP upon electrical stimulation of the left ADN. We observed that OVX rats from week 2 and week 3 post ovariectomy exhibited similar normalized reductions in mean arterial pressure (ΔMAP) to that of OVX rats from 24 days or later post ovariectomy (Figure 21B), thus, these animals were grouped together (G2, Figure 22). On average and much like the older OVX rats, considerably higher rates of nerve stimulation were required in G2-OVX rats in order to bring about a comparable peak reduction in the MAP evoked from OVI rats at much lower stimulation frequencies (Figure 22, compare 10 Hz in OVI rat to 30 Hz in G2 rats). In the case of OVX rats from week 1 post ovariectomy (G1, Figure 22), the average reductions in ΔMAP were significantly greater ($p < 0.05$) at nearly every frequency tested as compared with OVX rats from 24 days or later post ovariectomy (Figure 22, * denotes Student's t-test results for G0 vs. OVX). When compared to OVI rats, BRx responses from G1-OVX rats were consistently and significantly attenuated at the higher frequencies of stimulation (Figure 22, greater or equal to 20 Hz, # denotes Student's t-test results for G1 vs. OVI). Beyond 2 V of nerve stimulation (3 and 10 V, data not shown) there continued to be a trend towards greater frequency-dependent reductions in ΔMAP in G1-OVX as compared with older OVX rats. At these higher nerve stimulus intensities, BRx responses from G1-OVX were similar to that of OVI rats as demonstrated by the incremental loss in statistical significance.

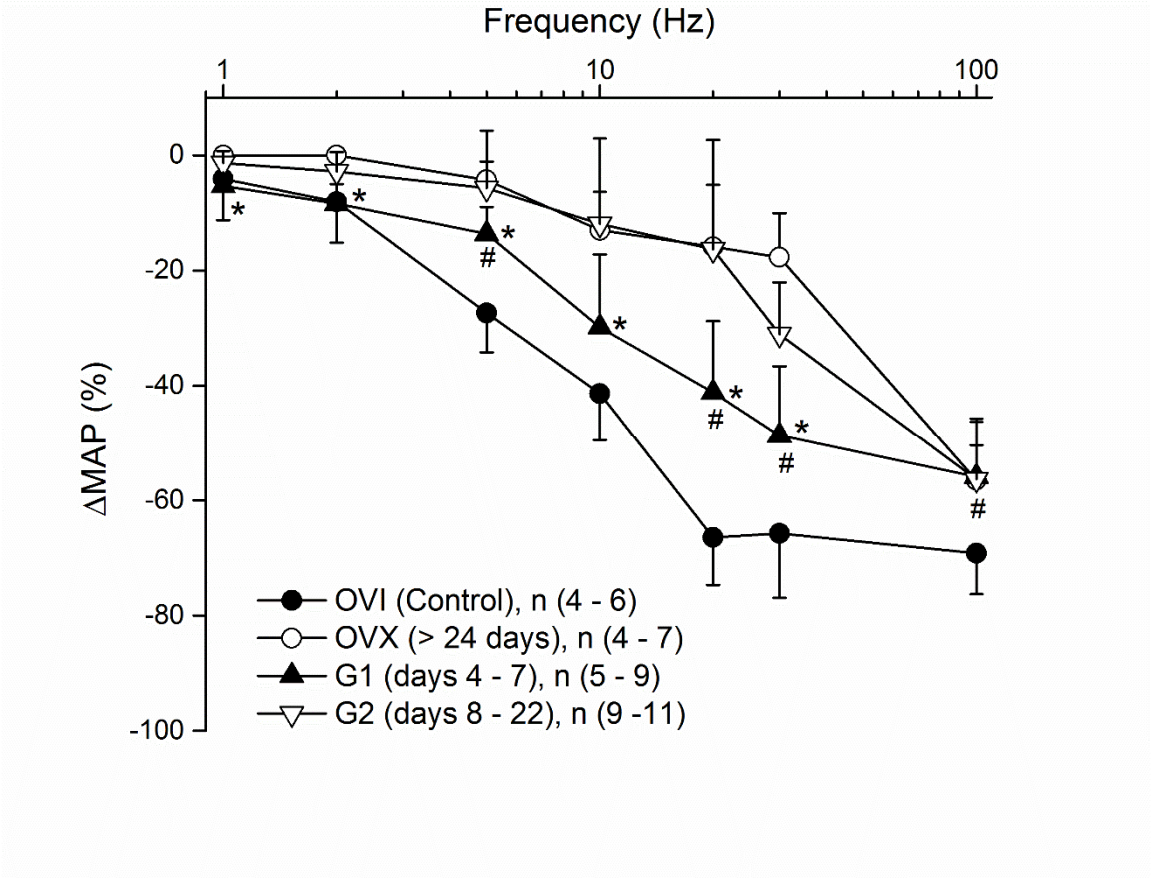

Figure 22: Baroreflex (BRx) responses measured in ovariectomized (OVX) female rats within the first week post ovariectomy are significantly greater than in older OVX rats but significantly attenuated compared to ovary intact (OVI) female rats. Average changes in left femoral mean arterial pressure (Δ MAP) evoked through bipolar stimulation of the left ADN using stimulus intensity (2V) that mostly recruits myelinated aortic baroreceptor fibers combined with randomly selected stimulus rates (1 to 100 Hz). OVX rats from days 8 to 22 post ovariectomy (G2) exhibited comparable peak reduction in MAP as those evoked from older OVX rats (24 days or later post ovariectomy). Conversely, BRx responses from OVX females up to one week post ovariectomy were significantly greater than those of the oldest OVX group, at nearly every frequency tested, but significantly attenuated as compared with OVI rats, at higher frequencies of stimulation. Data are means ± SD, * $p < 0.05$, G1 vs. OVX and # $p < 0.05$, G1 vs. OVI.

CHAPTER 4: DISCUSSION

I. General conclusions

The overarching goal of the studies described in this dissertation was to investigate the functional contributions of the sex specific myelinated Ah-type aortic BR afferents and whether they play a role in the sexual dimorphism observed in BRx function. Furthermore, we examined the effects of sustained loss of sex hormones, through ovariectomy, on the Ah-type aortic BR afferent fiber function and the aortic BRx response. We hypothesized that because myelinated aortic BR in female rat present as two distinct and comparably sized populations of afferents, while a far more homogeneous, mostly singular population of myelinated BR is found in male rats, female rats have an enhanced BRx response compared to male rats. Given our lab's previous findings that Ah-type vagal afferent neurons of the nodose ganglion lose excitability post ovariectomy (Li *et al.*, 2008; Qiao *et al.*, 2009), we also hypothesized that Ah-type BR afferent fiber function is affected by ovarian hormone depletion and normal BRx responses may be compromised.

The findings from this dissertation offer new perspectives concerning sexual dimorphism in autonomic cardiovascular reflexes and the effects of the loss of sex hormones, a hallmark of aging, on their function. The most notable findings being: (1) Increasing electrical stimulation of the ADN from sub-threshold values provides robust evidence for a second, distinct population of slower conducting myelinated BR fibers in female rats, presumably corresponding to the

Ah-type BR afferents, that is not apparent in recordings from male rats (Figures 11 to 13). (2) The functional impact of this additional population of low-threshold myelinated BR is a significant enhancement of the depressor response in female rats (Figures 14 to 16). This is most apparent at stimulation magnitudes just sufficient for recruitment of all myelinated fibers within the ADN but well below stimulation magnitudes required to evoke discharge in unmyelinated BR fibers. (3) Ovariectomy does not significantly disrupt the CV profile of myelinated BR afferent fibers in the ADN (Figures 17 to 19). Average RMS amplitudes from A-type and Ah-type fiber volleys in ovariectomized (OVX) and ovary intact (OVI) rats were comparable, although CAP recordings from OVX rats appeared desynchronized as compared to those from OVI rats. (4) BRx responses in OVX rats are significantly reduced as compared with OVI rats at stimulation magnitudes specific for total recruitment of myelinated BR fibers (Figures 20 and 22). Attenuations in peak reductions of femoral BP were observed as early as 4 days post ovariectomy.

II. Aim 1

A. Myelin profiles of the aortic depressor nerve are sexually dimorphic

Previous work from our lab suggests that vagal neurons functionally classified as myelinated and fluorescently identified as BR afferents present with approximately the same percentage of myelinated A- and Ah-type fibers in female rats while myelinated BR afferents in male rats are comprised almost exclusively of A-type (Li *et al.*, 2008). *In vitro*, Ah-type afferent neurons exhibit

higher electrical thresholds, broader action potentials and lower sustained rates of somatic evoked discharge as compared to A-type afferent neurons. However, both types of myelinated afferents exhibit a robust sensitivity to selective purinergic receptor (P2X) agonists while both are insensitive to selective vanilloid receptor (VR1) agonists (Jin *et al.*, 2004; Li & Schild, 2007). The range of fiber CVs for afferent neurons identified as A- and Ah-type were bimodal as measured using an intact vagal ganglion preparation at room temperatures (Li & Schild, 2007). The presumably larger, A-type fibers generally exhibited CV in the range of 10 to 18 m/sec while Ah-type fibers exhibited much slower CV from just under 4 to about 10 m/sec, although overlapping measures of CV were apparent in both afferent populations as were a small percentage of outliers with CV 2 to 3 times greater (Li & Schild, 2007).

Many factors affect action potential propagation in nerve but those most closely associated with CV are internodal anatomical parameters such as fiber diameter (Waxman, 1995). Whether using the long established quasi-linear relationship between fiber diameter (D) and CV of $1.5 \times D^{1.5}$ (Coppin & Jack, 1972) or the more simplistic linear scaling of $4.6 \times D$ (Boyd & Kalu, 1979), our *in vitro* measures of CV for A- and Ah-type afferents of the ADN align quite well with the propagation profiles typical of 1 to 4 μm diameter Group III sensory afferents and potentially Group II sensory afferents with diameters in the range of 10 to 12 μm. Such estimates are well within the range of measures from the Schild Lab's EM studies (Figure 10) where the average cross sectional area of myelinated fibers (myelin area + axon area) in female rat was significantly less than that of

male rats (Table 3). This difference was the result of considerably less myelin on average per fiber in female as compared to male rats as no significant difference in the axon area was observed (Table 3). Our EM data demonstrated that males trend toward larger magnitudes and females trend toward smaller magnitudes of myelin and axon areas (See histograms in Figure 10). An extreme example of this bias is evident in the observation that each ADN from male rat had at least one or a few myelinated fibers with diameters larger than 10 μm (Figure 10, inset) that were not found in the ADN of female rats. As a result, the sample distribution of myelin area from females was much more compact, exhibiting a much smaller coefficient of variation than that from males, i.e. 0.70 as compared to 1.58, respectively. This neuroanatomical study provided with experimental support for sexual dimorphism in the myelination of aortic barosensory fibers in Sprague-Dawley rat. Because myelin thickness has a role in determining fiber CV (Waxman, 1980; Harper & Lawson, 1985), the EM data was highly suggestive of potential sex differences in the recruitment pattern of ADN myelinated barosensory afferent fibers.

B. Sexually dimorphic conduction velocity profile of the aortic depressor nerve

A compound action potential is an electrophysiological event that represents the algebraic sum of all individual fiber action potentials of a nerve. Hence, the type and number of fibers contained in the nerve shape the nerve conduction profile since CV of single fibers depends on their diameter. Importantly, fiber diameter and discharge threshold for extracellular electrical stimulation are strongly

correlated (McNeal, 1976; Gorman & Mortimer, 1983; Sundar & Gonzalez-Cueto, 2005). The theory has been well tested with experimental inquiry confirming that larger diameter fibers exhibit thresholds for extracellular electrical excitation that are of lower magnitude than that required for smaller diameter myelinated fibers. Gradual increases in bipolar stimulus intensity brings about a cumulative recruitment of successively smaller myelinated axons within the nerve trunk. This graded recruitment from the myelinated fiber population within small diameter peripheral nerve trunks has been widely studied using the electrically evoked CAP as an electrophysiological correlate of the fraction of myelinated fibers recruited with each stimulus. This method also provides timing indexes that make possible reliable estimates of average fiber CV. With a population of myelinated fibers trending toward less total myelin and smaller diameters in female rats as compared to males, we hypothesized this would lead to differences in both the recruitment and CV profiles of the bipolar stimulus evoked CAP.

Previous ADN nerve conduction studies have shown that stimulus intensities that solely activate myelinated fibers are typically in the range of 0.3 to 3 V (Numao *et al.*, 1985; Fan & Andresen, 1998). Unmyelinated fibers with characteristically smaller diameters are concomitantly recruited at threshold intensities around and above 8 V (Fan & Andresen, 1998). Thus, low intensity stimuli at or below 5V allowed us to isolate the CAP responses corresponding to specific myelinated fiber activation without activating C-type BR fibers. For both male and female rats and at the lowest intensity tested (0.1 V, top trace in Figure 11), we detected only the peak corresponding to the lower threshold and

presumably larger diameter A-type barosensory fibers. This fast conducting volley had the shortest latency making it susceptible to the contaminating effects of the stimulus artifact. Dissecting ADN trunks longer than 15 mm combined with our electrophysiological recording technique featuring orthogonally-positioned bipolar stimulating and recording electrode pairs greatly reduced the artifact contamination (Figure 13B, see inset and grey arrows). In most instances, our recordings from rat ADN exhibited a maximum CV approaching 60 m/sec for male and 50 m/sec for female rats and always at the lowest stimulus magnitude tested of 0.1 V. Such low threshold and elevated measures of CV in ADN have been reported elsewhere but only in larger species such as cat with a max of 66 m/sec, and rabbit with a max of 40 m/sec (Paintal, 1953; Douglas *et al.*, 1956; Devanandan, 1964). Our measured high CV can reasonably be expected to cover the largest fibers (equal or greater than 10 μm) in male rats if utilizing the well accepted scaling factor of 4.6 (Boyd & Kalu, 1979). Similarly, our selection of a minimum threshold of 10 m/sec for CV in assigning afferent fiber type as myelinated A is consistent with estimates of average myelinated fiber diameter for males (2.45 ± 1.1 μm) and age-matched females (2.33 ± 0.8 μm). This estimated lower limit CV agrees with our lab *in vitro* electrophysiological (Li & Schild, 2007) data and CV measured *in situ* by other investigators although the upper limit is highly variable (Brown *et al.*, 1976; Reynolds *et al.*, 2006).

At stimulation intensities slightly higher than those required to recruit the fastest A-type axons and well below those necessary for activation of unmyelinated fibers, recruitment of a second slower component became evident

in the CAP traces of female rats (~ 0.5V, 3rd trace from top in Figure 11). This longer latency CAP waveform presented with a clear and distinct separation in timing from the faster CAP waveform of the lower threshold A-type fibers, although the differences between activation thresholds was quite small, i.e. 0.1 V threshold for A-type and 0.5 V threshold for Ah-type. A proposed explanation is that a significant overlap in fiber diameter between aortic BR afferent fiber populations exists in female rats although the distribution of myelinated fiber diameters appears unimodal (data not shown). Furthermore, structural factors such as differential myelin distribution, i.e. less in females compared to males, may be responsible for the female's two-component vs. the male's one-component myelinated CAP.For the long-latency component, the CV remained between 8 and 10 m/sec which corresponds to *in vitro* propagating speeds of slower conducting, presumably smaller diameter and lightly myelinated, Ah-type aortic BR fibers. It is likely that such observations have not been previously reported because the majority of CAP studies performed on the ADN of rat involves mostly male data (Numao *et al.*, 1985; Fan *et al.*, 1996; Fan & Andresen, 1998; Reynolds *et al.*, 2006). In the few instances where female rats were used, their data was combined with those of male rats and this may account for the slower conducting myelinated fiber volleys (between 3 and 12 m/sec) reported for Wistar-Lewis rats (Brown *et al.*, 1976). Importantly, as we increased the stimulus intensity, our CAP traces showed that the Ah-type fiber volley of female rats remained compact and well-defined, whereas in males it appeared desynchronized and without a well defined peak. These CAP features

were reflected in the Ah-type fiber volleys magnitude quantifications. The average RMS magnitudes in females were significantly greater than those from males for all but the lowest stimulation intensities (Figures 12B and 13C). Notably, both populations of myelinated A- and Ah-type fibers reached similar plateaus in CAP magnitude at about the same stimulus intensities (1.25 to 1.75 V), albeit the threshold of activation of the Ah-type fibers was slightly higher than that of the A-type fibers (0.5 V vs. 0.1 V). Furthermore, we only began to recruit unmyelinated C-type aortic BR fibers at stimulus intensities beyond 5 V (Figure 13D) with CV below 2 m/sec. The RMS magnitude of the CAP from A-type and C-type fibers in both sexes were remarkably similar (Figures 12A and 13D). Collectively, our electrophysiological data confirmed that in female rats two functionally distinct myelinated afferent sensory pathways to the integrated drive of the aortic BRx exist, whereas only one pathway is apparent in male rats.

C. An afferent basis for sexual dimorphism in the aortic baroreflex

The BRx responses attributed to activation of the myelinated A- and unmyelinated C-type aortic BR fibers have been extensively studied and these have distinct frequency-response characteristics (Douglas *et al.*, 1956; Kardon *et al.*, 1975; Numao *et al.*, 1985; Fan *et al.*, 1996; Fan & Andresen, 1998; Fan *et al.*, 1999). In rat, activation of A-type fiber volleys in the ADN evokes reflex changes in MAP only at frequencies greater than 10 Hz at low stimulus intensities, usually in the range of 1 to 3 V (Fan *et al.*, 1999). The recruitment of C-type fiber volleys (A + C) occurs at stimulus intensities greater than or equal to 15 V and at

frequencies lower than the ones required to elicit reflex MAP responses from A-type BR alone (Fan & Andresen, 1998). It is important to note that these studies comprise data from male rats only. To our knowledge, ADN stimulation studies in female rats have not been previously reported except for one study by Mohamed *et al.* (1999) (Mohamed *et al.*, 1999). These investigators used a supramaximal stimulus intensity of 30 V at frequencies ranging from 1 to 30 Hz in order to activate both A and C fibers in intact, sham-operated, and ovariectomized female rats. Our average MAP decreases at 18 and 20 V stimulus intensities (data not shown) appear to correlate with their results in intact females, although a one-to-one comparison could not be made because we normalized our decreases in MAP with respect to the baseline MAP.

Importantly, our *in situ* BRx experiments utilized bipolar stimulation of the left ADN to elicit graded recruitment of the myelinated A- and Ah-type, and unmyelinated C-type fibers via electrical excitation of voltage-gated ion channels independent of mechanotransduction. This type of stimulation allowed us to gradually recruit BR fibers in the ADN with precision timing and exquisite control over the stimulus intensities needed to evoke the volleys of action potentials corresponding to specific mixed populations of afferent fibers, that is: myelinated *vs.* myelinated + unmyelinated. One caveat associated with electrical stimulation is that the activation of all the sensory axons is synchronous and clearly unlikely to happen with natural stimuli and does not mimic the intrinsic natural distribution of multiple parallel sensory inputs to the CNS. This had to be taken into account when extrapolating our results to an *in vivo* scenario. Furthermore, we carried out

our reflex response studies under anesthesia, although techniques have been developed to stimulate the ADN in conscious freely moving rats (De Paula *et al.*, 1999; Salgado *et al.*, 2007). The choice of anesthetic can profoundly influence baseline parasympathetic and sympathetic tone, peripheral vascular resistance, and the central processing of the baroreflex. Therefore, we chose a urethane and α-chloralose "cocktail" as it has been shown, at the doses used in our experiments, to minimally inhibit the cardiovascular system while providing an adequate depth of anesthesia (Stornetta *et al.*, 1987; Jackson *et al.*, 2004; Usselman *et al.*, 2011).

Since the net effect of BR activation, regardless of the afferent fiber type, is the elevation of the parasympathetic and inhibition of the sympathetic autonomic pathways for neurocirculatory control, we expected to record the reflex contributions of the Ah-type aortic BR afferent at stimulus specific for the activation of myelinated fibers. Our electrophysiological findings showed that ADN A- and Ah-type fiber thresholds were typically less than or equal to 0.5 V, whereas thresholds of activation for C-type fibers usually occurred at around 5 V (Figures 11 to 13). Consequently, low intensity stimuli up to 5 V allowed us to examine reflex responses to selective activation of the myelinated BR fiber subpopulations without activating C-type fibers. Interestingly, no substantial decreases in MAP were recorded in female or male rats for stimulus intensities below 1 V. This implies that a minimum threshold level must be met at the CNS to elicit the BRx. Our raw BRx response recordings showed new evidence that stimulus intensities as low as 1.5 V elicited a rapid fall in femoral arterial pressure

at stimulation rates at or below 10Hz in female rats, whereas in males similar depressor responses were only achieved at 50 Hz and beyond (Figure 14). These observations were supported by our BRx response summary curves which demonstrated that low intensity combined with low frequency (ranging between 1 to 20 Hz) stimulation evoked substantial depressor reflex responses in female rats that was essentially lacking in male rats (Figure 15). Furthermore, our electrophysiological studies also determined that complete electrical recruitment of A- and Ah-type aortic BR fibers occurs at stimulus intensities close to 2 V (Figure 12). At this stimulus intensity, activation of A-type volleys in the ADN of male rats evoked reflex changes in MAP only at relatively high frequencies (≥ 10 Hz) compared with the responses evoked in female rats that were significantly greater at stimulation rates as low as 2 Hz (Figure 15C). This indicates that the Ah-type BR afferent has a distinctly different frequency range of operation and suggests a functional overlap in the submaximal regions of the A-type afferent frequency-response. Thus, when only the myelinated BR in the ADN are activated, the reflex MAP response in females is elicited over a wider range of frequencies compared to males (Figure 16C) and afferent summation (A + Ah) is responsible for the significantly greater depressor responses in female compared to male rats (Figure 16).

III. Aim 2

Surgical removal of both ovaries, ovariectomy, is commonly used as a translational model of human menopause, a hallmark of female aging. A pitfall of

surgical menopause is that gradual reduction in ovarian steroids and associated compensatory responses do not take place as in natural reproductive senescence (Diaz Brinton, 2012). Regardless, this model is appropriate for simulating short-term changes in autonomic cardiovascular regulation during menopause because it efficiently suppresses ovarian hormone levels. Sustained loss of female hormones due to ovariectomy can also have an impact on nerve fiber function since a range of neurosteroids have been shown to impart a protective effect upon peripheral nerve integrity (Melcangi *et al.*, 2005; Leonelli *et al.*, 2006). In this study, ovaries were removed at 9 weeks of age which allowed for ovarian maturation and establishment of reproductive cycling. All of our interventions occurred within 12 weeks post ovariectomy, a time frame in which extensive adaptive responses to ovariectomy have not yet occurred as predicted by sustained levels of circulating 17β-estradiol and testosterone (Zhao *et al.*, 2005).

A. <u>Ovariectomy does not significantly alter the conduction velocity profile of low-threshold myelinated fibers from aortic depressor nerve</u>

In peripheral nerves, the majority of age-related changes associated with the loss of sex hormones are related to changes in the myelin sheath (e.g. thickening of myelin sheaths, ballooning, splitting, and/or demyelination) (Melcangi *et al.*, 2000). This broadly supports our previous lab findings that distributions of myelinated A-type and Ah-type and unmyelinated C-type vagal afferents between OVI and OVX female populations were essentially similar (Li *et al.*, 2008). As a

normal part of a woman's aging process, menopause involves reductions in the production of estradiol and progesterone (Grady, 2006). These neuroactive steroids are able to influence the expression of myelin proteins and the proliferation of Schwan cells (Fex Svenningsen & Kanje, 1999; Magnaghi *et al.*, 2001). Hence, sustained loss of female hormones due to ovariectomy has the potential to affect myelinated BR function. In this study, we did not investigate if the ADN of OVX rats exhibited significant morphological changes in myelin, or the potential loss of myelin proteins. These could have been investigated by RT-PCR (changes in RNA levels), by Western analysis (changes in protein levels), and/or by visualization under the microscope using immunohistochemistry, and ultrastructural analysis by electron microscopy. However, these assays are limited because they are unable to measure the consequences of changes in myelin integrity in the context of axon function and the effects on axon conduction. A frequently used quantitative marker to assess such functional changes in nerve fibers is the speed at which the nerve propagates action potentials. CAP recordings yield this type of information and are used to assess overall nerve fiber function (Waxman, 1980, 1988). Ours results showed that ADN CAP recordings from OVI and OVX rats exhibited two distinct myelinated fiber volleys corresponding to A-type and Ah-type barosensory fibers (Figure 17). The myelinated CAP from OVI and OVX rats appeared qualitatively similar in threshold and latency, although an increased temporal dispersion (i.e. desynchronization) of individual nerve fiber activity was evident in the CAP of OVX rats, even at myelinated supramaximal stimulus. Temporal dispersion can

alter the waveform of sensory CAP, specifically a reduction in amplitude due to shifts in sensory spike latencies (Kimura, 1984). This effect was apparent when comparing the peak elevation of the Ah-type fiber volley in OVX and OVI rats (Figure 17). However, our RMS data for A- and Ah-type fiber volley showed that OVI and OVX CAP magnitudes were not significantly different (Figures 18 and 19) indicating that overall myelinated fiber recruitment was not altered. Collectively, our electrophysiological data suggests that the number of myelinated axons in the female rat ADN may be largely preserved post ovariectomy, but myelin integrity may be affected. This is consistent with studies investigating aging effects on autonomic nerve fibers in rat, although these did not include ovariectomized animals (Sato *et al.*, 1985; Soltanpour & Santer, 1996; Nakayama *et al.*, 1998) . For example, Soltanpour and Santer (1996) reported on the preservation of the total number of myelinated axons in the vagus nerve trunk with age, albeit with alterations in their ultrastructure and Schwann cells (Soltanpour & Santer, 1996). Thus, our findings emphasize the vulnerability of myelin sheaths to the loss of sex hormones independently of ageing. Importantly, our data strongly indicates that aortic myelinated BR fiber function may be preserved post ovariectomy. This is significant because BP information generated at the depressor nerve terminals can be transmitted to 2nd order barosensory neurons of the NTS. However, our CAP recordings were performed at 1 Hz and it is unclear whether OVX myelinated ADN fibers have the ability to sustain high-frequency impulse conduction. Previous work from our laboratory reported on the reduced excitability of isolated Ah-type vagal afferent

neurons from OVX rats (i.e. reduced firing frequency) despite exhibiting only subtle differences in the duration of their action potential waveforms (Qiao *et al.*, 2009). No such changes in excitability were observed in the OVX myelinated A-type and unmyelinated C-type vagal afferents. This suggests that ovariectomy, perhaps through combined reductions in the membrane excitability at the soma and nerve fiber of Ah-type barosensory neurons, may result in fewer repetitively discharging myelinated ADN fibers driving centrally mediated BRx pathways. Therefore, the diminished barosensory drive in OVX rats may contribute to their reduced aortic BRx responses compared to normal female rats.

B. Sustained loss of sex hormones is associated with significant attenuation of baroreflex responses in ovariectomized females

Our OVX reflex studies showed that bipolar electrical stimulation of barosensory afferent fibers in the ADN produced frequency-dependent responses that were not altered by ovariectomy (Figures 20 and 21). However, significant differences in average MAP reductions between OVI and OVX rats were present across most stimulation rates tested at stimulation magnitudes (1 to 5V) that presumably recruits only A-type and Ah-type BR fibers. Beyond 5 V of nerve stimulation, there continued to be a greater reflex reduction in MAP in OVI rats as compared to OVX rats, although with an incremental loss in statistical significance except at the lowest stimulus rates (Data not shown and Figure 21D).

Several plausible and likely concurrent explanations exist for the decrease in BRx response observed in OVX female rats. For example, a temporal

desynchronization of the afferent myelinated input transmitted to the CNS in OVX females may result in afferent summation below the minimum threshold required by the CNS to elicit BRx responses comparable to those of OVI females. Our nerve conduction studies revealed conspicuous changes in the synchronization of A- and Ah-type BR activity in both myelinated fiber volleys. Despite achieving simultaneously recruitment of A- and Ah-type barosensory fibers similar to that observed in OVI rats starting at intensities as low as 0.5 V (Figure 17) , the amplitude of the OVX Ah-fiber volley appeared qualitatively reduced across all stimulus intensities tested. This decrease in baseline to peak amplitude could be an indicative of a decrement in the recruitment of conducting Ah-type fibers. Interestingly, we found no significant differences in the average RMS amplitude of the Ah-type CAP between OVI and OVX rats (Figure 18B), suggesting an increase in the temporal dispersion of Ah-type BR activity in OVX females. Any reductions in the size and synchrony of the myelinated presynaptic fiber volley will diminish the spatial and temporal afferent summation of BR inputs at the NTS and may result in reduced BRx responses as observed in OVX females. Furthermore, previous work had shown that ovariectomy lessens the somatic excitability (i.e. ability to evoke repetitive discharge) of most but not all (~ 90 %) Ah-type vagal afferents, whereas no such changes in excitability were observed in myelinated A-type and unmyelinated C-type vagal afferents from OVX females (Li *et al.*, 2008; Qiao *et al.*, 2009). Although electrical excitability of the soma is not necessary for through-conduction of ascending afferent information (Amir & Devor, 2003) and cannot be directly compared to that of the axon, the reduced

ability of the soma to generate action potentials reflects system changes in the molecular architecture of the cell membrane that may also affect the axonal firing rate. This would imply that a large percentage of Ah-type barosensory neurons in OVX rats may have a reduced ability to follow sustained firing with high precision and fidelity and are unable to trigger appropriate responses at their central targets. Indeed, our reflex curves revealed stark differences in the magnitude of the frequency-dependent reflex responses between OVI and OVX rats (Figure 21). For example, OVI female rats exhibited substantial falls in femoral arterial pressure with stimulus intensities as low as 2 V and stimulus rates at or greater than 5 Hz (Figures 20 and 21B), whereas similar depressor responses were only achieved in OVX rats at frequencies greater than 30 Hz. In males, this latter combination of voltage and frequency stimulus brings about substantial decreases in MAP due to the activation of mostly A-type aortic BR afferents (Fan *et al.*, 1999). Interestingly, reflex responses from OVX rats are similar to those of male rats (Figure 23, grey curve), except at stimulus voltages beyond 5V. This suggests that additional functional changes may occur at other components of the BRx pathways, for example, the neurons in the brainstem.

Among all sex hormones, estrogen have been suggested to influence cardiovascular function through effects on the ANS (Huikuri *et al.*, 1996; Seely *et al.*, 1999; Menozzi *et al.*, 2000; Saleh & Connell, 2000). A proposed mechanism is that the exposure of neurons from the cardiovascular nuclei in the brain to circulating estrogen crossing the blood-brain barrier or generated from aromatase activity within the brain brings about various genomic and more rapid,

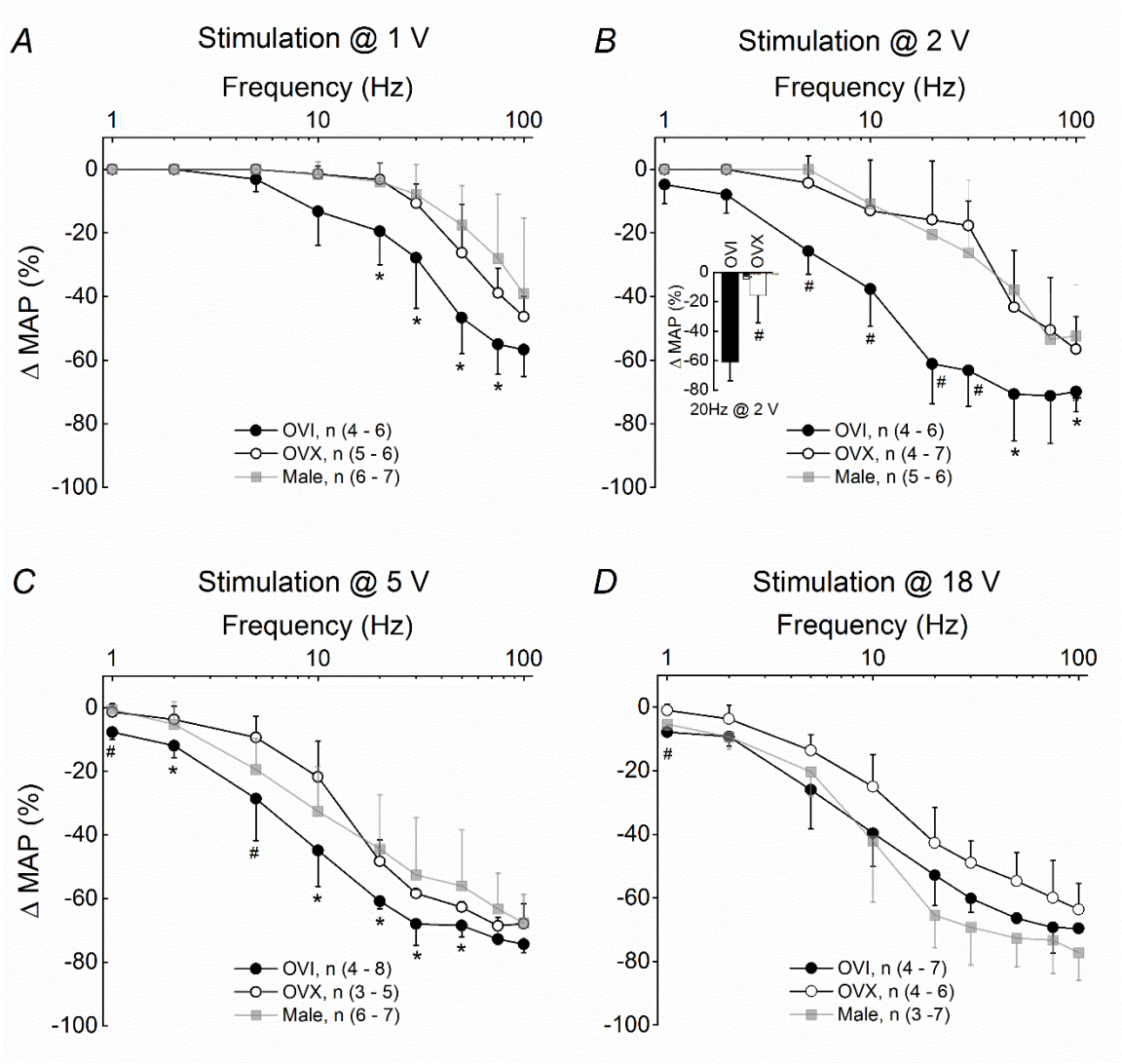

Figure 23: Comparison of average baroreflex responses in ovary intact (OVI), ovariectomized (OVX) female and male rats. Average changes in left femoral MAP (Δ MAP) evoked through bipolar stimulation of the left ADN using randomly selected pairs of voltage (1 to 18 V) and frequency (1 to 100 Hz). (A - C) Low intensity (≤ 5 V) stimulation of low- threshold myelinated baroreceptor afferents evoked significantly attenuated depressor reflexes in OVX rats compared to OVI rats (see inset) but comparable to those of male rats. (D) Higher intensity (≥ 5 V) stimulation results in graded recruitment of the higher threshold, unmyelinated baroreceptor afferents (see Figure 19) which bring about depressor responses that are quite similar in male and OVI female rats, but not in OVX females. Data are means ± SD, * $p < 0.05$ and # $p < 0.01$, both OVI vs. male.

non-genomic effects capable of modulating autonomic outflow and BRx function (McEwen, 1981; Maggi *et al.*, 2004). Evidence that supports this hypothesis comes from direct injections of E2 into central autonomic nuclei of adult rats (Saleh *et al.*, 2000; Saleh & Connell, 2000). These studies demonstrate that estrogen exerts influence on neurons located in the NTS and NA to increase parasympathetic tone, and may act on the neurons located in the RVLM to attenuate sympathetic tone. Consistent with these observations, variations in BP, HR, and BRx function have been correlated to changes in circulating estrogen levels that occur over the estrous cycle and following ovariectomy (El-Mas & Abdel-Rahman, 2009; Goldman *et al.*, 2009). However, systemic levels of estrogen do not reflect local concentrations in the brain or periphery. In OVX rats, the production of estrogen is shifted from the ovaries to extragonadal sites such as the adipose, vascular and brain tissues. In the brain, aromatization of androgens to estrogens is important to maintain synaptic connections and regulate neurotransmitter release and may counteract the effects of aging after menopause in females (Garcia-Segura *et al.*, 1994).

In the current study, we did not determine whether the magnitude of BRx responses in OVI rats is associated with the phase of estrous cycle. If such correlations between the level of circulating estrogen and MAP-reflex responses exist, ovariectomy may abolish them. This could be assessed by measuring the serum levels of estradiol in the OVI and OVX females before BRx studies. Such findings would be supported by reports that both classic nuclear estrogen receptors (ER), ERα and ER β, and the orphan G protein-coupled receptor

GPR30 are distributed in several rat brain areas including the NTS (Spary *et al.*, 2010; Spary *et al.*, 2013), and their expression is significantly reduced post ovariectomy. Interestingly, ERα and ERβ have been immunohistochemically located in the nuclei of a subpopulation of neurons in the vagal nodose ganglia (Papka *et al.*, 1997; Papka *et al.*, 2001). This suggests that estrogen could influence structural and functional parameters of this group of sensory vagal neurons. Since it is currently unknown if this subpopulation of neurons include aortic mechanosensitive neurons, further investigation is warranted, and this may support our interpretations related to alterations in nerve conduction post ovariectomy.

C. Initial and long-term changes in rat aortic BRx responses post ovariectomy

Hormonal replacement therapy (HRT) in postmenopausal women failed to reduce adverse cardiovascular events (Hulley *et al.*, 1998; Rossouw *et al.*, 2002). Given the documented effects of estrogen to improve vascular function and BRS, data from these studies suggest that timing of HRT therapy may be a critical factor in decreasing postmenopausal CVD. This is supported by studies that demonstrate time-dependent cardiovascular effects following either surgical or natural menopause (Dubey *et al.*, 2005; Goldman *et al.*, 2009). Such findings lead us to speculate on the time course of changes in the female aortic BRx response following ovariectomy and this warranted further study. Our results showed that reductions in BRx responses post ovariectomy are time-dependent (Figure 22). Significant attenuations occurred within the first week post

ovariectomy (G1 group), but even greater reductions were measured 2 to 3 weeks after surgery (G2 group) that were comparable to those of OVX females 24 or more days post ovariectomy. Likewise, Goldman *et al.* (2009) reported that spontaneous cardiovagal BRS in OVX female Sprague-Dawley rats was significantly reduced 1 to 4 days following ovariectomy as compared to intact female rats, although further reductions were not found (Goldman *et al.*, 2009). These changes in BRx function could be explained, at least in part, by estrogenic modulation of autonomic and baroreflex function elicited via ER. Indeed, elevated levels of ER expression in areas of the brain with descending projections to medullary autonomic nuclei have been reported 3 days after ovariectomy, whereas a dramatic down-regulation of ERα mRNA occurs 3 weeks after surgery (Shughrue *et al.*, 1992; Spary *et al.*, 2010). Interestingly, in the NTS GPR30 mRNA levels appeared to be increased in OVX rats at 3 weeks following ovariectomy suggesting that the non-genomic regulation of neural activity by estrogen may be dependent on local aromatase enzyme activity (Spary *et al.*, 2013). Importantly variations in BP and BRS in rat following ovariectomy are well documented, but most studies performed in OVX females supplemented with estrogen and do not examine the effects of estrogen withdrawal following ovariectomy. Such studies have the potential to bring further insight into the mechanisms involved in the development of hypertension.

IV. Clinical implications

BR activate to stabilize sudden changes in BP. A transient or sustained increase in arterial pressure leads to the activation of barosensory pathways that elicit a rapid reduction of HR via the parasympathetic arm of the BRx or withdrawal of sympathetic drive. With such a powerful influence over the cardiovascular system, BR dysfunction has been linked to a diverse array of cardiovascular pathologies from acute and chronic hypertension to orthostatic hypotension (OH) (Grassi *et al.*, 1998; Ufnal, 2012; Aung *et al.*, 2013; La Rovere *et al.*, 2013). Regardless of type, the function of the BR is to accurately transduce the mechanical distortion of its nerve endings to a frequency-modulated train of action potentials and convey this electrical signal to the CNS via its afferent fibers. Their pressure-discharge attributes have been extensively studied. Myelinated A-type BR or low-threshold pressoreceptors are generally active at normal arterial pressures and produce a regular discharge pattern that faithfully encodes the pressure pulse (Katona *et al.*, 1968; Coleridge & Coleridge, 1980). In stark contrast, unmyelinated C-type BR or high-threshold pressoreceptors require more elevated arterial pressures for activation and exhibit irregular discharge frequencies not well correlated with arterial hemodynamics (Thoren *et al.*, 1977). Although as yet unproven, it is reasonable to speculate that the myelinated Ah-type BR exhibit pressure-discharge properties similar to the A-type BR because they have similar *in vitro* excitability characteristics, albeit with lower rates of repetitive discharge (Li *et al.*, 2008). Our current data supports the role of the Ah-type BR afferents as an additional myelinated barosensory

pathway to the integrated afferent drive of the BRx. This would imply that for comparable arterial pressures, females but not males exhibit substantially elevated BR input driving centrally mediated BRx pathways. Such an augmented barosensory drive may account for, at least in part, the sex-related differences observed in baseline arterial pressure, cardiovagal BRx, and OH, as these implicate a more active parasympathetic control in females compared to males.

Although it is not clear which component(s) of the parasympathetic branch of the BRx arc mediates the sex-related differences observed in autonomic reflex function, a BR-mediated elevation in parasympathetic drive is a plausible explanation for the gap in baseline arterial pressure and cardiovagal BRx between the sexes. Emerging evidence shows that healthy young and middle-aged women have lower tonic sympathoadrenal activity-related support of BP (Peckerman *et al.*, 2001; Christou *et al.*, 2005; Tank *et al.*, 2005; Hogarth *et al.*, 2007) and significantly higher parasympathetic markers for HRV compared to age-matched men (Kuch *et al.*, 2001; Britton *et al.*, 2007). A BR-mediated elevation in parasympathetic drive and concomitant reduction in sympathetic activity could significantly contribute to the higher resting parasympathetic tone in women compared to men. Likewise, given the potential role of BR for long-term control of MAP (Thrasher, 2006), a myelinated BR-mediated reduction of sympathetic activity on BP may contribute to the “cardioprotective” lower baseline arterial pressure often observed in premenopausal women (Christou *et al.*, 2005; Fallen, 2005). Furthermore, A recent study by Kim *et al.* (2011) concluded that sex differences in the BRx control of BP appear to be less evident during BR

unloading (i.e. simulated hypotension) than BR loading(i.e. simulated hypertension), and in response to the latter women exhibited “an exaggerated reduction in BP compared to men” (Kim *et al.*, 2011; Fisher *et al.*, 2012). These findings broadly support our observations that acute hypertension evoked by electrical stimulation of the ADN results in greater hypotensive responses in female compared to male rats. Noteworthy is that several studies have reported on women being less capable than men to compensate for postural changes, for example, from a supine to an upright position (Convertino, 1998; Barantke *et al.*, 2008). This phenomenon also referred to as OH may be manifested with extreme symptoms such as vasovagal or reflex syncope ensuing an abrupt fall in systemic BP ((Chen-Scarabelli & Scarabelli, 2004; Cheng *et al.*, 2011). Differences in body size and contributing factors such as sex-hormones and genetics do not explain the sex differences observed in OH between the sexes (Franke *et al.*, 2003; Cheng *et al.*, 2011). Because orthostatic BP regulation in women occurs via parasympathetic withdrawal more than sympathetic activation (Harm *et al.*, 2001; Arzeno *et al.*, 2013), a BR-mediated increase in tonic resting parasympathetic activity could result in women requiring a larger increase in heart rate compared to men to achieve orthostatic stabilization.

Several lines of evidence support the idea that female sex hormones have a cardioprotective effect in young women (Dart *et al.*, 2002). Although aging is a risk factor in developing hypertension in both males and females, females are at a greater risk after natural or surgical menopause. This is demonstrated through measures of cardiovascular reflex function such as BRS, which has been shown

to be markedly reduced in hypertensive as compared with normotensive women, whereas no such reduction occurs in hypertensive men (Sevre *et al.*, 2001). Interestingly, postmenopausal females present with BRS and hypertension that are more closely aligned with those of age-matched males, suggesting that ovarian hormones may play an important role in modulation of neurocirculatory control (Dubey *et al.*, 2005). Likewise, our BRx studies showed that sustained loss of sex hormones, through ovariectomy, resulted in evoked hypotensive responses from OVX females that were comparable to those from male rats, at stimulus intensities specific for the activation of mostly myelinated barosensory afferents. Importantly, growing evidence supports the idea of a transition from vagal parasympathetic to sympathetic control of neurocirculation in females with aging (Lavi *et al.*, 2007). We contend that Ah-type barosensory afferents may have a role in promoting vagal tone in females, and that ovarian sex hormone depravation after ovariectomy brings about functional changes in the Ah-type afferent pathway that may account for, a least in part, the increased sympathetic drive observed in aging females.

CHAPTER 5: SUMMARY

The differential myelination of aortic BR fibers of male and female rats gives rise to sexually dimorphic recruitment patterns of myelinated afferent fibers. In female rats, we consistently observed an additional myelinated fiber volley corresponding to low-threshold Ah-type BR fibers with CV ranging from 2 to 10 m/sec. *In situ* BRx experiments demonstrate that the functional contributions of this low-threshold myelinated barosensory afferent pathway bring about greater BRx responses in females compared to males at lower frequencies than previously reported for myelinated-specific stimulus. Collectively, our findings suggest that *in vivo* the physiological role of the Ah-type BR afferents is to mediate the low-pressure-threshold drive of the BRx resulting in a better parasympathetic control of BP in females compared to males. Although we did not determine the independent contributions of the Ah-type BR afferent to BRx function, our study presents the Ah-type BR as a potential afferent explanation, or at least, a contributor to the sexual dimorphism observed in basal autonomic BRx function. Furthermore, the “cardioprotection” observed in premenopausal women may be associated to this sex specific BR afferent. Since sex hormones have been suggested to serve a neuromodulatory role, our correlative nerve conduction and BRx studies in intact *vs*. ovariectomized female rats bring insight to the impact ovarian sex steroids may have on BR afferent and BRx function. Lastly, the aortic BR form part of a larger population of multi-modal vagal sensory neurons whose cell bodies reside in the nodose ganglia, therefore, our findings

have the potential to explain other sexually dimorphic disorders involving vagal afferent dysfunction such as irritable bowel syndrome and asthma.

REFERENCES

Abraham A. (1969). *Microscopic innervation of the heart and blood vessels in vertebrates including man*. Pergamon Press, Oxford.

Adrian ED. (1926). The impulses produced by sensory nerve endings: Part I. *J Physiol* **61,** 49-72.

Amir R & Devor M. (2003). Electrical excitability of the soma of sensory neurons is required for spike invasion of the soma, but not for through-conduction. *Biophys J* **84,** 2181-2191.

Andresen MC, Doyle MW, Bailey TW & Jin YH. (2004). Differentiation of autonomic reflex control begins with cellular mechanisms at the first synapse within the nucleus tractus solitarius. *Braz J Med Biol Res* **37,** 549-558.

Andresen MC & Kunze DL. (1987). Ionic sensitivity of baroreceptors. *Circ Res* **61,** I66-71.

Andresen MC & Kunze DL. (1994). Nucleus tractus solitarius--gateway to neural circulatory control. *Annu Rev Physiol* **56,** 93-116.

Arai K, Nakagawa Y, Iwata T, Horiguchi H & Murata K. (2013). Relationships between QT interval and heart rate variability at rest and the covariates in healthy young adults. *Auton Neurosci* **173,** 53-57.

Arndt JO, Dorrenhaus A & Wiecken H. (1975). The aortic arch baroreceptor response to static and dynamic stretches in an isolated aorta-depressor nerve preparation of cats in vitro. *J Physiol* **252,** 59-78.

Arzeno NM, Stenger MB, Lee SM, Ploutz-Snyder R & Platts SH. (2013). Sex differences in blood pressure control during 6 degrees head-down tilt bed rest. *Am J Physiol Heart Circ Physiol* **304,** H1114-1123.

Aumonier FJ. (1972). Histological observations on the distribution of baroreceptors in the carotid and aortic regions of the rabbit, cat and dog. *Acta Anat (Basel)* **82,** 1-16.

Aung T, Fan W & Krishnamurthy M. (2013). Recurrent syncope, orthostatic hypotension and volatile hypertension: think outside the box. *J Community Hosp Intern Med Perspect* **3**.

Aviado DM & Guevara Aviado D. (2001). The Bezold-Jarisch reflex. A historical perspective of cardiopulmonary reflexes. *Ann N Y Acad Sci* **940,** 48-58.

Barantke M, Krauss T, Ortak J, Lieb W, Reppel M, Burgdorf C, Pramstaller PP, Schunkert H & Bonnemeier H. (2008). Effects of gender and aging on differential autonomic responses to orthostatic maneuvers. *J Cardiovasc Electrophysiol* **19,** 1296-1303.

Barnes JN, Matzek LJ, Charkoudian N, Joyner MJ, Curry TB & Hart EC. (2012). Association of cardiac baroreflex sensitivity with blood pressure transients: influence of sex and menopausal status. *Front Physiol* **3,** 187.

Benarroch EE. (2008). The arterial baroreflex: functional organization and involvement in neurologic disease. *Neurology* **71,** 1733-1738.

Beske SD, Alvarez GE, Ballard TP & Davy KP. (2001). Gender difference in cardiovagal baroreflex gain in humans. *J Appl Physiol (1985)* **91,** 2088-2092.

Bock P & Gorgas K. (1976). Fine structure of baroreceptor terminals in the carotid sinus of guinea pigs and mice. *Cell Tissue Res* **170,** 95-112.

Boyd IA & Kalu KU. (1979). Scaling factor relating conduction velocity and diameter for myelinated afferent nerve fibres in the cat hind limb. *J Physiol* **289,** 277-297.

Bristow MR, Ginsburg R, Umans V, Fowler M, Minobe W, Rasmussen R, Zera P, Menlove R, Shah P, Jamieson S & *et al*. (1986). Beta 1- and beta 2-adrenergic-receptor subpopulations in nonfailing and failing human ventricular myocardium: coupling of both receptor subtypes to muscle contraction and selective beta 1-receptor down-regulation in heart failure. *Circ Res* **59,** 297-309.

Britton A, Shipley M, Malik M, Hnatkova K, Hemingway H & Marmot M. (2007). Changes in heart rate and heart rate variability over time in middle-aged men and women in the general population (from the Whitehall II Cohort Study). *Am J Cardiol* **100,** 524-527.

Brodde OE & Leineweber K. (2004). Autonomic receptor systems in the failing and aging human heart: similarities and differences. *Eur J Pharmacol* **500,** 167-176.

Bronk DW & Stella G. (1932). Afferent impulses in the carotid sinus nerve I. The relation of the discharge from single end organs to arterial blood pressure. *Journal of Cellular Physiology* **1,** 113-130.

Bronzino JD. (2006). *Biomedical Engineering Fundamentals*. CRC Press, Boca Raton, Fl.

Brown AM. (1980). Receptors under pressure. An update on baroreceptors. *Circ Res* **46,** 1-10.

Brown AM, Saum WR & Tuley FH. (1976). A comparison of aortic baroreceptor discharge in normotensive and spontaneously hypertensive rats. *Circ Res* **39,** 488-496.

Cai Y, Hay M & Bishop VS. (1996). Synaptic connections and interactions between area postrema and nucleus tractus solitarius. *Brain Res* **724,** 121-124.

Campos LA, Pereira VL, Jr., Muralikrishna A, Albarwani S, Bras S & Gouveia S. (2013). Mathematical biomarkers for the autonomic regulation of cardiovascular system. *Front Physiol* **4,** 279.

Chan RK, Jarvina EV & Sawchenko PE. (2000). Effects of selective sinoaortic denervations on phenylephrine-induced activational responses in the nucleus of the solitary tract. *Neuroscience* **101,** 165-178.

Chen-Scarabelli C & Scarabelli TM. (2004). Neurocardiogenic syncope. *BMJ* **329,** 336-341.

Cheng YC, Vyas A, Hymen E & Perlmuter LC. (2011). Gender differences in orthostatic hypotension. *Am J Med Sci* **342,** 221-225.

Christou DD, Jones PP, Jordan J, Diedrich A, Robertson D & Seals DR. (2005). Women have lower tonic autonomic support of arterial blood pressure and less effective baroreflex buffering than men. *Circulation* **111,** 494-498.

Ciriello J & Calaresu FR. (1979). Separate medullary pathways mediatiating reflex vagal bradycardia to stimulation of buffer nerves in the cat. *J Auton Nerv Syst* **1,** 13-32.

Coleman TG. (1980). Arterial baroreflex control of heart rate in the conscious rat. *Am J Physiol* **238,** H515-520.

Coleridge HM & Coleridge JC. (1980). Cardiovascular afferents involved in regulation of peripheral vessels. *Annu Rev Physiol* **42,** 413-427.

Coleridge HM, Coleridge JC & Schultz HD. (1987). Characteristics of C fibre baroreceptors in the carotid sinus of dogs. *J Physiol* **394,** 291-313.

Conte MR. (2003). Gender differences in the neurohumoral control of the cardiovascular system. *Ital Heart J* **4,** 367-370.

Convertino VA. (1998). Gender differences in autonomic functions associated with blood pressure regulation. *Am J Physiol* **275,** R1909-1920.

Coppin CM & Jack JJ. (1972). Internodal length and conduction velocity of cat muscle afferent nerve fibres. *J Physiol* **222,** 92P-93P.

Coulter SA. (2011). Epidemiology of cardiovascular disease in women: risk, advances, and alarms. *Tex Heart Inst J* **38,** 145-147.

Cowley AW, Jr. (1992). Long-term control of arterial blood pressure. *Physiol Rev* **72,** 231-300.

Cowley AW, Jr., Liard JF & Guyton AC. (1973). Role of baroreceptor reflex in daily control of arterial blood pressure and other variables in dogs. *Circ Res* **32,** 564-576.

Curtis BM & O'Keefe JH, Jr. (2002). Autonomic tone as a cardiovascular risk factor: the dangers of chronic fight or flight. *Mayo Clin Proc* **77,** 45-54.

Dart AM, Du XJ & Kingwell BA. (2002). Gender, sex hormones and autonomic nervous control of the cardiovascular system. *Cardiovasc Res* **53,** 678-687.

Davos CH, Davlouros PA, Wensel R, Francis D, Davies LC, Kilner PJ, Coats AJ, Piepoli M & Gatzoulis MA. (2002). Global impairment of cardiac autonomic nervous activity late after repair of tetralogy of Fallot. *Circulation* **106,** I69-75.

De Hert S. (2012). Physiology of hemodynamic homeostasis. *Best Pract Res Clin Anaesthesiol* **26,** 409-419.

De Paula PM, Castania JA, Bonagamba LG, Salgado HC & Machado BH. (1999). Hemodynamic responses to electrical stimulation of the aortic depressor nerve in awake rats. *Am J Physiol* **277,** R31-38.

Dean C & Seagard JL. (1997). Mapping of carotid baroreceptor subtype projections to the nucleus tractus solitarius using c-fos immunohistochemistry. *Brain Res* **758,** 201-208.

Debanne D, Campanac E, Bialowas A, Carlier E & Alcaraz G. (2011). Axon physiology. *Physiol Rev* **91,** 555-602.

Deighton NM, Motomura S, Borquez D, Zerkowski HR, Doetsch N & Brodde OE. (1990). Muscarinic cholinoceptors in the human heart: demonstration, subclassification, and distribution. *Naunyn Schmiedebergs Arch Pharmacol* **341,** 14-21.

Devanandan MS. (1964). A Study of the Myelinated Fibres of the Aortic Nerve of Cats. *J Physiol* **171,** 361-367.

Diaz Brinton R. (2012). Translational animal models of human menopause: Challenges and emerging opportunities. *Endocrinology***,** 3571-3578.

Donald DE & Shepherd JT. (1980). Autonomic regulation of the peripheral circulation. *Annu Rev Physiol* **42,** 429-439.

Douglas WW, Ritchie JM & Schaumann W. (1956). Depressor reflexes from medullated and non-medullated fibres in the rabbits aortic nerve. *J Physiol* **132,** 187-198.

Drummond HA, Price MP, Welsh MJ & Abboud FM. (1998). A molecular component of the arterial baroreceptor mechanotransducer. *Neuron* **21,** 1435-1441.

Duan YF, Kopin IJ & Goldstein DS. (1999). Stimulation of the paraventricular nucleus modulates firing of neurons in the nucleus of the solitary tract. *Am J Physiol* **277,** R403-411.

Dubey RK, Imthurn B, Barton M & Jackson EK. (2005). Vascular consequences of menopause and hormone therapy: importance of timing of treatment and type of estrogen. *Cardiovasc Res* **66,** 295-306.

Dworkin BR & Dworkin S. (1995). Learning of physiological responses: II. Classical conditioning of the baroreflex. *Behav Neurosci* **109,** 1119-1136.

Ead HW, Green JH & Neil E. (1952). A comparison of the effects of pulsatile and non-pulsatile blood flow through the carotid sinus on the reflexogenic activity of the sinus baroceptors in the cat. *J Physiol* **118,** 509-519.

El-Mas MM & Abdel-Rahman AA. (2009). Longitudinal assessment of the effects of oestrogen on blood pressure and cardiovascular autonomic activity in female rats. *Clin Exp Pharmacol Physiol* **36,** 1002-1009.

Fallen EL. (2005). Vagal afferent stimulation as a cardioprotective strategy? Introducing the concept. *Ann Noninvasive Electrocardiol* **10,** 441-446.

Fan W & Andresen MC. (1998). Differential frequency-dependent reflex integration of myelinated and nonmyelinated rat aortic baroreceptors. *Am J Physiol* **275,** H632-640.

Fan W, Reynolds PJ & Andresen MC. (1996). Baroreflex frequency-response characteristics to aortic depressor and carotid sinus nerve stimulation in rats. *Am J Physiol* **271,** H2218-2227.

Fan W, Schild JH & Andresen MC. (1999). Graded and dynamic reflex summation of myelinated and unmyelinated rat aortic baroreceptors. *Am J Physiol* **277,** R748-756.

Fazan VP, Junior RF, Salgado HC & Barreira AA. (1999). Morphology of aortic depressor nerve myelinated fibers in normotensive Wistar-Kyoto and spontaneously hypertensive rats. *J Auton Nerv Syst* **77,** 133-139.

Fazan VP, Salgado HC & Barreira AA. (1997). A descriptive and quantitative light and electron microscopy study of the aortic depressor nerve in normotensive rats. *Hypertension* **30,** 693-698.

Fex Svenningsen A & Kanje M. (1999). Estrogen and progesterone stimulate Schwann cell proliferation in a sex- and age-dependent manner. *J Neurosci Res* **57,** 124-130.

Fisher JP, Kim A, Hartwich D & Fadel PJ. (2012). New insights into the effects of age and sex on arterial baroreflex function at rest and during dynamic exercise in humans. *Auton Neurosci* **172,** 13-22.

Franke WD, Johnson CP, Steinkamp JA, Wang R & Halliwill JR. (2003). Cardiovascular and autonomic responses to lower body negative pressure: do not explain gender differences in orthostatic tolerance. *Clin Auton Res* **13,** 36-44.

Frenneaux MP. (2004). Autonomic changes in patients with heart failure and in post-myocardial infarction patients. *Heart* **90,** 1248-1255.

Fukuda Y, Sato A, Suzuki A & Trzebski A. (1989). Autonomic nerve and cardiovascular responses to changing blood oxygen and carbon dioxide levels in the rat. *J Auton Nerv Syst* **28,** 61-74.

Furukawa Y, Narita M, Takei M, Kobayashi O, Haniuda M & Chiba S. (1991). Differential intracardiac sympathetic and parasympathetic innervation to the SA and AV nodes in anesthetized dog hearts. *Jpn J Pharmacol* **55,** 381-390.

Garcia-Segura LM, Chowen JA, Parducz A & Naftolin F. (1994). Gonadal hormones as promoters of structural synaptic plasticity: cellular mechanisms. *Prog Neurobiol* **44,** 279-307.

Glazebrook PA, Schilling WP & Kunze DL. (2005). TRPC channels as signal transducers. *Pflugers Arch* **451,** 125-130.

Glick G & Braunwald E. (1965). Relative Roles of the Sympathetic and Parasympathetic Nervous Systems in the Reflex Control of Heart Rate. *Circ Res* **16,** 363-375.

Go AS, Mozaffarian D, Roger VL, Benjamin EJ, Berry JD, Borden WB, Bravata DM, Dai S, Ford ES, Fox CS, Franco S, Fullerton HJ, Gillespie C, Hailpern SM, Heit JA, Howard VJ, Huffman MD, Kissela BM, Kittner SJ, Lackland DT, Lichtman JH, Lisabeth LD, Magid D, Marcus GM, Marelli A, Matchar DB, McGuire DK, Mohler ER, Moy CS, Mussolino ME, Nichol G, Paynter NP, Schreiner PJ, Sorlie PD, Stein J, Turan TN, Virani SS, Wong ND, Woo D & Turner MB. (2013). Heart disease and stroke statistics--2013 update: a report from the American Heart Association. *Circulation* **127,** e6-e245.

Goldman RK, Azar AS, Mulvaney JM, Hinojosa-Laborde C, Haywood JR & Brooks VL. (2009). Baroreflex sensitivity varies during the rat estrous cycle: role of gonadal steroids. *Am J Physiol Regul Integr Comp Physiol* **296,** R1419-1426.

Gorman PH & Mortimer JT. (1983). The effect of stimulus parameters on the recruitment characteristics of direct nerve stimulation. *IEEE Trans Biomed Eng* **30,** 407-414.

Grady D. (2006). Clinical practice. Management of menopausal symptoms. *N Engl J Med* **355,** 2338-2347.

Grady D, Herrington D, Bittner V, Blumenthal R, Davidson M, Hlatky M, Hsia J, Hulley S, Herd A, Khan S, Newby LK, Waters D, Vittinghoff E & Wenger N. (2002). Cardiovascular disease outcomes during 6.8 years of hormone therapy: Heart and Estrogen/progestin Replacement Study follow-up (HERS II). *JAMA* **288,** 49-57.

Grassi G, Cattaneo BM, Seravalle G, Lanfranchi A & Mancia G. (1998). Baroreflex control of sympathetic nerve activity in essential and secondary hypertension. *Hypertension* **31,** 68-72.

Guyton AC. (1980). *Circulatory Physiology III: Arterial Pressure and Hypertension*. WB Saunders, Philadelphia, PA.

Guyton AC. (2006). *Textbook of Medical Physiology*. Elsevier Inc., Philadelphia, PA.

Hall JE, Granger JP, do Carmo JM, da Silva AA, Dubinion J, George E, Hamza S, Speed J & Hall ME. (2012). Hypertension: physiology and pathophysiology. *Compr Physiol* **2,** 2393-2442.

Harm DL, Jennings RT, Meck JV, Powell MR, Putcha L, Sams CP, Schneider SM, Shackelford LC, Smith SM & Whitson PA. (2001). Invited review: gender issues related to spaceflight: a NASA perspective. *J Appl Physiol (1985)* **91,** 2374-2383.

Harper AA & Lawson SN. (1985). Conduction velocity is related to morphological cell type in rat dorsal root ganglion neurones. *J Physiol* **359,** 31-46.

Hay M & Kunze DL. (1994). Calcium-activated potassium channels in rat visceral sensory afferents. *Brain Res* **639,** 333-336.

Heidenreich PA, Trogdon JG, Khavjou OA, Butler J, Dracup K, Ezekowitz MD, Finkelstein EA, Hong Y, Johnston SC, Khera A, Lloyd-Jones DM, Nelson SA, Nichol G, Orenstein D, Wilson PW & Woo YJ. (2011). Forecasting the future of cardiovascular disease in the United States: a policy statement from the American Heart Association. *Circulation* **123,** 933-944.

Hendrix SL, Wassertheil-Smoller S, Johnson KC, Howard BV, Kooperberg C, Rossouw JE, Trevisan M, Aragaki A, Baird AE, Bray PF, Buring JE, Criqui MH, Herrington D, Lynch JK, Rapp SR & Torner J. (2006). Effects of conjugated equine estrogen on stroke in the Women's Health Initiative. *Circulation* **113,** 2425-2434.

Hering H. (1923). Der Karotis druck versuch. *Munch Med Wochenschr* **70,** 1278-1290.

Herrington DM. (1999). The HERS trial results: paradigms lost? Heart and Estrogen/progestin Replacement Study. *Ann Intern Med* **131,** 463-466.

Higgins CB, Vatner SF & Braunwald E. (1973). Parasympathetic control of the heart. *Pharmacol Rev* **25,** 119-155.

Hines T, Toney GM & Mifflin SW. (1994). Responses of neurons in the nucleus tractus solitarius to stimulation of heart and lung receptors in the rat. *Circ Res* **74,** 1188-1196.

Hogarth AJ, Mackintosh AF & Mary DA. (2007). Gender-related differences in the sympathetic vasoconstrictor drive of normal subjects. *Clin Sci (Lond)* **112,** 353-361.

Hsia J, Margolis KL, Eaton CB, Wenger NK, Allison M, Wu L, LaCroix AZ & Black HR. (2007). Prehypertension and cardiovascular disease risk in the Women's Health Initiative. *Circulation* **115,** 855-860.

Huikuri HV, Pikkujamsa SM, Airaksinen KE, Ikaheimo MJ, Rantala AO, Kauma H, Lilja M & Kesaniemi YA. (1996). Sex-related differences in autonomic modulation of heart rate in middle-aged subjects. *Circulation* **94,** 122-125.

Hulley S, Grady D, Bush T, Furberg C, Herrington D, Riggs B & Vittinghoff E. (1998). Randomized trial of estrogen plus progestin for secondary prevention of coronary heart disease in postmenopausal women. Heart and Estrogen/progestin Replacement Study (HERS) Research Group. *JAMA* **280,** 605-613.

Huxley VH. (2007). Sex and the cardiovascular system: the intriguing tale of how women and men regulate cardiovascular function differently. *Adv Physiol Educ* **31,** 17-22.

Jackson DN, Noble EG & Shoemaker JK. (2004). Y1- and alpha1-receptor control of basal hindlimb vascular tone. *Am J Physiol Regul Integr Comp Physiol* **287,** R228-233.

Janig W. (2008). *The integrative action of the autonomic nervous system*. Cambridge University Press, Cambridge, UK.

Jin YH, Bailey TW, Li BY, Schild JH & Andresen MC. (2004). Purinergic and vanilloid receptor activation releases glutamate from separate cranial afferent terminals in nucleus tractus solitarius. *J Neurosci* **24,** 4709-4717.

Johnson MS, DeMarco VG, Heesch CM, Whaley-Connell AT, Schneider RI, Rehmer NT, Tilmon RD, Ferrario CM & Sowers JR. (2011). Sex differences in baroreflex sensitivity, heart rate variability, and end organ damage in the TGR(mRen2)27 rat. *Am J Physiol Heart Circ Physiol* **301,** H1540-1550.

Jordan J, Heusser K, Brinkmann J & Tank J. (2012). Electrical carotid sinus stimulation in treatment resistant arterial hypertension. *Auton Neurosci* **172,** 31-36.

Jose AD & Collison D. (1970). The normal range and determinants of the intrinsic heart rate in man. *Cardiovasc Res* **4,** 160-167.

Kardon MB, Peterson DF & Bishop VS. (1975). Reflex heart rate control via specific aortic nerve afferents in the rabbit. *Circ Res* **37,** 41-47.

Kassab GS. (2006). Biomechanics of the cardiovascular system: the aorta as an illustratory example. *J R Soc Interface* **3,** 719-740.

Katona PG, Poitras JW, Pantelakis N, Jensen EW & Barnett GO. (1968). Deterministic nature of baroreceptor firing. *Am J Physiol* **215,** 1-7.

Ketch T, Biaggioni I, Robertson R & Robertson D. (2002). Four faces of baroreflex failure: hypertensive crisis, volatile hypertension, orthostatic tachycardia, and malignant vagotonia. *Circulation* **105,** 2518-2523.

Kim A, Deo SH, Fisher JP & Fadel PJ. (2012). Effect of sex and ovarian hormones on carotid baroreflex resetting and function during dynamic exercise in humans. *J Appl Physiol (1985)* **112,** 1361-1371.

Kim A, Deo SH, Vianna LC, Balanos GM, Hartwich D, Fisher JP & Fadel PJ. (2011). Sex differences in carotid baroreflex control of arterial blood pressure in humans: relative contribution of cardiac output and total vascular conductance. *Am J Physiol Heart Circ Physiol* **301,** H2454-2465.

Kimura J. (1984). Principles and pitfalls of nerve conduction studies. *Ann Neurol* **16,** 415-429.

Kirchheim HR. (1976). Systemic arterial baroreceptor reflexes. *Physiol Rev* **56,** 100-177.

Kobayashi M, Cheng ZB, Tanaka K & Nosaka S. (1999). Is the aortic depressor nerve involved in arterial chemoreflexes in rats? *J Auton Nerv Syst* **78,** 38-48.

Korner PI. (1971). Integrative neural cardiovascular control. *Physiol Rev* **51,** 312-367.

Koster G & Tschermak A. (1903). Ueber den nervus depressor als reflex nerv der aorta. *Pflueger Arch* **93,** 24.

Kougias P, Weakley SM, Yao Q, Lin PH & Chen C. (2010). Arterial baroreceptors in the management of systemic hypertension. *Med Sci Monit* **16,** RA1-8.

Krauhs JM. (1979). Structure of rat aortic baroreceptors and their relationship to connective tissue. *J Neurocytol* **8,** 401-414.

Kuch B, Hense HW, Sinnreich R, Kark JD, von Eckardstein A, Sapoznikov D & Bolte HD. (2001). Determinants of short-period heart rate variability in the general population. *Cardiology* **95,** 131-138.

Kuhn C & Werdan K. (2001). Hemodynamic monitoring. In *Surgical treatment: Evidence-based and problem-oriented*, ed. Holzheimer RG & Mannick JA. Zuckschwerdt, Munich.

Kunze DL, Andresen MC & Torres LA. (1986). Do calcium antagonists act directly on calcium channels to alter baroreceptor function? *J Pharmacol Exp Ther* **239,** 303-310.

La Rovere MT, Bersano C, Gnemmi M, Specchia G & Schwartz PJ. (2002). Exercise-induced increase in baroreflex sensitivity predicts improved prognosis after myocardial infarction. *Circulation* **106,** 945-949.

La Rovere MT, Bigger JT, Jr., Marcus FI, Mortara A & Schwartz PJ. (1998). Baroreflex sensitivity and heart-rate variability in prediction of total cardiac mortality after myocardial infarction. ATRAMI (Autonomic Tone and Reflexes After Myocardial Infarction) Investigators. *Lancet* **351,** 478-484.

La Rovere MT, Pinna GD, Hohnloser SH, Marcus FI, Mortara A, Nohara R, Bigger JT, Jr., Camm AJ & Schwartz PJ. (2001). Baroreflex sensitivity and heart rate variability in the identification of patients at risk for life-threatening arrhythmias: implications for clinical trials. *Circulation* **103,** 2072-2077.

La Rovere MT, Pinna GD, Maestri R & Sleight P. (2013). Clinical value of baroreflex sensitivity. *Neth Heart J* **21,** 61-63.

La Rovere MT, Pinna GD & Raczak G. (2008). Baroreflex sensitivity: measurement and clinical implications. *Ann Noninvasive Electrocardiol* **13,** 191-207.

Lahiri MK, Kannankeril PJ & Goldberger JJ. (2008). Assessment of autonomic function in cardiovascular disease: physiological basis and prognostic implications. *J Am Coll Cardiol* **51,** 1725-1733.

Landgren S. (1952a). The baroceptor activity in the carotid sinus nerve and the distensibility of the sinus wall. *Acta Physiol Scand* **26,** 35-56.

Landgren S. (1952b). On the excitation mechanism of the carotid baroceptors. *Acta Physiol Scand* **26,** 1-34.

Lavi S, Nevo O, Thaler I, Rosenfeld R, Dayan L, Hirshoren N, Gepstein L & Jacob G. (2007). Effect of aging on the cardiovascular regulatory systems in healthy women. *Am J Physiol Regul Integr Comp Physiol* **292,** R788-793.

Leonelli E, Ballabio M, Consoli A, Roglio I, Magnaghi V & Melcangi RC. (2006). Neuroactive steroids: A therapeutic approach to maintain peripheral nerve integrity during neurodegenerative events. *J Mol Neurosci* **28,** 65-76.

Li BY, Glazebrook P, Kunze DL & Schild JH. (2011). KCa1.1 channel contributes to cell excitability in unmyelinated but not myelinated rat vagal afferents. *Am J Physiol Cell Physiol* **300,** C1393-1403.

Li BY, Qiao GF, Feng B, Zhao RB, Lu YJ & Schild JH. (2008). Electrophysiological and neuroanatomical evidence of sexual dimorphism in aortic baroreceptor and vagal afferents in rat. *Am J Physiol Regul Integr Comp Physiol* **295,** R1301-1310.

Li BY & Schild JH. (2002). Patch clamp electrophysiology in nodose ganglia of adult rat. *J Neurosci Methods* **115,** 157-167.

Li BY & Schild JH. (2007). Electrophysiological and pharmacological validation of vagal afferent fiber type of neurons enzymatically isolated from rat nodose ganglia. *J Neurosci Methods* **164,** 75-85.

Liao D, Cai J, Barnes RW, Tyroler HA, Rautaharju P, Holme I & Heiss G. (1996). Association of cardiac autonomic function and the development of hypertension: the ARIC study. *Am J Hypertens* **9,** 1147-1156.

Lu Y, Ma X, Sabharwal R, Snitsarev V, Morgan D, Rahmouni K, Drummond HA, Whiteis CA, Costa V, Price M, Benson C, Welsh MJ, Chapleau MW & Abboud FM. (2009). The ion channel ASIC2 is required for baroreceptor and autonomic control of the circulation. *Neuron* **64,** 885-897.

Maggi A, Ciana P, Belcredito S & Vegeto E. (2004). Estrogens in the nervous system: mechanisms and nonreproductive functions. *Annu Rev Physiol* **66,** 291-313.

Magnaghi V, Cavarretta I, Galbiati M, Martini L & Melcangi RC. (2001). Neuroactive steroids and peripheral myelin proteins. *Brain Res Brain Res Rev* **37,** 360-371.

Manson JE, Hsia J, Johnson KC, Rossouw JE, Assaf AR, Lasser NL, Trevisan M, Black HR, Heckbert SR, Detrano R, Strickland OL, Wong ND, Crouse JR, Stein E & Cushman M. (2003). Estrogen plus progestin and the risk of coronary heart disease. *N Engl J Med* **349,** 523-534.

Maranon R & Reckelhoff JF. (2013). Sex and gender differences in control of blood pressure. *Clin Sci (Lond)* **125,** 311-318.

Martini FH. (1998). *Fundamentals of Anatomy and Physiology*. Prentice Hall, Inc., Upper Saddle River, NJ.

McCubbin JW, Green JH & Page IH. (1956). Baroceptor function in chronic renal hypertension. *Circ Res* **4,** 205-210.

McEwen BS. (1981). Neural gonadal steroid actions. *Science* **211,** 1303-1311.

McKitrick DJ, Krukoff TL & Calaresu FR. (1992). Expression of c-fos protein in rat brain after electrical stimulation of the aortic depressor nerve. *Brain Res* **599,** 215-222.

McNeal DR. (1976). Analysis of a model for excitation of myelinated nerve. *IEEE Trans Biomed Eng* **23,** 329-337.

Melcangi RC, Cavarretta IT, Ballabio M, Leonelli E, Schenone A, Azcoitia I, Miguel Garcia-Segura L & Magnaghi V. (2005). Peripheral nerves: a target for the action of neuroactive steroids. *Brain Res Brain Res Rev* **48,** 328-338.

Melcangi RC, Magnaghi V & Martini L. (2000). Aging in peripheral nerves: regulation of myelin protein genes by steroid hormones. *Prog Neurobiol* **60,** 291-308.

Menozzi R, Cagnacci A, Zanni AL, Bondi M, Volpe A & Del Rio G. (2000). Sympathoadrenal response of postmenopausal women prior and during prolonged administration of estradiol. *Maturitas* **34,** 275-281.

Miura M & Reis DJ. (1972). The role of the solitary and paramedian reticular nuclei in mediating cardiovascular reflex responses from carotid baro- and chemoreceptors. *J Physiol* **223,** 525-548.

Mohamed MK, El-Mas MM & Abdel-Rahman AA. (1999). Estrogen enhancement of baroreflex sensitivity is centrally mediated. *Am J Physiol* **276,** R1030-1037.

Mraovitch S, Kumada M & Reis DJ. (1982). Role of the nucleus parabrachialis in cardiovascular regulation in cat. *Brain Res* **232,** 57-75.

Nakayama H, Noda K, Hotta H, Ohsawa H & Hosoya Y. (1998). Effects of aging on numbers, sizes and conduction velocities of myelinated and unmyelinated fibers of the pelvic nerve in rats. *J Auton Nerv Syst* **69,** 148-155.

Nonidez JF. (1935). The aortic (depressor) nerve and its associated epithelioid body, the glomus aorticum. *American Journal of Anatomy* **57,** 259-301.

Numao Y, Siato M, Terui N & Kumada M. (1985). The aortic nerve-sympathetic reflex in the rat. *J Auton Nerv Syst* **13,** 65-79.

Olshansky B, Sabbah HN, Hauptman PJ & Colucci WS. (2008). Parasympathetic nervous system and heart failure: pathophysiology and potential implications for therapy. *Circulation* **118,** 863-871.

Opthof T. (2000). The normal range and determinants of the intrinsic heart rate in man. *Cardiovasc Res* **45,** 177-184.

Pagani M, Lucini D & Porta A. (2012). Sympathovagal balance from heart rate variability: time for a second round? *Exp Physiol* **97,** 1141-1142.

Paintal AS. (1953). The conduction velocities of respiratory and cardiovascular afferent fibres in the vagus nerve. *J Physiol* **121,** 341-359.

Papka RE, Srinivasan B, Miller KE & Hayashi S. (1997). Localization of estrogen receptor protein and estrogen receptor messenger RNA in peripheral autonomic and sensory neurons. *Neuroscience* **79,** 1153-1163.

Papka RE, Storey-Workley M, Shughrue PJ, Merchenthaler I, Collins JJ, Usip S, Saunders PT & Shupnik M. (2001). Estrogen receptor-alpha and beta-immunoreactivity and mRNA in neurons of sensory and autonomic ganglia and spinal cord. *Cell Tissue Res* **304,** 193-214.

Patterson D, Dick JB & Struthers AD. (2002). Intensive statin treatment improves baroreflex sensitivity: another cardioprotective mechanism for statins? *Heart* **88,** 415-416.

Peckerman A, Hurwitz BE, Nagel JH, Leitten C, Agatston AS & Schneiderman N. (2001). Effects of gender and age on the cardiac baroreceptor reflex in hypertension. *Clin Exp Hypertens* **23,** 645-656.

Perge JA, Niven JE, Mugnaini E, Balasubramanian V & Sterling P. (2012). Why do axons differ in caliber? *J Neurosci* **32,** 626-638.

Pickering TG & Davies J. (1973). Estimation of the conduction time of the baroreceptor-cardiac reflex in man. *Cardiovasc Res* **7,** 213-219.

Pilowsky PM & Goodchild AK. (2002). Baroreceptor reflex pathways and neurotransmitters: 10 years on. *J Hypertens* **20,** 1675-1688.

Purves D, Augustine GJ, Fitzpatrick D, Hall WC, LaMantia A-S & White LE. (2012). *Neuroscience*. Sunderland, MA.

Qiao GF, Li BY, Lu YJ, Fu YL & Schild JH. (2009). 17Beta-estradiol restores excitability of a sexually dimorphic subset of myelinated vagal afferents in ovariectomized rats. *Am J Physiol Cell Physiol* **297,** C654-664.

Randall WC & McNally H. (1960). Augmentor action of the sympathetic cardiac nerves in man. *J Appl Physiol* **15,** 629-631.

Reynolds PJ, Fan W & Andresen MC. (2006). Capsaicin-resistant arterial baroreceptors. *J Negat Results Biomed* **5,** 6.

Reynolds PJ, Yang M & Andresen MC. (1994). Contribution of potassium channels to the discharge properties of rat aortic baroreceptor sensory endings. *Brain Res* **665,** 115-122.

Ribatti D. (2009). William Harvey and the discovery of the circulation of the blood. *J Angiogenes Res* **1,** 3.

Robertson D, Biaggioni I, Burnstock G, Low PA & Paton JFR. (2012). *Primer on the Autonomic Nervous System*. Elsevier Inc.

Rossouw JE, Anderson GL, Prentice RL, LaCroix AZ, Kooperberg C, Stefanick ML, Jackson RD, Beresford SA, Howard BV, Johnson KC, Kotchen JM & Ockene J. (2002). Risks and benefits of estrogen plus progestin in healthy postmenopausal women: principal results From the Women's Health Initiative randomized controlled trial. *JAMA* **288,** 321-333.

Rudy B. (1988). Diversity and ubiquity of K channels. *Neuroscience* **25,** 729-749.

Sabbatini M, Molinari C, Grossini E, Mary DA, Vacca G & Cannas M. (2004). The pattern of c-Fos immunoreactivity in the hindbrain of the rat following stomach distension. *Exp Brain Res* **157,** 315-323.

Saleh MC, Connell BJ & Saleh TM. (2000). Medullary and intrathecal injections of 17beta-estradiol in male rats. *Brain Res* **867,** 200-209.

Saleh TM & Connell BJ. (2000). 17beta-estradiol modulates baroreflex sensitivity and autonomic tone of female rats. *J Auton Nerv Syst* **80,** 148-161.

Salgado HC, Barale AR, Castania JA, Machado BH, Chapleau MW & Fazan R, Jr. (2007). Baroreflex responses to electrical stimulation of aortic depressor nerve in conscious SHR. *Am J Physiol Heart Circ Physiol* **292,** H593-600.

Samodelov LF, Godehard E & Arndt JO. (1979). A comparison of the stimulus-response curves of aortic and carotid sinus baroreceptors in decerebrated cats. *Pflugers Arch* **383,** 47-53.

Sanders JS, Ferguson DW & Mark AL. (1988). Arterial baroreflex control of sympathetic nerve activity during elevation of blood pressure in normal man: dominance of aortic baroreflexes. *Circulation* **77,** 279-288.

Santa Cruz Chavez GC, Li B-Y, Glazebrook P, Kunze DL & Schild JH. (2014). An afferent explanation for sexual dimorphism in the aortic barorefelx of rat. *In Submission*.

Santa Cruz Chavez GC, Li BY, Glazebrook P, Kunze DL & schild JH. (2012). An afferent basis for sexual dimorphism in the aortic baroreceptor reflex of rat. In *Experimental Biology* San Diego, CA. Poster session, 684.24.

Santa Cruz Chavez GC & Schild JH. (2014). Diminished baroreflex function following ovariectomy is a consequence of the reduced excitability of a sex specific population of low threshold myelinated baroreceptor afferents in the rat. *In Preparation*.

Sapru HN, Gonzalez E & Krieger AJ. (1981). Aortic nerve stimulation in the rat: cardiovascular and respiratory responses. *Brain Res Bull* **6,** 393-398.

Sato A, Sato Y & Suzuki H. (1985). Aging effects on conduction velocities of myelinated and unmyelinated fibers of peripheral nerves. *Neurosci Lett* **53,** 15-20.

Scheffers IJ, Kroon AA & de Leeuw PW. (2010). Carotid baroreflex activation: past, present, and future. *Curr Hypertens Rep* **12,** 61-66.

Schild JH, Alfrey KD & Li BY. (2005). Voltage-gated ion channels in vagal afferent neurons. In *Advances in vagal afferent neurobiology*, ed. Undem BJ & Weinreich D, pp. 77-100. CRC Press, USA.

Schild JH & Kunze DL. (1997). Experimental and modeling study of Na+ current heterogeneity in rat nodose neurons and its impact on neuronal discharge. *J Neurophysiol* **78,** 3198-3209.

Schild JH & Kunze DL. (2012). Differential distribution of voltage-gated channels in myelinated and unmyelinated baroreceptor afferents. *Auton Neurosci* **172,** 4-12.

Schneider CA, Rasband WS & Eliceiri KW. (2012). NIH Image to ImageJ: 25 years of image analysis. *Nat Methods* **9,** 671-675.

Seagard JL, Dean C & Hopp FA. (1995). Discharge patterns of baroreceptor-modulated neurons in the nucleus tractus solitarius. *Neurosci Lett* **191,** 13-18.

Seagard JL, Hopp FA, Drummond HA & Van Wynsberghe DM. (1993). Selective contribution of two types of carotid sinus baroreceptors to the control of blood pressure. *Circ Res* **72,** 1011-1022.

Seely EW, Walsh BW, Gerhard MD & Williams GH. (1999). Estradiol with or without progesterone and ambulatory blood pressure in postmenopausal women. *Hypertension* **33,** 1190-1194.

Sevre K, Lefrandt JD, Nordby G, Os I, Mulder M, Gans RO, Rostrup M & Smit AJ. (2001). Autonomic function in hypertensive and normotensive subjects: the importance of gender. *Hypertension* **37,** 1351-1356.

Shughrue PJ, Bushnell CD & Dorsa DM. (1992). Estrogen receptor messenger ribonucleic acid in female rat brain during the estrous cycle: a comparison with ovariectomized females and intact males. *Endocrinology* **131,** 381-388.

Sleight P. (1997). The importance of the autonomic nervous system in health and disease. *Aust N Z J Med* **27,** 467-473.

Sleight P. (2004). Arterial baroreflexes can determine long-term blood pressure. Baroreceptors and hypertension: time for a re-think? *Exp Physiol* **89,** 337-341.

Soltanpour N & Santer RM. (1996). Preservation of the cervical vagus nerve in aged rats: morphometric and enzyme histochemical evidence. *J Auton Nerv Syst* **60,** 93-101.

Spary EJ, Chapman SE, Sinfield JK, Maqbool A, Kaye J & Batten TF. (2013). Novel G protein-coupled oestrogen receptor GPR30 shows changes in mRNA expression in the rat brain over the oestrous cycle. *Neurosignals* **21,** 14-27.

Spary EJ, Maqbool A & Batten TF. (2010). Changes in oestrogen receptor alpha expression in the nucleus of the solitary tract of the rat over the oestrous cycle and following ovariectomy. *J Neuroendocrinol* **22,** 492-502.

Stornetta RL, Guyenet PG & McCarty RC. (1987). Autonomic nervous system control of heart rate during baroreceptor activation in conscious and anesthetized rats. *J Auton Nerv Syst* **20,** 121-127.

Straznicky NE, Lambert EA, Lambert GW, Masuo K, Esler MD & Nestel PJ. (2005). Effects of dietary weight loss on sympathetic activity and cardiac risk factors associated with the metabolic syndrome. *J Clin Endocrinol Metab* **90,** 5998-6005.

Sundar S & Gonzalez-Cueto J. (2005). Selective activation of small nerve fibers for assessing carpal tunnel syndrome. *Conf Proc IEEE Eng Med Biol Soc* **4,** 3668-3671.

Taha AA, Abdel-Magied EM & King AS. (1983). Ultrastructure of aortic and pulmonary baroreceptors in the domestic fowl. *J Anat* **137 (Pt 1),** 197-207.

Tanaka M, Sato M, Umehara S & Nishikawa T. (2003). Influence of menstrual cycle on baroreflex control of heart rate: comparison with male volunteers. *Am J Physiol Regul Integr Comp Physiol* **285,** R1091-1097.

Tank J, Diedrich A, Szczech E, Luft FC & Jordan J. (2005). Baroreflex regulation of heart rate and sympathetic vasomotor tone in women and men. *Hypertension* **45,** 1159-1164.

Thoren P & Jones JV. (1977). Characteristics of aortic baroreceptor C-fibres in the rabbit. *Acta Physiol Scand* **99,** 448-456.

Thoren P, Saum WR & Brown AM. (1977). Characteristics of rat aortic baroreceptors with nonmedullated afferent nerve fibers. *Circ Res* **40,** 231-237.

Thrasher TN. (2002). Unloading arterial baroreceptors causes neurogenic hypertension. *Am J Physiol Regul Integr Comp Physiol* **282,** R1044-1053.

Thrasher TN. (2004). Baroreceptors and the long-term control of blood pressure. *Exp Physiol* **89,** 331-335.

Thrasher TN. (2006). Arterial baroreceptor input contributes to long-term control of blood pressure. *Curr Hypertens Rep* **8,** 249-254.

Todo K. (1977). Vagal preganglionic innervation of the cat heart--an attempt to identify the medullary "heart area" by the retrograde axoplasmic transport of horseradish peroxidase. *Jpn Circ J* **41,** 1341-1352.

Todo K, Yamamoto T, Satomi H, Ise H, Takatama H & Takahashi K. (1977). Origins of vagal preganglionic fibers to the sino-atrial and atrio-ventricular node regions in the cat heart as studied by the horseradish peroxidase method. *Brain Res* **130,** 545-550.

Ufnal M. (2012). Essential hypertension--is erroneous receptor output to blame? *Med Hypotheses* **78,** 454-458.

Usselman CW, Mattar L, Twynstra J, Welch I & Shoemaker JK. (2011). Rodent cardiovascular responses to baroreceptor unloading: effect of plane of anaesthesia. *Appl Physiol Nutr Metab* **36,** 376-381.

van Brummelen P, Jie K & van Zwieten PA. (1986). Alpha-adrenergic receptors in human blood vessels. *Br J Clin Pharmacol* **21 Suppl 1,** 33S-39S.

Vasquez EC, Meyrelles SS, Mauad H & Cabral AM. (1997). Neural reflex regulation of arterial pressure in pathophysiological conditions: interplay among the baroreflex, the cardiopulmonary reflexes and the chemoreflex. *Braz J Med Biol Res* **30,** 521-532.

Verdu E, Ceballos D, Vilches JJ & Navarro X. (2000). Influence of aging on peripheral nerve function and regeneration. *J Peripher Nerv Syst* **5,** 191-208.

Wachter SB & Gilbert EM. (2012). Beta-adrenergic receptors, from their discovery and characterization through their manipulation to beneficial clinical application. *Cardiology* **122,** 104-112.

Waxman SG. (1980). Determinants of conduction velocity in myelinated nerve fibers. *Muscle Nerve* **3,** 141-150.

Waxman SG. (1988). Biophysical mechanisms of impulse conduction in demyelinated axons. *Adv Neurol* **47,** 185-213.

Waxman SG. (1995). *The Axon: Structure, Function and Pathophysiology*. Oxford University Press, New York, NY.

Wladyka CL, Feng B, Glazebrook PA, Schild JH & Kunze DL. (2008). The KCNQ/M-current modulates arterial baroreceptor function at the sensory terminal in rats. *J Physiol* **586,** 795-802.

Wladyka CL & Kunze DL. (2006). KCNQ/M-currents contribute to the resting membrane potential in rat visceral sensory neurons. *J Physiol* **575,** 175-189.

Young J. (1929). Malpighi's "De Pulmonibus". *Proc R Soc Med* **23,** 1-11.

Yu YG & Lindsey CJ. (2003). Baroreceptor-sensitive neurons in the rat paratrigeminal nucleus. *Auton Neurosci* **105,** 25-34.

Zhao H, Tian Z, Hao J & Chen B. (2005). Extragonadal aromatization increases with time after ovariectomy in rats. *Reprod Biol Endocrinol* **3,** 6.

Zhuo H, Ichikawa H & Helke CJ. (1997). Neurochemistry of the nodose ganglion. *Prog Neurobiol* **52,** 79-107.

CURRICULUM VITAE

Grace C. Santa Cruz Chavez

EDUCATION

1993 - 1997	B.S.	Electrical Engineering, Trine University (Angola, IN)
2007 - 2009	M.S.	Biomedical Engineering, Purdue University (Indianapolis, IN)
2010 - 2014	Ph.D.	Medical Neuroscience, Indiana University (Indianapolis, IN)

PROFESSIONAL EXPERIENCE

1998	Electrical Engineer (Biomedical Equipment) Roca S.A. Lima, Peru
1998 - 2003	Graduate Research Assistant (Atomic Force Microscopy / Biofilms / Digital image processing) Mentors: Indira Chatterjee, Ph.D. and James Henson, Ph.D. Program of Biomedical Engineering University of Nevada, Reno, NV
2008 - 2009	Thesis Research (Tissue Engineering / Bone cements) Mentor: Tien-Min Gabriel Chu, D.D.S., Ph.D. Advanced Biomaterial Lab Department of Biomedical Engineering Purdue University, Indianapolis, IN
2009 - 2010	Research Associate Experimental and Computational Neurobiology Lab Department of Biomedical Engineering Indiana University - Purdue University Indianapolis, IN
2010	Lab Rotation (Trigeminal hyperalgesia / Estrogen receptors / RT-PCR) Mentor: Jill C. Fehrenbacher, Ph.D. Department of Pharmacology and Toxicology Indiana University, Indianapolis, IN

2011	Lab Rotation (Optogenetics) Mentor: Xiaoming Jin, Ph.D. Spinal Cord and Brain Injury Research Group Indiana University, Indianapolis, IN
2011	Lab Rotation (Neuropathic pain / Fura-2 imaging) Mentor: Fletcher White, Ph.D. Stark Neurosciences Research Institute Indiana University, Indianapolis, IN
2011 - 2014	Dissertation Research (Baroreflex / Baroreceptor / Whole nerve electrophysiology) Mentor: John H. Schild, Ph.D. Experimental and Computational Neurobiology Laboratory Department of Biomedical Engineering Stark Neurosciences Research Institute Indiana University - Purdue University Indianapolis, IN

SPECIAL HONORS, AWARDS AND RECOGNITIONS

1993 - 1997	International Scholar Award, Trine University, Angola, IN
1997	Eta Kappa Nu
1997	Order of the Engineer
2008	Wm. Wrigley Jr. Company Graduate Student Award, first place poster competition, Indiana University, Indianapolis
2008	Honorable Mention Award, presenting author, Indiana University, Indianapolis
2011 - 2014	NHLBI Graduate Research Supplement Fellowship (R01HL072012), principal investigator: John H. Schild, Ph.D.
2014	Invited oral presentation at New England Science Symposium. Harvard Medical School, Boston, MA

PUBLICATIONS AND CONFERENCE ABSTRACTS

1. Alge DL, Santa Cruz G, Goebel WS, Chu TM, Characterization of dicalcium phosphate dihydrate cements prepared using a novel hydroxyapatite-based formulation. *Biomedical Materials, April 2009, 4(2): 25016*

2. G. Santa Cruz Chavez *(2009)* Evaluation of powder to liquid ratio and additive concentration effects on hydroxyapatite-based DCPD cements. M.S. thesis. Purdue University, Indianapolis, IN

3. Santa Cruz Chavez G, Alge DL, Chu TM, Additives concentration effects on dicalcium phosphate dihydrate cements prepared using monocalcium phosphate monohydrate and hydroxyapatite. *Biomedical Materials, 2011, 6: 65007*

4. Grace Santa Cruz Chavez, Bai-Yan Li, and John H. Schild. An afferent basis for sexual dimorphism in the aortic baroreceptor reflex of rat. *FASEB J March 29, 2012 26:684.24* (Abstract)

5. Grace Corina Santa Cruz Chavez, Bai-Yan Li, John H. Schild. Diminished baroreflex function following ovariectomy is a consequence of the reduced excitability of a sex specific population of low threshold myelinated baroreceptor afferents in the rat. *FASEB J April 9, 2013 27:1118.21* (Abstract)

6. Grace C. Santa Cruz Chavez, Bai-Yan Li, Patricia A. Glazebrook, Diana L. Kunze, John H. Schild. An afferent explanation for the sexually dimorphic aortic baroreflex response in rat. New England Science Symposium, Harvard Medical School, Boston, MA. April 6, 2014 (Abstract)

7. Grace C. Santa Cruz Chavez, Bai-Yan Li, Patricia A. Glazebrook, Diana L. Kunze, and John H. Schild. An afferent explanation for sexual dimorphism in the aortic baroreflex of rat. *In submission.*

8. Grace C. Santa Cruz Chavez and John H. Schild. Diminished baroreflex function following ovariectomy is a consequence of reduced excitability of low-threshold myelinated aortic baroreceptor afferents in rat. *In preparation.*

SEMINARS

2011 "The baroreflex" (with Principal Investigator)
Sensory Neuron Lab Meeting
Indiana University, Indianapolis

2011 "Sexual dimorphism in aortic baroreflex based on *in situ* electrophysiological approach"
Department of Medical Neuroscience graduate student meeting
Indiana University, Indianapolis

2012 "Gender differences in rat aortic baroreflex"
Biomedical Engineering Research Day
Purdue University, Indianapolis

2012 "Sex-related differences and the effects of aging on rat cardiovagal baroreflex"
Department of Medical Neuroscience graduate student meeting
Indiana University, Indianapolis

2013 "Sexually dimorphic function of low-threshold myelinated aortic baroreceptor afferents in rat"
Biomedical Engineering graduate student association
Purdue University, Indianapolis

2014 “Sexual dimorphism in aortic baroreceptor afferents”
Stark Neurosciences Research Institute
Indiana University, Indianapolis

2014 “An afferent explanation for the sexually dimorphic aortic baroreflex response in rat”
New England Science Symposium
Harvard Medical School, Boston

CONFERENCES AND SCIENTIFIC MEETINGS

2012 Experimental Biology, San Diego, CA (poster)
2013 Experimental Biology, Boston, MA (poster)
2013 Hypertension Summer School, Columbia University, Columbia, SC
2013 Society for Neuroscience, Indianapolis, IN
2013 6th International IEEE EMBS Neural Engineering, San Diego, CA
2014 New England Science Symposium, Harvard Medical School, Boston, MA
2014 Biomedical Science Student Conference, Boston, MA

PROFESSIONAL SOCIETIES

2012 - Present American Association for the Advancement of Science (AAAS)
2012 - Present American Physiological Society (APS)
2012 - Present Society for Neuroscience (SFN)
2013 - Present Institute of Electrical and Electronics Engineers (IEEE) / Engineering in Medicine and Biological Society (EMBS)
2013 - Present Biomedical Engineering Society (BMES)
2013 - Present Society for Hispanic Professional Engineers (SHPE)

OUTREACH

2012 - Present Volunteer intermediate school Science fair judge
2012 - 2014 Medical Neuroscience Graduate Student Association
2013 Journal of Physiology Reviewer Training (with Principal Investigator)
2013 Volunteer intermediate school Science class
2013 - Present Underrepresented Professional and Graduate Student Organization
2013 - 2014 Biomedical Engineering Graduate Student Association